EVALUATION OF OXYGEN BOMB METHODOLOGY FOR STUDYING FRYING CHEMISTRY

by

Teng Peng

A thesis submitted to the

Graduate School-New Brunswick

Rutgers, The State University of New Jersey

in partial fulfillment of the requirements

for the degree of

Master of Science

Graduate Program in Food Science

written under the direction of

Professor Karen M. Schaich

and approved by

_____

_____

_____

_____

New Brunswick, New Jersey

[October, 2010]

ABSTRACT OF THE THESIS

Evaluation of Using Oxygen Bomb Methodology for Studying Frying Chemistry

By Teng Peng

Thesis Director: Professor Karen M. Schaich

Oxipres™ oxygen bomb instrumentation was evaluated for measuring oxygen consumption in studying reactions of food oils at frying temperatures. High oleic sunflower oil:corn oil blends (60:40 w/w) were heated in Oxipres™ cells over a range of temperatures from 100 to 180 °C under different gases and pressures. Effects of sample size, temperature, pressure, pressurizing gas, heating time, mixing, and oil characteristics were determined. Conjugated dienes, peroxide values, aldehydes, and free fatty acids were measured to relate oxygen consumption curves to other chemical changes during lipid oxidation.

At 150 °C and above, oxygen consumption exhibited no induction periods and did not follow Arrhenius kinetics. Curves showed an initial pressure increase associated with oil heating, followed by a period of rapid decline, then a slowing in pressure decrease with continued heating. Limitations of oxygen diffusion may contribute to but do not fully explain this decreasing reactivity.

Oxygen consumption rates and net uptake increased with headspace oxygen concentration (2, 5, 20, and 100%) and pressure (0.5 to 5 bars). The system accurately differentiated oxidation sensitivity of oils with different degrees of unsaturation with high reproducibility (average variation 2.27%). Oxygen consumption correlated with aldehyde oxidation products, particularly under high oxygen, but not conjugated dienes or hydroperoxides. Patterns of volatile products collected by short path thermal

desorption tubes connected to Oxipres cells showed a homologous series of C2-C12 alkanes, alkenes, fatty acids, and aldehydes. These products are more consistent with thermal scission reactions than lipid autoxidation initiated by pre-formed hydroperoxides.

Overall, the Oxipres system provides very stable, sensitive control of pressure and temperature, but three modifications would improve its design. At frying temperatures, headspace pressure reflects oxygen consumption balanced against release of volatile products and oxygen produced in reactions. Replacing the current pressure transducer with an oxygen-specific sensor would eliminate complications from volatile products. The closed system with slow eddy currents in the oil is a useful research tool but does not accurately model real-life frying. Addition of a stirring mechanism would facilitate oxygen diffusion. Finally, a thermocouple to monitor the actual oil temperature and rates of heating would be very useful.

ACKNOWLEDGEMENTS

I would like to thank the following people, whose contributions were critical for completion of this thesis:

Dr. Karen M. Schaich, my thesis advisor, for her support through the years. Her kindness, generosity and patient tutoring helped me achieve this long sought-after pursuit of higher education. I am grateful for the privilege of having known and worked with her.

Dr. Thomas Hartman and Dr. Chi-Tang Ho for serving on my thesis committee. Their comments and suggestions are gretly appreciated.

Dr. Thomas Hartman for providing GC-MS instrumentation and laboratory facilities and assisting me with analyses to complete my experiments.

Mr. Yakov Uchitel for his technical assistance with computers.

Lili You, my wife, and my parents for their continual support from the first moment that I decided to pursue higher education in the U.S. I couldn't achieve all this without their support and understanding.

TABLE OF CONTENTS

LIST OF TABLES

LISTS OF FIGURES

2. BACKGROUND

2.1. Oil Oxidation

For decades lipid oxidation has been notorious as the main chemical reaction responsible for shortening the shelf life of food. The process requires initiators, but once started is self-propagating and very difficult to stop. Lipid oxidation not only produces off-flavors by generating aldehydes, alcohols and other oxidized products, but many of these products are toxic to some extent (Claxson 1994; Eldin 1997; Moreno 1999) and almost all lipid oxidation products react with other food molecules to alter the texture and other qualities of foods in both positive and negative ways.

For the past twenty to thirty years, the food industry has considered that everything about lipid oxidation and how to prevent it in foods was known. Following standard understanding, the common stabilization practice used in industry has been to formulate with saturated or mono-unsaturated fats and add synthetic anti-oxidants. However, with the new emphasis on the health, there is great pressure on industry to replace saturated fats with poly-essential unsaturated fatty acids (PUFAs) and to use natural anti-oxidants instead of synthetics. High PUFA oils oxidize much more readily, and former standard approaches are inadequate for stabilizing them. It's clear that a new understanding of lipid oxidation in a wide range of systems is needed.

According to the classical theory of lipid oxidation, the process is divided into three distinctive stages -- initiation, propagation and termination (Figure 1). These have been reviewed in detail by Schaich (Schaich 2005). Lipid autoxidation is a free radical

CLASSICAL FREE RADICAL CHAIN REACTION OF LIPID OXIDATION

Initiation ***(formation of ab initio lipid free radical)***

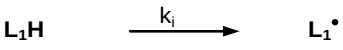

Propagation

Free radical chain reaction established

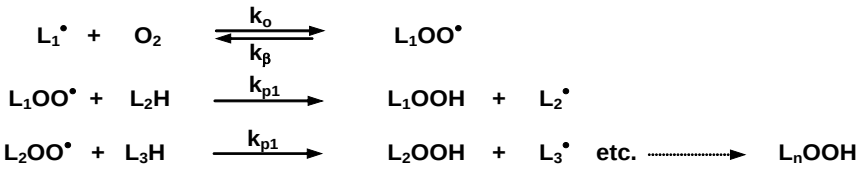

Free radical chain branching (initiation of new chains)

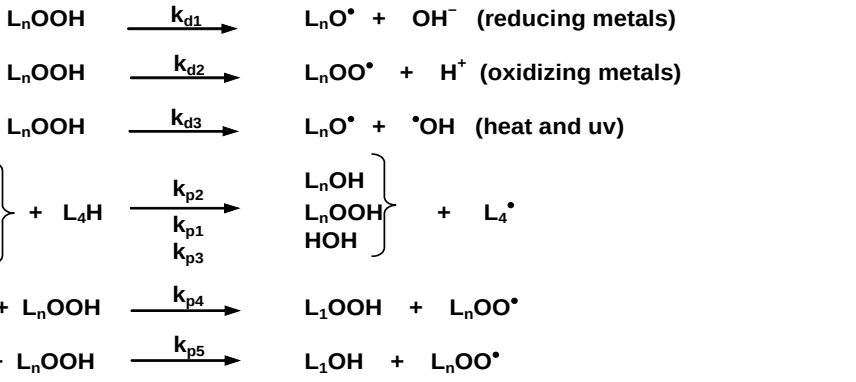

Termination ***(formation of non-radical products)***

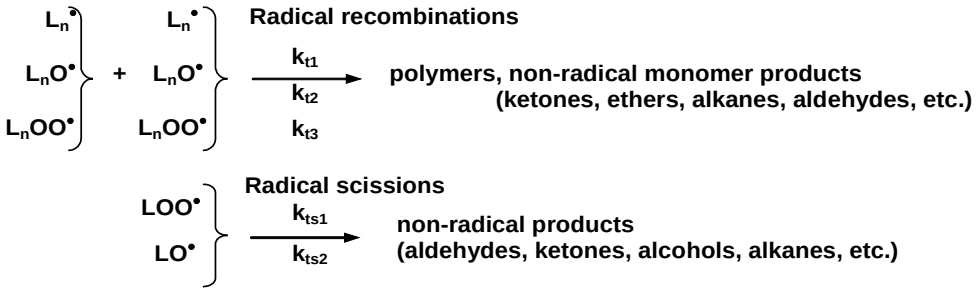

i - initiation; o-oxygenation; β- O_2 scission; p-propagation; d-dissociation; t-termination; ts–termination/scission

Figure 1. Sequence of free radical reactions in lipid oxidation described by classical theory (Schaich 2005)

chain reaction that is not thermodynamically spontaneous, but requires initiators such as metals, light, other free radicals, photosensitizers, heat, radiation, etc. In the propagation stage, a free radical produced during initiation first reacts with oxygen to form a peroxyl radical, which then abstracts a hydrogen atom from a nearby lipid molecule to produce a hydroperoxide and a new acyl radical. This radical repeats peroxyl radical formation and hydrogen abstraction to generate still another new free radical and continue the chain. This cycle continues indefinitely, potentially producing very high levels of hydroperoxides. However, hydroperoxides themselves are decomposed by ultraviolet light, heat, and metals to produce alkoxyl radicals, which are even more reactive than peroxyl radicals. They, too, abstract radicals to initiate new chains and broaden the oxidation; this process is called branching. In the last stage -- termination -- radicals recombine with themselves to form a wide range of non-radical monomer, dimers, and polymer products, and alkoxyl radicals undergo scission to generate aldehydes, alkanes, and other oxidation fragments. The full process has been shown to be much more complex than normally depicted, with multiple alternate reaction pathways competing with hydrogen abstraction for each major intermediate (Schaich, 2005; Figure 2). However, for the purpose of the current study, the simple classical sequence is sufficient.

The following discussion presents additional details of the reactions in each of the three stages of lipid oxidation.

2.1.1. Initiation

Based on quantum mechanics, oxygen in the air is in a triplet state and thus cannot react with singlet state carbon-carbon double bonds, so direct addition of oxygen to double bonds cannot occur(Schaich 2005). Nevertheless, common observation shows lipid oxidation to be extremely easy to set off, so obviously, something is connecting oxygen and lipid molecules to make the reaction much easier than it should be thermodynamically. This connection is a variety of initiators which are able to react directly with the double bond to form a species capable of initiating oxidation free radical chains. As mentioned previously, metals, light, heat, preformed radicals or hydroperoxides, and photosensitizer are all common initiators that trigger the whole process on set. The discussion below shows briefly how each of these catalysts work.

2.1.1.1. Metals

Transition metals are well-known catalysts of lipid oxidation and probably the most active initiators in foods. The catalytic mechanism of metals can be divided into two major categories: direct initiation through higher valence metals and indirect initiation and propagation or chain branching (Schaich 1992).

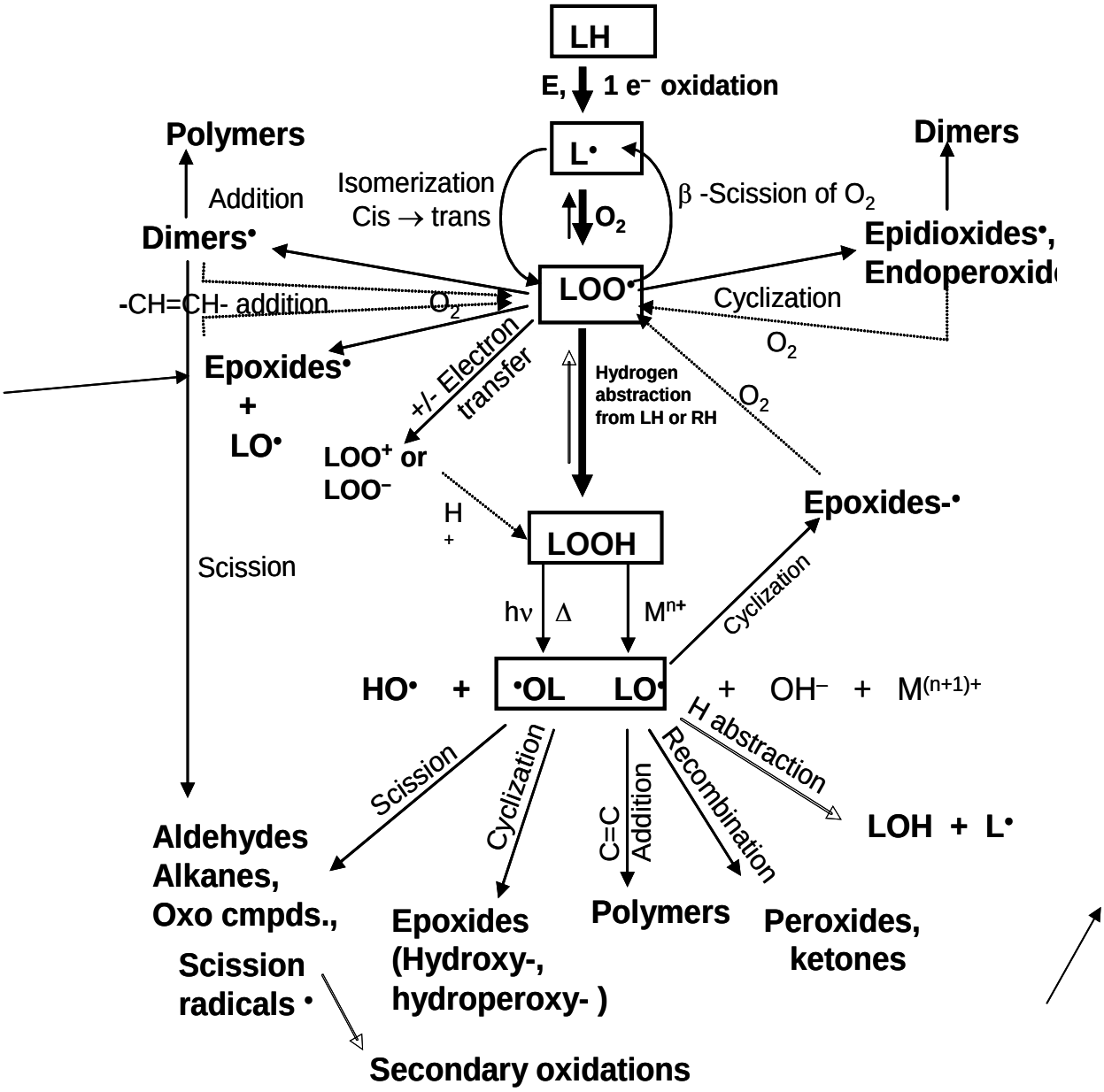

Figure 2. Integrated theory of lipid oxidation showing alternate reactions that compete with hydrogen abstraction (Schaich 2005).

Direct initiation through higher valence metals.

Electron transfer from high valence metal to lipid molecules generates radicals that then initiate radical abstraction chains. Electron transfer to –CH=CH– oxidizes one bond from the double bond (Schaich 2005), forming a free radical on one carbon atom and reducing the metal ion to its lower valence state. The carbon-centered free radical adds oxygen and then is able to attack any lipid molecules nearby and start the chain reaction:

$$RCH{=}CHR + M^{(n+1)+} \longrightarrow RCH{-}\overset{\bullet}{C}H{-}\overset{+}{C}HR + M^{n+} \left[\xrightarrow{LH} L^{\bullet} + RH\right] \quad (1)$$

Carbon-centered radicals are similarly formed when the electron is transferred to carbon-hydrogen bonds; the radical thus generated also adds oxygen and abstracts another hydrogen from adjacent lipids and start the chain reaction:

$$RH + M^{(n+1)+} \longrightarrow R^{\bullet} + H^{+} + M^{n+} \xrightarrow{LH} L^{\bullet} + \left[RH\right] \quad (2)$$

Higher valence ions can also affect the lipid oxidation during propagation by causing chain branching. This reaction will be discussed under Propagation.

Initiation through lower valence metals. Lower valence metals such as Fe^{2+} reduce oxygen to form superoxide ($O_2^{-\bullet}$) and hydroxyl ($^{\bullet}OH$) radicals that can react directly with lipid molecules (Reactions 3 and 4).

$$Fe^{2+} + O_2 \longrightarrow Fe^{3+} + O_2^{-\bullet} \xleftrightarrow{H^{+}} HOO^{\bullet} \xrightarrow{LH} L^{\bullet} + H_2O_2 \quad (3)$$

$$Fe^{2+} + H_2O_2 \longrightarrow Fe^{3+} + HO^{-} + {}^{\bullet}OH \xrightarrow{LH} L^{\bullet} + H_2O \quad (4)$$

Fe^{2+} can also reduce preformed hydroperoxides from lipids or other molecules. For example, as shown in Reaction 5, Fe^{2+} reduces LOOH into alkoxyl radicals that can

propagate the chain reaction; at the same time, Fe^{2+} is oxidized to Fe^{3+}, which is also a strong catalyst for lipid oxidation (Reaction 1). Fe^{3+} also oxidizes hydroperoxides to peroxyl radicals (Reaction 6). Thus, when both ferrous and ferric iron are present, the catalytic effect is very much enhanced redox cycles continuously generate radicals and recycle reactive iron forms..

$$M^{n+} + LOOH \longrightarrow M^{n+1} + LO^{\bullet} + HO^{-} \longrightarrow LOH + L_2^{\bullet} \quad (5)$$

$$M^{(n+1)+} + LOOH \longrightarrow M^{n+} + LOO^{\bullet} + H^{+} \xrightarrow{L_2H} LOOH + L_2^{\bullet} \quad (6)$$

2.1.1.2. Light

Light radiation impinges energy on bonds of lipid molecules to directly initiate the chain reaction (Schaich 2005). However, initiation by this mechanism is considerably less efficient than by metals or other methods. Bond scission to generate carbon-centered radicals from carbon-carbon bonds (double or single) or from carbon-hydrogen bonds, which are dominant chemical bonds one would expect in fresh oil, requires tremendous energy. Only light in the lower wavelength range of UV light, which is not very abundant in in-door lighting, has sufficient energy (Table 1), and even when radicals do form, there is usually not enough energy to push them apart, so they recombine and seldom start chain reactions (Schaich 2005).

Ultraviolet light is most active in scission of hydroperoxides where the O-O bond energy is only 157 KJ/mol. This means that if the oils or lipids are oxidized before use and even tiny amount hydroperoxides form, exposure of samples to light will

decompose any hydroperoxides present and initiate lipid oxidation chains:

Table 1. Energy at various light wavelength compared to the bond dissociation energies for typical chemical bonds (Schaich 2005).

	eV[a] (Physicists)	kJ[b] (Chemists)	kCal[b] (Biologists)	Bond Dissociation Energy ΔE		
				Bond	kJ/mol[c]	kCal/mol[d]
200	6.2	596	143	C=C	612	146
230	5.4	518	124	O–H	463	111
260	4.8	458	110	C–H	412	99
290	4.3	411	98	C–O	360	86
320	3.9	372	89	C–C	348	83
350	3.5	341	82	C–N	305	73
380	3.3	314	75	O–O	157	35
410	3.0	291	70			
440	2.8	271	65			
470	2.6	254	61			
510	2.4	234	56			
540	2.3	221	53			
570	2.2	209	50			
600	2.1	199	48			
630	2.0	189	45			
660	1.9	181	43			
700	1.8	170	41			

$$ROOH \xrightarrow{uv} RO^{\bullet} + {}^{\bullet}OH \xrightarrow{LH} ROH + L^{\bullet} \quad (7)$$

$$HOOH \xrightarrow{uv} HO^{\bullet} + {}^{\bullet}OH \xrightarrow{LH} H_2O + L^{\bullet} \quad (8)$$

$$LOOH \xrightarrow{uv} LO^{\bullet} + {}^{\bullet}OH \xrightarrow{LH} LOH + L_2^{\bullet} \quad (9)$$

Visible light does not have enough energy to break bonds, but in the presence of photosensitizers that harvest and transform light energy to usable chemical energy, it can still initiate lipid oxidation. As shown below, there are two types of photosensitizations: free radical (Type 1) and singlet oxygen (Type 2) (Schaich 2005). In Type 1 photosensitization, low energy light is collected by the sensitive molecules, transformed to excited state chemical energy, and transferred directly to lipid molecules

to form free radicals. Except in kinetics, this is indistinguishable from normal autoxidation. In contrast, in Type 2 reactions, the photosensitizer transfers the excitation energy to oxygen, forming singlet oxygen which can now add directly to double bonds (also in singlet state) to form hydroperoxides with no radicals involved:

Unlike autoxidation, singlet oxygen photosensitization has no induction period, is independent of oxygen but dependent on concentration and type of photosensitizer(s), and forms internal non-conjugated hydroperoxides as readily as external conjugated products because the oxygen addition across bonds is non-selective for double bond position in the acyl chain and hydroperoxide formation is non-selective for carbon position in the double bond (Reaction 10).

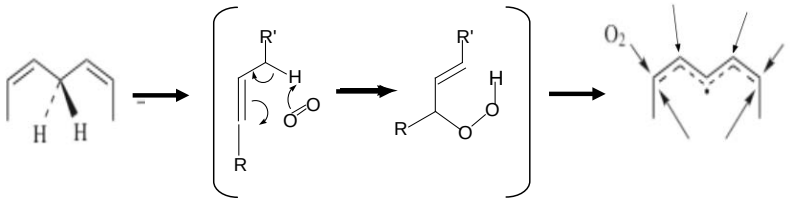

(10)

2.1.1.3. Heat

Of the various reactions in the sequence of lipid oxidation, all have very low activation energy except decomposition of the hydroperoxides. Thus, at moderately elevated temperatures, the major effect of heat is to provide the energy to drive decomposition of lipid hydroperoxides (Lundberg and Chipault 1947; Labuza 1971). The alkoxyl radicals produced in the decomposition then abstract hydrogens to start new chains, now at a much faster rate than early peroxyl radicals. The net effect is to double the rate of oxidation for every 20 °C rise in temperature(Labuza 1971).

At high temperatures such as are used in frying, thermal energy provides enough energy

to break chemical bonds. According to extensive research by Nawar (Nawar 1985),

Table 2. Activation energy of different radicals (Labuza 1971).

Reaction	Activation energy (E_a)
k_o ($L^\bullet + O_2$)	0 kcal/mole
k_p ($LOO^\bullet$ + LH)	~5-15
k_t (2 $ROO^\bullet$)	~4
k_t (2 $R^\bullet$)	5
k_t ($R^\bullet + ROO^\bullet$)	1
k_d (monomolecular) (LOOH →)	31
k_d (bimolecular) (2 LOOH →)	50 uncatalyzed system

C-C bonds alpha, beta and gamma to the carboxylic group in saturated fatty acids and to double bonds for unsaturated fatty acids will preferentially undergo scission reactions generating $C^\bullet$ free radicals at an extremely rapid rate. A general summary of expected thermal scission products in oils during high temperature frying are shown in Figure 3. More details of thermal degradation reactions will be presented in Section 1.2.

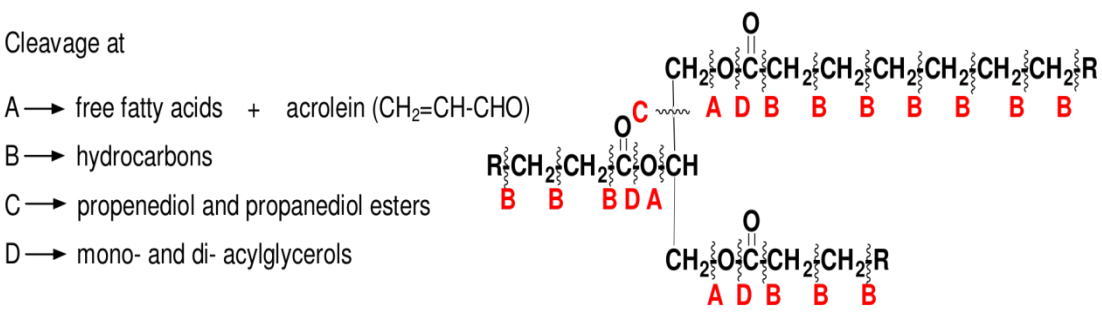

Figure 3. Thermal scission patterns observed in heated triacylglycerols (Nawar 1985).

2.1.2. Propagation

In the propagation stage, two major intermediate products, peroxyl radicals ($LOO^{\bullet}$) and alkoxyl radicals ($LO^{\bullet}$), transfer radicals to new lipid molecules, keeping the chain reaction going (Schaich 2005). Each radical dominates at different stages. Peroxyl radicals form at the very beginning of the chain reaction, and their relatively slow, specific reactions dictate kinetics and pathways during early stages of oxidation. Alkoxyl radicals are generated from decomposition of hydroperoxides, the product of $LOO^{\bullet}$ hydrogen abstraction reactions, so they become important later in the chain reaction after peroxyl radicals and hydroperoxides have accumulated. Since $LO^{\bullet}$ reaction rates are several orders of magnitude higher than $LOO^{\bullet}$, these radicals are responsible for the rapid rate period commonly observed in lipid oxidation. As will be outlined below, both radicals undergo rearrangement/cyclization, addition, and scission reactions in addition to hydrogen abstraction to keep the chain reaction going. Both propagators are of importance when studying lipid oxidation.

2.1.2.1. Propagation by peroxyl radicals

The classical reaction by which peroxyl radicals propagate the radical chain is by H-abstraction as shown in reaction 11 and 12.

$$L_1OO^{\bullet} + L_2H \longrightarrow L_1OOH + L_2^{\bullet} \quad (11)$$

$$L_1OO^{\bullet} + L_3OOH \longrightarrow L_1OOH + L_3OO^{\bullet} \quad (12)$$

Peroxyl radicals simply abstract hydrogen atoms from neighboring H sources, in this

case lipids, to form a hydroperoxide and another carbon centered radical which will then react with oxygen to give a new peroxyl radical and start another oxidation cycle. Theoretically, as long as there is no intervention and susceptible targets are available, this process can repeat itself indefinitely. H abstraction can also occur from hydroperoxides, which results in an overall slow-down of the oxidation.

It is important to note, however, that other reactions compete with and supplement H abstraction for propagating the chain, and these alternate reactions change both the kinetics and product mix of lipid oxidation. Peroxyl radicals undergo internal rearrangement, reacting with a double bond within the same lipid molecule to form epidioxides (internal cyclic peroxides). The prerequisite for this reaction is a cis-double bond at the beta-position relative to $LOO^{\bullet}$, and the reaction proceeds by a 1,3-addition (Reaction 13). For fatty acid with four double bonds, e.g. EPA and DHA, 1.4-addition of the peroxyl radical to the gamma double bond forms a 6-oxo ring (Reaction 14) (Schaich 2005).

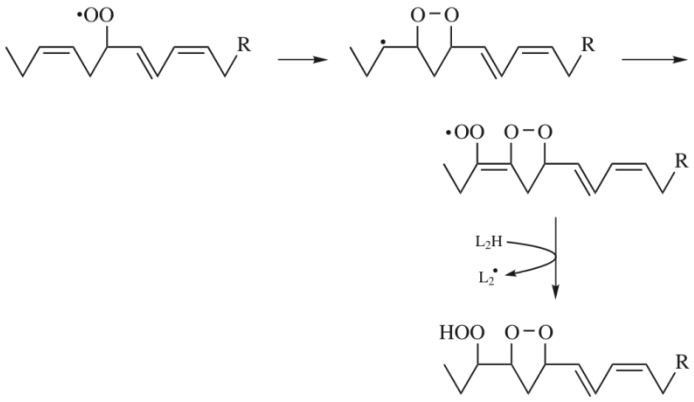

(13)

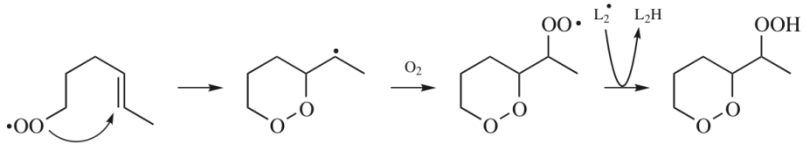

(14)

A third alternate reaction occurs when allylic hydrogens are not readily available. $LOO^{\bullet}$ then preferentially adds to conjugated or terminal double bonds to form a dimer and an acyl radical as shown in Reaction 15 (Schaich 2005). The LOO- then undergoes beta scission to release epoxy alkyl and alkoxyl radicals that continue to propagate the chain reaction (Reaction 16).

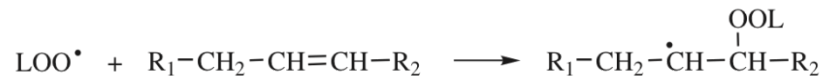

(15)

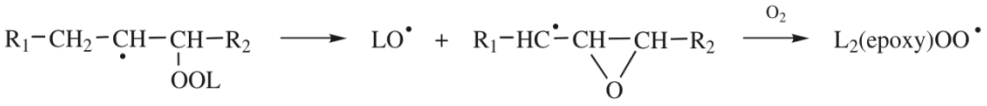

(16)

Other pathways that carry the radical chain include recombination of $LOO^{\bullet}$ and $LOO^{\bullet}$ and beta scission of $LOO^{\bullet}$, which will release oxygen and more reactive alkoxyl radicals. Reactions of these radicals will be discussed in the following section.

2.1.2.2. Propagation by alkoxyl radicals

After a period time of accumulation, hydroperoxides decompose to $LO^{\bullet}$ and $^{\bullet}OH$ or OH^{-} by metals, lights and heats or other mechanisms. $LO^{\bullet}$ then becomes the main radical chain carrier. $LO^{\bullet}$ reactions are much faster that $LOO^{\bullet}$, but the pathway alternatives are quite similar: 1, H abstraction, 2 Rearrangement, 3, Addition and 4, alpha and beta scission.

When hydrogen sources are abundant and immediately available to alkoxyl radicals (e.g. high lipid concentrations or lipid alignment as in membranes), H abstraction leads the chain reaction (Reaction 17).

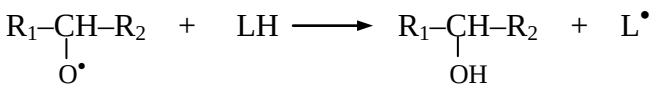

(17)

$LO^{\bullet}$ abstracts both allylic (next to a double bond) and bis-allylic (between two double bonds) hydrogens on lipid molecules, while $LOO^{\bullet}$ can only be effective on the latter ones (Schaich 2005). Therefore, the degree of unsaturation of the component free fatty acid is crucial to the rate of abstraction.

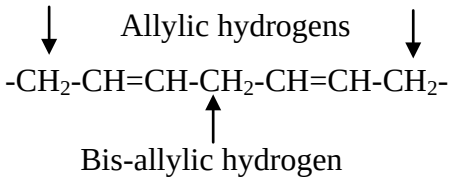

As with peroxyl radicals, when H accessibility becomes more limited (e.g. low lipid concentrations) or double bond targets become more accessible (chains aligned on surfaces), other reaction pathways compete to propagate the chain reaction. Generally speaking, when lipid concentration or oxygen pressure are low, or the system is at room temperature, or lipid molecules are in high polarity solvents or aligned in monolayers, the dominant reaction shifts to internal rearrangement or cyclization in which $LO^{\bullet}$ add to a beta double bond in 1,2 cyclization, forming epoxides and epoxyalkyl radicals which then add oxygen and propagate the chain (Reaction 18):

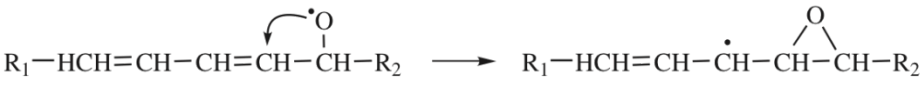

(18)

Addition of $LO^{\bullet}$ to double bonds on other lipid molecules is another alternative

pathway, but very difficult to happen since alkoxyl radicals have such a strong preference for allylic hydrogens (Reaction 19, Table 3). However, when allylic hydrogens are limited in quantity or accessibility, addition reactions become more favorable. $LO^{\bullet}$ then adds to a cis double bond, forming a dimer adduct with a free radical that adds oxygen and propagates the radical chain.

(19)

Table 3. Effect of alkene structure on preference for addition vs. abstraction by t-BuO• radicals at 40°C (Kochi 1973).

Alkene	Abstraction (%)	Addition (%)
R-CH=CH-R (trans)	95	3-4
R-CH=CH-R (cis)	83	17
R-CH=CH_2	97	3
R_2-CH=CH_2	83	17

Beta scission is the fourth alternative pathway for radical transfer. C-C bonds on either side of the alkoxyl radical are cleaved, producing two radicals that transform to aldehydes and new propagating peroxyl radicals (Reaction 20). This reaction is particularly responsible for generation of off-flavors and odors when oils or fat-containing foods become rancid.

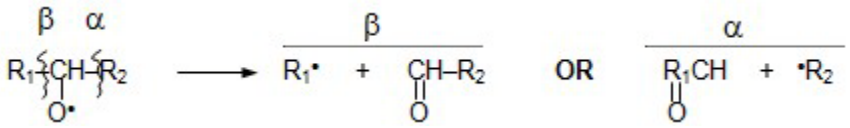

(20)

Beta scission is favored by polar solvents that support formation of polar transition states that facilitate transformation of non-polar alkoxyl radicals to polar aldehyde products (Reaction 21).

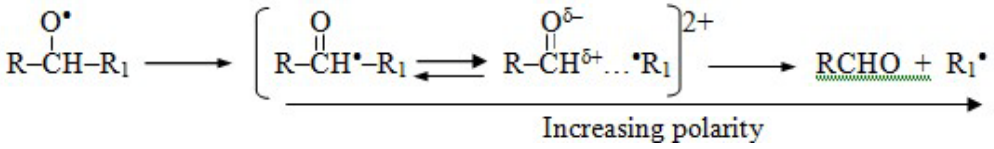

(21)

Table 4 shows how solvent polarity increases relative rates of beta scission reactions over H abstraction. Heat also promotes scission reactions since thermal energy offered by heat helps the reaction to overcome the high Ea of disrupting bonds (Schaich 2005)

Table 4. Solvent effect on the rate of H abstraction and the rate of beta scission (Schaich 2005).

	H Abstraction	β-Scission	
	$k_a \times 10^{-6}$ $M^{-1}s^{-1}$	$k\beta \times 10^{-5}$ s^{-1}	$k_a/k\beta$ M^{-1}
CCl_4	1.1	2.6	4.5
C_6H_6	1.2	3.7	3.2
C_6H_5Cl	1.1	5.5	2.0
$(CH_3)_3COH$	1.3	5.8	2.3
CH_3CN	1.2	6.3	1.9
CH_3COOH	1.3	19	0.7

2.1.3. Termination

Lipid oxidation is a problem from the moment of harvest of plants or slaughter of animals, where lipids are protected by their natural environments, through food processing, to packaging and storage of finished food products. Theoretically, as long as oxygen is available, the chain reaction will proceed indefinitely. In an open system where oxygen from air is limitless, plus light energy and other possible catalysts, the reaction will not stop until the lipids or oils are completely decomposed. From a practical standpoint, however, this never occurs for two major reasons. First, in most processed foods, vacuum or nitrogen-flushed headspaces limit the amount of available oxygen, freezers and refrigerators keep thermodynamic energy low, and packaging limits light, so oxidation can be tremendously slowed. In addition, as products accumulate, self-reactions turn the chain off in the third stage: termination.

Termination is usually cited and shown as a series of radical recombinations. Peroxyl radicals recombine in multiple processes that involve both non-radical and radical termination (Figure 4). When non-radical termination happens, alcohols, ketones, dimers, and peroxides are formed. Radical propagation is more complex since resulting alkoxyl and peroxyl radicals recycle to propagate the chain. Interestingly, when $LOO^{\bullet}$ recombination occurs by either mechanism, oxygen is released back to the headspace and becomes available to fuel additional oxidations. Oxygen release in termination reactions complicates measurement of lipid oxidation kinetics by oxygen consumption. This is also one of the major difficulties in our project when using

Oxypres^{TM} oxygen bomb instrumentation to measure the net oxygen consumption.

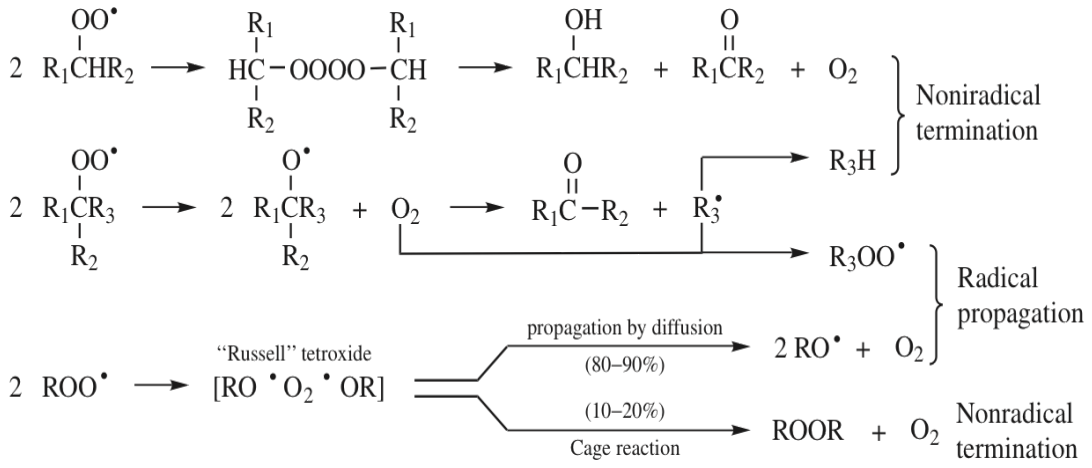

Figure 4. Propagating radicals and non-radical products formed from recombination of peroxyl radicals during lipid oxidation(Schaich 2005)

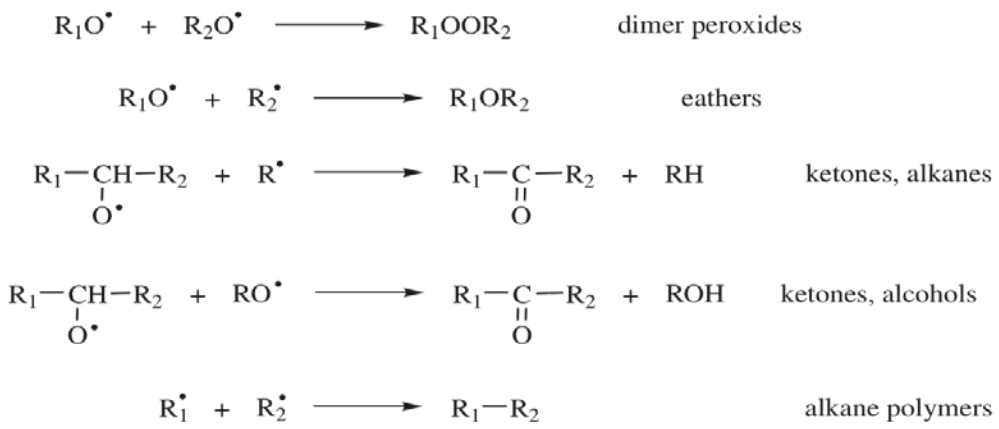

Figure 5. Products formed via recombination of various intermediate radicals in lipid oxidation(Schaich 2005).

2.2. Thermal degradation of lipids

Thermal degradation of lipids at high temperatures (e.g. frying) is an enormously complex process complicated by the presence of two modes of degradation (thermal scission and autoxidation), Arrhenius effects of heat on reaction kinetics, and the presence of water (introduced with foods) that facilitates hydrolysis. Although frying chemistry of oils has been studied extensively (Kamal-Eldin 1997; Shen, Fehr et al. 1997; Saguy 2003; Coni 2004; Frankhauser-Noti 2006), the detailed mechanisms of thermal degradation remain poorly understood and highly controversial, with several schools of thinking.

The global reaction scheme in Figure 6 shows the current general thinking about what happens during frying(Schaich 2008). Because foods always introduce water into oils, hydrolysis to free fatty acids has long been considered the first degradation at high temperatures.

Free fatty acids are quite reactive and go on several possible ends.

1) They oxidize to a variety of small products, including aldehydes, methyl ketones, and lactones that are characteristic flavor and aroma compounds((Kamal-Eldin 1997).

2) They polymerize to dimers, trimers, and higher polymers, with and without oxygen bridges that increase viscosity of oils (Nawar 1985).

3) They react with any soft metals present to form soaps that contribute to foaming and formation of off-flavors.

This scheme has been developed largely from observations in commercial frying

or in research settings that model commercial frying, where heating under abusive conditions is common. However, it is clear that much remains to be learned about reactions connecting the various intermediates and end products and how the reactions involved differ from autoxidation.

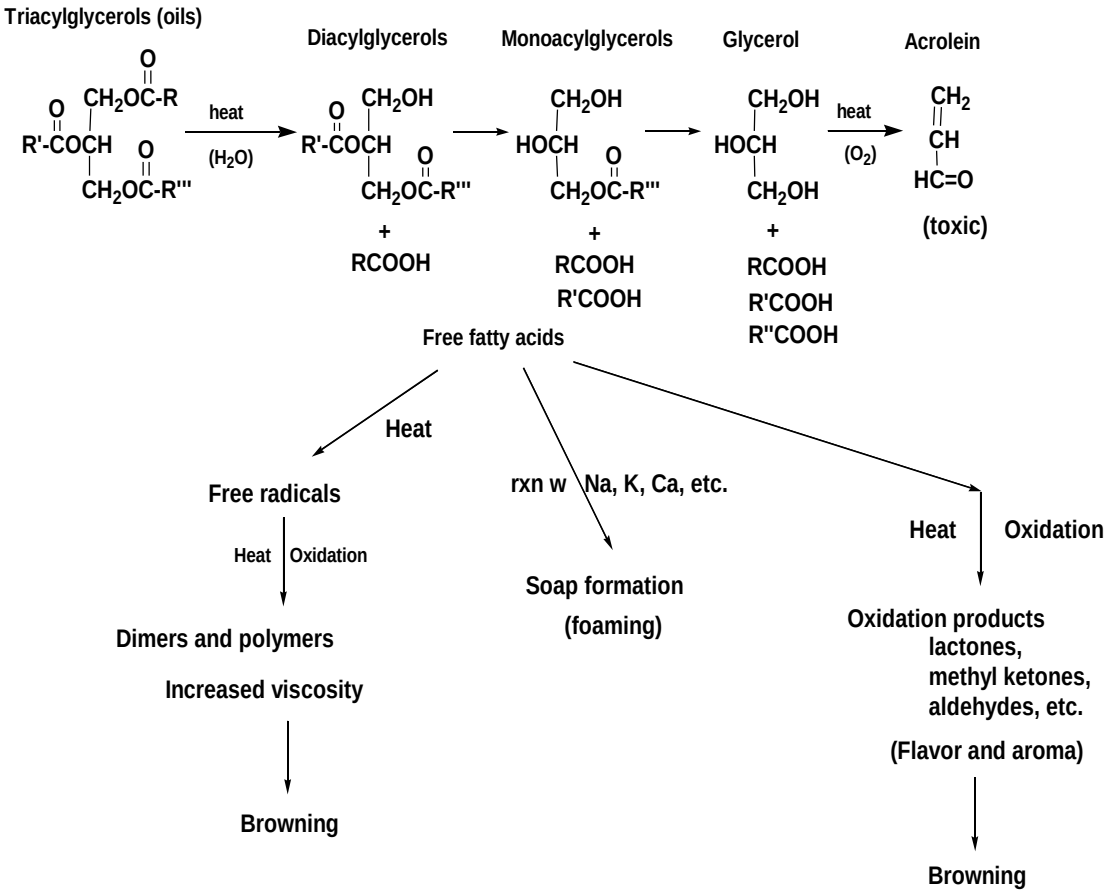

Figure 6. Generalized scheme for oil degradation during frying (Schaich 2008).

2.2.1. Degradation reactions of lipids at high temperatures

There is a large volume of data in the literature describing oil performance during heating under a wide range of conditions and fry times. Review of this body of literature is beyond the scope of this thesis, except to note that most studies have been oriented towards use performance; very few studies have investigated degradation mechanisms and kinetics in general, let alone in detail. This is not surprising considering the rapid kinetics and complex product mixtures of thermal oxidation.

At room temperature, lipid oxidation requires an initiator such as metals, radiation, or light to form the *ab initio* radical that starts the radical chain. Initiators are required at high temperatures as well, and two are available:

a) Thermal energy preferentially cleaves C-C bonds alpha, beta and gamma to the carboxylic acid group in saturated fatty acid and double bonds for unsaturated fatty acids (Nawar 1985), although products from radical scissions all along the chain have been observed (Yu 1997). A simplified schematic flow showing the possible thermal scission products during high temperature frying was presented in Figure 3 (heat as initiator section). Theoretically, thermal energy is able to cleavage any of the C-C bonds in the acyl chain, and our GC-MS data of volatiles confirms this, as will be discussed in more detail later. The radicals so formed generate a wide range of non-characteristic scission and radical recombination products under inert atmospheres; in air, thermal scission fragments add oxygen to form terminal peroxyl radicals that initiate chains of autoxidation.

b) Preformed hydroperoxides in oils are decomposed to $LO^{\bullet}$ + $^{\bullet}OH$ (lipid alkoxyl and hydroxyl) radicals that then drive the degradation strictly by hydrogen abstraction as in normal autoxidation chains (Frankel 1987; Muik 2005). In autoxidation, chain cleavage also occurs, but only as a secondary reaction and the product mix is selective for specific positions on the acyl chain (Frankel 1987; Choe 2006). Therefore, in autoxidation, the secondary products are predictable according known hydroperoxide formation and alkoxyl radical scission points. For example, with oxidation of oleic acid, 9-oxo-nonanoic acid and 2-decenal are expected as final products. These may or may not be formed by thermal pathways.

Whatever the mechanisms and reaction pathways, the kinetics of degradation increase dramatically with temperature. At room temperature, initiation by trace concentrations of metals, etc. and propagation by hydrogen abstraction are relatively slow, so oxidation has a very long induction period and it usually takes days to weeks for fast oxidation to develop. In thermal degradation, the first free radicals are generated by thermal scission reactions, probably many occurring at the same time. Each scission forms two free radicals that can add oxygen to form peroxyl radicals, or perhaps add $-O^{\bullet}$ to form aldehydes or epoxides directly. Thus, high radical concentrations may be reached rapidly and maintained as long as heat is applied, as reflected in loss of induction periods and much faster oxygen consumption as well as faster formation and accumulation of all products.

There are several practical consequences of this rapid radical generation. First are

challenges in determining what products to analyze and how to detect products with short lifetimes. High temperatures alter kinetics, reaction mechanisms, and products, in particular shifting distributions and forming some products not present at lower temperatures(Nawar 1985). It is well known that autoxidation is marked with high yields of hydroperoxide which are very unstable and decompose readily; with the addition of heats, the breakdown proceeds even faster. Kamal-Eldin (Kamal-Eldin 1997) and coworkers found unusually high levels of methyl 8-oxooctanoate, 9-oxononanoate, 10 oxo-8-decenoate, 11-oxo-9-undecenoate, 12-dodecenoate formed from hydroperoxide decomposition in used hydrogenated rapeseed/palm oil mixture, conventional sunflower oil and high oleic sunflower oil. They also found small fragments, supporting thermal scission at multiple sites on the acyl backbone.

During early stages of oxidation under heating conditions, carbonyl groups begin forming as soon as 150 °C is reached (Moreno 1999) and they increase linearly with heating time at 170 °C (Farhoosh 2008). Since, as mentioned above (Nawar's data), thermal scission occurs randomly at all positions of acyl chains, aldehydes of a greater variety than in autoxidation, particularly short chain aldehydes, have been reported (Gillat 2001). Pentane, acrolein, pentanal, hexanal, heptenal and octenal are commonly reported, heptanes, octane, 2- decenal and 2-undecenal are reported as unique frying products (Warner 2008)

High levels of epoxides are also typical in frying oils. Methyl trans-9,10-epoxystearate and methyl cis-9,10-epoxystearate were observed in methyl

oleate while methyl trans-9,10-epoxyoleate, methyl cis-9,10-epoxyoleate, trans-12,13-epoxyoleate and cis-12,13-epoxyoleate were also detected from methyl linoleate (Frankhauser-Noti 2006; Marmeasat 2008). Under heating conditions, the amount of epoxide formation was proportional to the heating time (Frankhauser-Noti 2006) .

Dimers and polymers also form during heating (Byrdwell 1999; Marmeasat 2008) because the radical load can be extremely high and the radicals are too short lived to migrate so they connect with whatever is nearby. Radical recombinations are also facilitated by current industrial practice of carefully limiting oxygen by flushing oils with nitrogen and providing water vapor blankets over fryers. Dimers and polymers form from linear radical recombinations between molecules, but radical reactions within molecules lead also to cyclic and bicylic products (Dobson 1997) in much higher levels than present during autoxidation at lower temperatures.

Another consequence of high radical loads is rapid consumption and thus decreased efficiency of antioxidants added to frying oils. Although diminished antioxidant effectiveness has most often been attributed to decomposition of antioxidants at high temperatures (Pellegrini 2001; Pokorny 2003), the very high thermal radical load from scission and hydroperoxide decomposition also contributes to "using up" antioxidant capacity rapidly (Reblova 2006). Differing balances between these two factors probably account for the large number of conflicting research reports.

For example, Reblova (Reblova 2006) found that the antioxidative activity of

gamma tocopherol decreased as temperature increased from 80°C to 150°C, alpha tocopherol activity remained constant from the temperature range of 80°C to 110°C, and both tocopherols were totally ineffective at 150°C. Similar results were reported by Tomaino (Tomaino 2005). De Maria (Maria 2000) found that while quercetin and 5-caffeoylquinic acid (5-CQA) were not effective in stabilizing soybean oil under heating conditions, quercetin decreased oxidation significantly, and 5-CQA also protected the oil but less effectively. With the addition of ferric palmitate, quercetin showed a decrease in antioxidation activity while 5-CQA didn't, demonstrating that a major effect of quercetin was through metal binding rather than or in addition to radical scavenging. Antioxidant volatility is another issue, which may explain why natural antioxidants are more effective than synthetics at elevated temperatures (Gertz 2000)

In summary, the high energy available from heat makes thermal degradation of oils and fats very different from autoxidation in initiation mechanism, the ways to propagate free radicals, final products, and kinetics (Shahina Naz 2005). Thus, studying thermal degradation requires different approaches than autoxidation at lower temperatures, especially when it comes to the analysis of degradation products. Because of the multiple pathways, altered product distributions, and high concentration of volatile products which do not remain in the oil (Nawar 1985), using any single product assay will very likely yield a totally inaccurate result. In addition, the rapid kinetics make it extremely difficult to monitor degradation by sampling. Traditional methods of frying research typically use long heating times (days to even weeks) in

open fryers with little or no control over headspace, while monitoring hydroperoxides, total polars, and free fatty acids. Under these conditions, sorting out reaction pathways and early versus late products is virtually impossible. Clearly new research approaches are needed to more clearly elucidate the sequence and hierarchy of reactions in thermal degradation of oils.

There currently is considerable controversy over the existence of thermal scissions and the relative roles of thermal scission vs decomposition of preformed hydroperoxides as the major initiators of lipid degradation at frying temperatures. While this difference may seem to be of academic interest only, it becomes critically important in light of current interest in replacing saturated and mono-unsaturated oils with more healthy polyunsaturated (PUFA) oils for frying. PUFAs are already highly sensitive to oxidation, and their degradation at high temperatures is rapid. Thus, it is very important for the food industry to learn more details of the reactions and mechanisms involved in thermal degradation of oils so improved stabilization mechanisms can be developed.

2.3. Methods for detecting and following kinetics of lipid degradation

2.3.1. Traditional chemical assays

Based on knowledge of lipid degradation pathways, several classes of key degradation products have traditionally been major targets for monitoring oil degradation, namely, conjugated dienes, peroxide values, and aldehydes for oxidation, and free fatty acids for hydrolysis (thermal, chemical, or enzymatic).

Conjugated dienes. Conjugated dienes (CDs) are the first permanent change in oxidizing lipids so is almost universally used to monitor lipid oxidation at very early stages. Formation of conjugated dienes requires poly-unsaturated fatty acids, and occurs when a hydrogen is abstracted from the methylene group between two double bonds and the electron density becomes delocalized over the 1,4 diene system. This leaves electron "holes" on the exterior carbons of the diene system, e.g. C9 and C13 of linoleic acid. Oxygen adds rapidly to one of these positions (not both), forming a peroxyl radical. At the same time, two electrons from the original double bond migrate one carbon over and reform a double bond in conjugation with the second double bond of the diene system (Reaction 22).

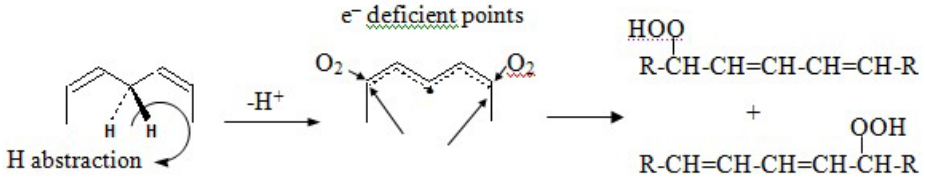

(22)

Fatty acids with more than two double bonds have the potential for forming conjugated

systems in more than one position, e.g.

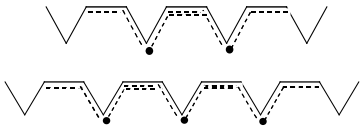

whereas linoleic acid can form only one conjugated system per molecule. Since one CD is formed per H abstraction, the stoichiometry of conjugated diene formation is one CD per molecule for linoleic acid but can be 2:1 or more for higher PUFAs and is zero for mono-unsaturated fatty acids which also oxidize. Thus, although CD's are calculated on a molar basis (moles of conjugated diene per kg oil), the CD value of an oil with mixed fatty acids is difficult to interpret on a mol CD / mol triacylglycerol basis.

Table 3

When interpreting CD, it is also important to recognize that it represents initiation of new chains. Thus, when incubating oils or pulling them from storage for analysis, conjugated dienes will be detected as long as new oxidation chains continue to be formed. Also, even though lipid molecules containing CDs continue to oxidize and degrade into a variety of products, some of the products retain the conjugated diene structure and will be detected at 233 nm. However, as oxidation progresses and scission reactions and radical recombinations become dominant, conjugated dienes are no longer an accurate reflection of the extent of lipid oxidation. Similarly, conjugated dienes may be used to calculate kinetics of oxidation in early stages but not after termination processes become substantial.

Conjugated diene levels in oils are usually determined at 233 (or 234) nm(AOCS

2003) where this unique structure of conjugated double bonds absorbs light. However, this method is not accurate for food matrix systems because conjugated double bonds are present in other molecules and are not specific for lipid oxidation, and it cannot be used with oils that have significant level of carotenoids, which also contain long chains of conjugated dienes (El-Agamey 2008).

Hydroperoxides (LOOH). Lipid hydroperoxides are the second major chemical change and the first isolatable product in lipid oxidation so provide another measure of early stages of reaction. Hydroperoxides form in the first step of propagation when a peroxyl radical abstracts a hydrogen from another molecule:

$$L^{\bullet} + O_2 \longrightarrow LOO^{\bullet} + LH \longrightarrow LOOH + L^{\bullet} \quad (23)$$

Conjugated dienes and peroxides values are both early stage products, formed approximately in parallel, and conjugated dienes usually contain hydroperoxide groups. However, CDs and PVs are not equivalent or interchangeable except under limited conditions in linoleic acid (McClements 2008). Hydroperoxides form wherever there is a double bond but CDs are not formed in saturated and mono-unsaturated fatty acids and, as noted above, they are not formed stoichiometrically in higher polyunsaturated fatty acids. Furthermore, hydroperoxides can decompose to alkoxyl radicals without losing the conjugated dienes. Nevertheless, divergence of the values can provide insights into system chemistry, so the two products are commonly measured together in oxidizing oils.

The standard method for determining Peroxide Values (PV) is an iodometric

titration (AOCS 1986) in which hydroperoxides first oxidize iodide ions to iodine, then the released I_2 is reacted with standardized thiosulfate to determine peroxide equivalents:

$$2\,S_2O_3^{2-} + I_2 \longrightarrow S_4O_6^{2-} + 2I^- \quad (24)$$

$$2I^- + H_2O + ROOH \longrightarrow ROH + 2OH^- + I_2 \quad (25)$$

Starch solution is added as a reaction indicator since starch binds I_2 and forms a blue complex. The peroxide value is defined as the milliequivalents of peroxide oxygen per kilogram fat or oil.

Secondary products. It is well-documented that hydroperoxides are highly unstable and can easily break down to secondary products, particularly aldehydes (Ellis 1966; Ellis 1968; Frankel 1982; Frankel 1987; Esterbauer 1989). Aldehydes therefore are another class of major products measured when studying lipid oxidation (Claxson 1994; Eldin 1997; Moreno 1999; Muik 2005; Schaich 2005; Smith 2007; Guillen 2009), although the techniques are less well defined and more problematic.

Scission of alkoxyl radicals is one of the major reactions that form aldehydes. Table 1 has already shown that the O-O bond in hydroperoxides has very low bond energy (157 kJ/mol), so it readily decomposes to alkoxyl radicals when exposed to heat, UV radiation, or reducing metals. The alkoxyl radicals then undergo either alpha or beta scission reactions to form alkanes plus terminal alkoxyl radicals that transform to aldehydes (Schaich 2005).

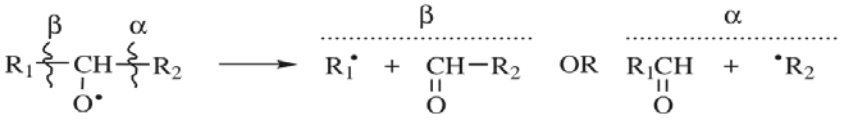

(26)

Aldehydes are determined by three reactions. 2-alkenals are detected by reactions with anisidine, which is called p-anisidine value (AOCS 1989). The sample dissolved in trimethylpentane is reacted with p-anisidine in glacial acetic acid to form a complex that absorbs at 350 nm. The method is simple but not very sensitive and not fully representative of oxidation extent since it measures only a single type of aldehyde which is not formed by all fatty acids (Foo 2006; Osawa 2007).

The thiobarbituric acid or TBA (AOCS 1989) test is another widely used chemical method for the detection of aldehydes. As with anisidine, it detects a single product – malonaldehyde, a late-stage breakdown product of linolenic or higher PUFAs. The reaction is based on the reaction between TBA and carbonyl group to form a red, fluorescent complex under acidic conditions (Sinnhuber 1967).

Despite its common use, the TBA test is valid only in highly unsaturated lipids since malonaldehyde is a scission product formed from the middle of a three double bond segment. It is not accurate with most vegetable oils since they are dominantly linoleic acid and have little or no linolenic or higher acids. It is used extensively with meat products where arachidonic acid is a major component. However, the method is plagued by side reactions with carbonyls in a wide range of non-lipid impurities, including sugars and proteins, and it reacts with all lipid carbonyl compounds including, ketones, carboxylic acid and the ones from other ingredient of foods (Rossell 1994).

Overall, the traditional chemical methods for determination of the major classes of oxidation products do not require sophisticated instrumentation, but each has specific problems and limitations. For measuring lipid oxidation, the major issue is that monitoring a single product in a reaction with multiple products and pathways cannot accurately represent the true rate or full extent of oxidation. In addition, the detection limits of traditional chemical methods are relatively high, and the methods are highly empirical – huge differences in results can be produced by small differences in handling. From a practical standpoint, several of the methods are time-consuming, very difficult to handle large number of samples, and most use lots of glassware as well as large volumes of oils and solvents. Clearly, alternative approaches are needed to provide accurate and sensitive analysis of lipid oxidation rates.

Commercial kits for detection of lipid oxidation.

To overcome some of the working limitations noted above for traditional chemical analyses of lipid oxidation (e.g many reagents, much glassware) and to provide rapid, reproducible analyses that are easy to handle in large numbers, several commercial kits have been developed and brought into the market. The Saftest^{TM} (MP Biomedical) and DiaMed F.A.T.S (DiaMed) kits are two examples of kits developed for both research and quality control (Gordon 2001; Gordon 2005)

These commercial kits analyze classes of lipid oxidation products, specifically, peroxides, aldehydes, and free fatty acids. For each test kit, standardized reagents were developed to react with a characteristic functional group of each product to form

colored compound that can be monitored optically and quantitated by extinction coefficient or standard curves. The advantages of the commercial kits are 1) they use standardized reagents which minimize variation in analyses, 2) the detection limits are much lower than the traditional chemical methods (Foo 2006; Osawa 2007), and 3) the methods are simple and easy to handle with large number of samples.

Despite these positive attributes, in practice, the correlation of ALK Safe is very low with TBA test, it's highly correlated with p-anisidine method though (Osawa 2007). Osawa also reported in another paper that the presence of color in degummed and crude oil interferes with the result gained from kit method (Osawa 2007). However, Foo claims that AldeSafe is the most suitable Saftest assay, FaSafe test has a moderate strong correlation with AOCS official method (Ca5a-40) (AOCS) and Peroxide Safe has the poorest method. According to these reports, Saftest and other fast test methods should have limited applications.

2.3.2. Instrumentation for analyzing lipid oxidation

As technology has advanced, sophisticated instrumentation methods with much higher accuracy, precision, and selectivity have now become the mainstream of studying lipid oxidation chemistry. Gas and liquid chromatography (GC andLC), Fourier transfer spectrometry (FTIR), nuclear magnetic resonance (NMR) and mass spectrometry (MS) are several major techniques that have been widely employed for more detailed identification of lipid oxidation products.

Gas and Liquid Chromatography

GC and LC separate mixture of compounds into individual chemicals that are then analyzed by a wide range of detectors. GC is used to separate and quantitate compounds that are either volatile or can be made volatile by derivatization (Kinter 1995). In studies of lipid oxidation, GC has been used to detect hydroperoxides and hydroxy lipids (Guido et al 1993) individual scission reaction products (Kamal-Eldin 1997) e.g. aldehydes, short chain carboxylic acids, alkanes alkenes, etc. GC has also been used to measure oxygen consumption during oil storage (Jonsdottir 2005).

LC is the complement to GC in that it separates non-volatile products and cannot detect any products that volatilize from oils before analysis. Since there are many ways to manipulate separation parameters (polarity of the mobile phase and stationary phase, oxidized lipid compounds, flow rate, etc.), separation methods vary a lot from paper to paper. Both reverse phase and normal phase methods have been reported (Kaufmann

2001) (Uran 2001) (Palmer 1984). High performance size-exclusion chromatography is widely used in the separation of polar and non-polar fractions from oils and fats (Caponio 2006; Summo 2008). However, a major limitation of HPLC is detection since lipids have no chromo except absorption of conjugated dienes at 234 nm.Thus, conventional UV detector is not so feasible for determination of oxidation products of fats and oils quantitatively without derivatizing functional group to them. Schulte (Schulte 2002) reported a method by reacting carbonyl groups in aldehydes and ketone with 2,4-dinitrophenylhydrazine(DNPH), then measure the concentration of derivatized compound at 370nm. Electro-chemical detector, which discriminate products by its redox potential, has also been employed for study of lipid(Toth 2004) (Jin-Hyang 1993). Other detectors like evaporative light scattering detector (Makinen 1996) and mass spectrometer coupled with HPLC (Kerwin 1996; Schneider 1997; Sjovall 1997) are also very widely used for detailed detection of lipid oxidation products

Although tentative identification of products can be obtained for both GC and HPLC by comparison to standards, coupling these technologies with mass spectrometry greatly improves capabilities for providing details of molecular structures (Byrdwell 1998; Oliw 1998; Spickett 1998). Chromatographic methods can provide both class and very detailed product analyses, and detect products accurately at ppm to ppb levels. However, chromatography usually involves complex sample pretreatment such as extraction, derivitization, clean-up, condensation, etc (Yamada 1987; Mullertz

1990; Yang 1992; Walker 1996). Complex pretreatments may reduce recovery, increase oxidation, and alter products, therefore complicating the results. In addition, the high temperatures of GC can decompose hydroperoxides and cause rearrangements of functional groups (Dobarganes 2002), also yielding inaccurate results.

Fourier Transfer Infrared Spectroscopy (FTIR).

FTIR is light spectroscopy that uses wavelengths in the range of infra-red to induce vibration of covalent bonds. FTIR is a rapid, non-destructive testing method that is increasing in popularity as instrumentation improves. Vibrations in different bonds and functional groups occur with different energies, and this is reflected in the wavelength of absorption, called the resonant frequency. By measuring how much light is absorb by the chemical compound at each wavelength, quantitative analysis can be done. Infrared lights are typically divided into 3 regions: far-infrared (1000-30um), mid-infrared (30-2.5um) and near infrared (2.5-0.8um), in which, mid and near infrared have been employed greatly in monitoring the stability and quality of fats and oils in frying (Gonzaga 2006; Moros 2009). Near infrared absorption was also use for classification and determination of the extent of oil oxidation (Moreno 1999). It has been used to study formation of aldehyde, unsaturated aldehydes and conjugated double bonds with cis-trans isomers (Muik 2005) and anti-oxidant stability (El-Abssy 2009)in oils after heating. Saturation level as an indication of quality of food oil was also monitored by FTIR to measure the concentration of double bonds (Moros 2009).

Nuclear Magnetic Resonance (NMR)

NMR is an even more advanced technology that has been applied to research of lipid oxidation. In NMR, magnetic nuclei have a magnetic field and applied electromagnetic pulses that cause the nuclei to absorb energy from electromagnetic pulses and radiate back. To cause the nuclei to absorb energy, a same frequency of magnetic field should be applied. Based on this feature, NMR is also capable of conducting very detailed products with extremely high precision. Secondary oxidation products, e.g. alkenals, alkanals, dienals and their isomers have been detected by NMR (Claxson 1994; Moreno 1998; Guillen 2009). Guillen also reported the detection of aldehydes and epoxides and their isomers by using NMR.

However, this technology is not very frequently used for routine food analysis due to high cost (so low availability) and sophisticated training needed for operation of instrumentation and interpretation of spectra.

Oxygen Bombs

All the methods described above for studying lipid oxidation have a common characteristic -- they measure some downstream oxidative product. However, as shown in Figure 2, a critical limitation in this approach is that here are many more products generated than measured in common assays. If the products monitored do not match the active degradation pathway(s) or extent of oxidation in a sample, erroneous pictures of lipid oxidation will be generated. Following single products may be acceptable for quality control when only one class of products affects key quality characteristics such

as flavor or aroma. However, when determining kinetics and reaction mechanisms in basic research, more accuracy is needed.

An alternative approach that avoids these issues is to bypass products, go to the very beginning of the lipid oxidation chain reactions, and measure oxygen consumption. Because oxygen addition to free radicals is diffusion controlled and essentially instantaneous ($k>10^9$ L $M^{-1}sec^{-1}$) and one molecule of oxygen adds to each radical, oxygen consumption is a sensitive and stoichiometric reflection of the rate of initiation and also chain propagation. Oxygen consumption offers the additional advantage that it occurs in the earliest stages of all pathways and is independent of downstream products that form afterwards.

One method used to measure oxygen consumption is the oxygen bomb (not to be confused with the oxygen bomb calorimeter), a technique that provides a closed chamber for reactions to proceed under specific conditions of atmosphere and temperature. In oxygen bomb analyses, high oxygen pressures are routinely applied to accelerate autoxidation, and consumption is considered to reflect initiation rates which provide radical sites for addition of oxygen. Three values are measured:

(1) Antioxidant capability: Determine induction period taking the point when the O2 pressures begin to drop as the starting point of oxidation. The more delayed the drop, the better the antioxidant capability

Oxidation rate: Determine linear regression on the part of the curve that is the most close to linear. The slope is the oxidation rate.

(3) Net oxygen consumption: The total oxygen consumption is an indicator of extent of oxidation.

Contemporary oxygen bombs all consist of four major components in various configurations – heating block, pressurized sample cell, control unit, and recorder. Examples of commercial instruments include the Parr calorimeter, Mikrolab Oxidograph, and Mikrolab Oxipres. The configuration for the Mikrolab Oxipres™ used in this study is shown in Figure 7. The heart of the unit is the reaction cylinder (Figure 8), a closed reaction chamber into which the oil or fat-containing sample is placed. On the very top of the reaction cylinder, a pressure transducer sensor monitors the total gas pressure in the headspace. The reaction cell is pressurized from a gas tank via the valve on the middle of the rod. Depending on experimental requirements, different gases can be pressurized into the cylinder. Pressurized reaction cylinders are placed into heating blocks for reaction. This unit works together with the control unit (situated underneath it) that provides precisely controlled temperatures for analyses. The working temperature range is 25°C to 199.5°C. LCD screens on the control units also allow researchers to monitor the actual gas pressure and working temperature during the experiment. The heating block temperature and reaction cylinder pressure are transmitted to a computer for recording and analysis.

Figure 9 shows a typical data curve generated by oxygen bombs. The flat part of the curve, which is known as induction period, is used as the major indicator of stability of oils and fat containing food. The slope of the curve after the induction period

indicates the reaction rate.

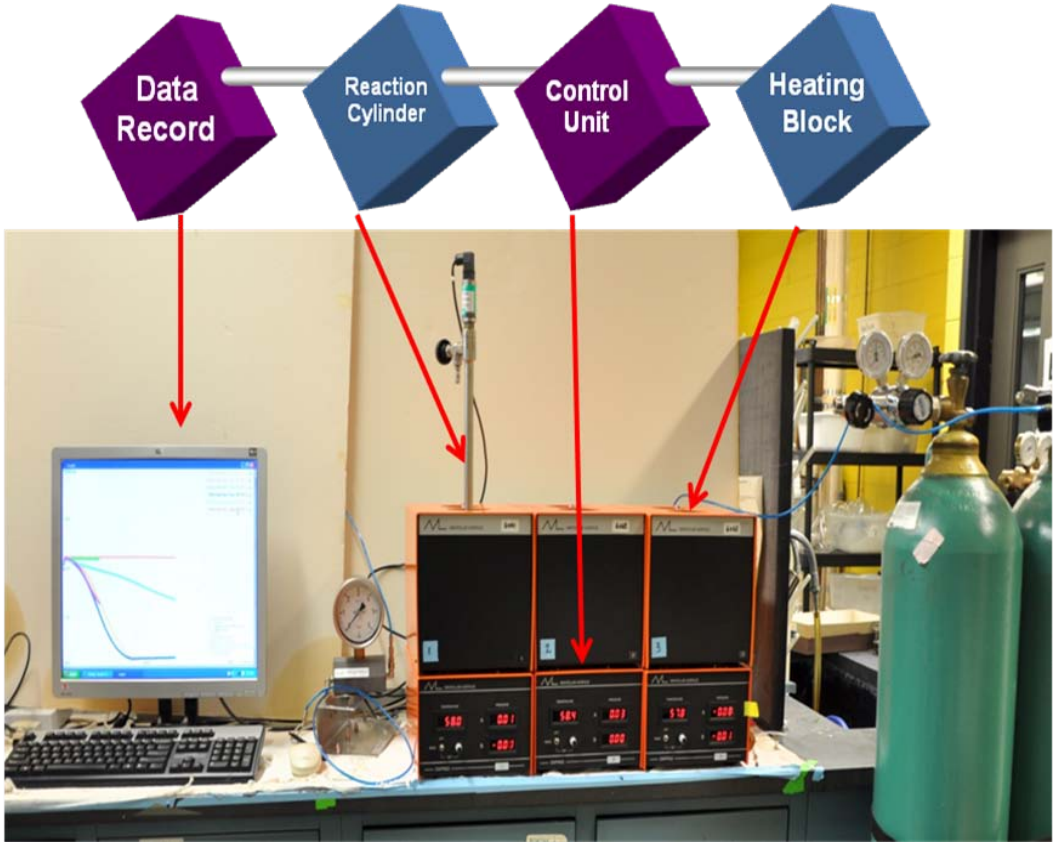

Figure 7. Instrumental configuration of the Mikrolab OxiPres™ Oxygen Bomb.

Figure 8. Reaction cylinder of oxygen bomb and short path thermal desorption trap for collection of volatiles when bomb is opened.

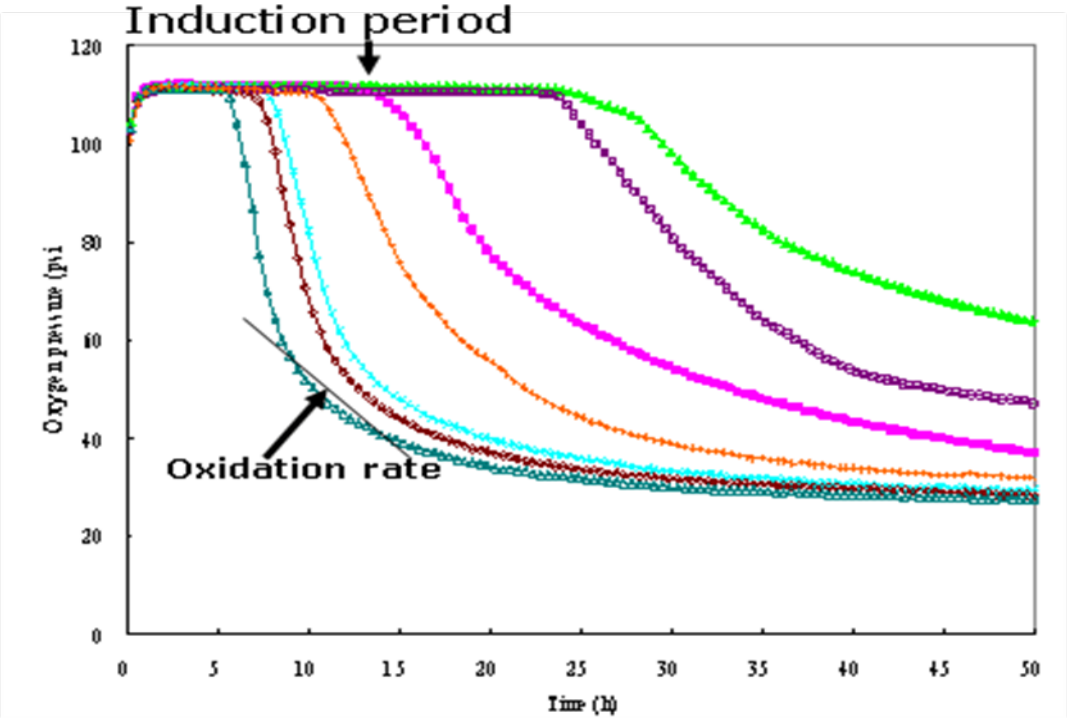

Figure 9 Typical oxygen consumption curves acquired by oxygen bomb. These curves were generated from food oils containing various levels of antioxidants

This technology has been used extensively to test stability of machine oils, and standardized protocols have been developed (Sheppard 1962); (Reiners 1972). For example, 5 g samples at 99 °C and 88-110 psi (~6-8 bar) or higher pure oxygen are the specified conditions for ASTM standard method D942 for oxidation of greases and engine oils (ASTM 2007)

Oxygen bombs have seen more limited applications to food oils or foods even though the methodology has been available for nearly fifty years (Stuckey 1958; Pohle 1962; Pohle 1963; Blankenship 1973; Cooper 1979; Drozdowsk 1987). Pokorny and his co-workers used the oxygen bomb to study oil degradation at ambient temperatures

(Trojakova 2001) and antioxidant activity of tocopherols (Reblova 2006). Liang and Schwarzer (1998) (Liang 1998) used this technique to study the stability of lard and tallow and compare the effectiveness of it with other accelerated stability methods.

All the research reported previously with oxygen bombs were conducted are temperatures less than 150°C. Under these conditions, the degree of the oil and fat oxidation and the activity of antioxidants can be determined by measuring the length of the induction period. There is no corresponding experience using this technology at frying temperatures (150 to 180 °C). However, given current industry trends toward increasing polyunsaturation of oils and extending shelf life of lipid-containing foods, the oxygen bomb with its controlled environment and ability to monitor oxygen consumption directly and continuously would seem to offer a very useful testing tool. The main purpose of this project, therefore, was to evaluate the suitability of oxygen bomb methodology for studying degradation kinetics in oil heated at frying temperatures, and to provide new parameters other than induction period for quantitation of changes.

3. MATERIALS AND METHODS

3.1. Materials

Oils. Initial testing of the instrumentation conditions was performed using TriSun high oleic oil. Some experiments used also soybean oil, Enova diglyceride oil, and olive oil purchased from local supermarkets. Systematic studies were conducted using a blend of 40% NuSun oil and 60% corn oil in three forms: fresh, stripped, and steady-state (partially degraded as used in actual frying). These oils were supplied by FritoLay (Plano, TX).. This 60:40 blended oil will be referred to hereafter as Blend.

Analytical reagents. HPLC grade iso-octane and 2-propanol were purchased from Fisher Scientific. Thermal desorption traps (Scientific Instrument Services, Ringoes, NJ) were packed with Tenax (50mg) and carboxen (50mg) mixed in the ratio1:1 get remaining details of GC and MS analyses. GC is purchased from Varian(Sugar Land, Texas), model: Varian 3400. Finnigan MAT 8230 is purchased from Finnigan(Cincinnati, OH). Short path thermal desorption TD-2 is purchased from Scientific Instrument Services, Inc. All Saftest reagents, include Peroxysafe^{TM}, AlkalSafe^{TM} and FaSafe^{TM} were purchased from MP Biomedicals (Solon, OH). The MicroChem^{TM} II used to read optical absorbances of SafTest samples was purchased from Source Scientific (Irvine, CA). Disposable culture tubes made of borosilicate glass with the dimension of 10*75mm for the SafTests were purchased from VWR (West Chester, PA).

3.2. Experiment Procedures

3.2.1. Glassware cleaning

All Oxipres flasks and tops are routinely washed using a three-step procedure:

a) Wash with Citranox detergent, rinse three times with tap water to remove detergent residues, rinse three times with 18 MΩ resistivity high purity water (Milli-Q water purification system).

Citranox is preferred over other standard lab detergents because it is phosphate free and leaves no films. Composed of a blend of organic acids (including citric acid), anionic and non-ionic surfactants and alkanolamines, it removes scale, metal oxides, metal complexes, trace inorganics, milkstone, soil, grit, buffing compound, grime, grease, fats, oils, particulates, deposits, chemical and solvents.

b) Transfer flasks and tops to denatured alcohol saturated with potassium hydroxide, soak overnight to saponify any traces of lipid materials. Remove from alcohol bath and repeat washing/rinsing as in Step a).

c) Transfer flasks and tops to 1 to 3 N HCl (high purity) to remove traces of metals from glassware, soak overnight, remove from bath, rinse 3-6 times with Milli-Q water, and dry.

3.2.2. Oil handling and storage

All oils (reagents and samples) were stored frozen (-20 °C) under argon headspace after receipt from FLNA and between experiments. Reagent oils were stored in the brown HDPE bottles shipped from FLNA. After heating, all samples were frozen in glass flasks or vials under argon headspace until analysis (usually within 24 hours).

For Oxipres analyses, oils were removed from the freezer and allowed to come to room temperature. Oil samples were then weighed into Oxipres flasks as rapidly as possible under subdued light and transferred immediately to the Oxipres cells.

In some experiments, oils were sparged in the Oxipres cells to replace oxygen with argon or nitrogen before heating. To accomplish this, a Pasteur pipette connected to the inert gas line is placed in the flask, the flask opening was plugged loosely with crushed KimWipes to limit air influx, and inert gas was bubbled through the oil for 15-30 minutes. The flasks were then transferred immediately to Oxipres cells, closed, and pressurized for heating experiments. The same procedure was used to saturate oils with oxygen before heating.

When heating experiments were completed, cells were removed from the heating blocks, pressure valves were opened and the headspace was released directly into the air (early experiments) or through a Tenax trap for volatiles analysis (current procedures). Oil samples were then cooled to room temperature and transferred to 25 ml Erlenmeyer flasks, flushed with argon, sealed (stopper plus Parafilm wrap), and stored frozen out of the light until analyzed for oxidation products. In current protocols,

oils were heated one day and the oxidation products were analyzed the next day.

3.2.3. Oxygen bomb analyses

General procedures. Oxygen consumption analyses were conducted using Oxipres^{TM} oxygen bombs (Mikrolab, Aarhus, Denmark). Temperature in the heating block for the bomb cells was set electronically and controlled to 0.1 °C. All heating blocks were equilibrated at test temperatures before beginning experiments. Pressure and temperature of each cell was monitored continually by computer and also shown on LED panels on each unit. Heating times varied but in most cases were 3 hours. Heating course and data recording was managed by computer using the Oxipres software. Asci data files were transferred to Excel for analysis and graphing.

Oil samples to be tested were weighed into Oxipres flasks and transferred to the Oxipres pressure cylinder, then the glass top was put into place. The cylinder top with pressure transducer was screwed into place and hand tightened, then the cell was pressurized with test gas to experimental pressure specified for each experiment. Cylinders were held at room temperature on the lab bench until all samples were loaded, then all cells were transferred to the heating blocks at the same time and data recording was initiated.

Although most Oxipres methods allow 30 minutes for temperature equilibration before recording oxygen pressure changes, reactions at the elevated temperatures used in this study are so rapid that recording of pressure changes was initiated as soon as the cells were placed in the heating block. Consequently, all pressure curves initially increased with temperature, a peak was reached, and then rapid oxygen consumption

began. Time to peak pressure, peak pressure, initial oxygen consumption rate, and total oxygen consumption were calculated for all runs (Figure 10).

All experiments were conducted at least in duplicate.

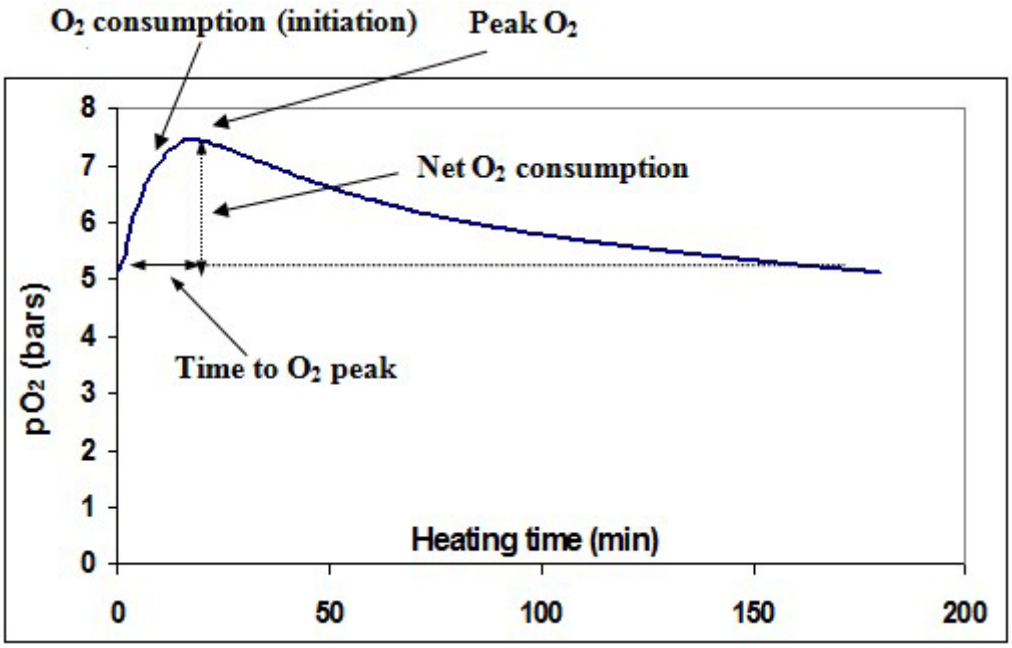

Figure 10. Typical Oxipres oxygen consumption generated when oils are heated to high temperatures (180 °C) under 5 bars oxygen pressure, showing parameters measured for each run.

3.2.3.1. Effects of sample size

Although the manufacturer recommends 5 g samples sizes for Oxipres analyses, heating at frying temperatures (150-180 °C) is a new application of this instrumentation, so effects of sample size were investigated to optimize sensitivity while preventing oxygen limitation and excess degradation. Standard conditions as described above were followed, using 3, 5, 10, 15, 20, 30, 40, and 50 g samples of Blend oil, heated at 180 °C under 5 bars oxygen for 3 hours.

3.2.3.2. Effects of heating time

To test whether the Oxipres could be used as a model of actual frying conditions which may continue for up to about eight hours (maximum turnover time) in industrial continuous frying operations and for days to weeks in commercial batch frying

operations, 10 g samples of Blend oil were heated under 5 bars oxygen for 48, 24, 12, 6, 4.8, and 3 hours following standard procedures described above.

3.2.3.3. Effects of oil composition

To assess the sensitivity of the Oxipres™ instrumentation in detecting differences in degradation susceptibility between oils, 10 g samples of TriSun (high oleic), soybean oil (polyunsaturated), olive oil (monounsaturated) with expected high antioxidant content, and Enova diglyceride oil based on soybean oil were heated at 180 °C under 5 bars oxygen for 3 hours.

3.2.3.4. Reproducibility

Six replicates of 10 g samples each of TriSun, soybean, and olive oils were heated at 180 °C under 5 bars oxygen for 3 hours. Averages, standard deviations, and coefficients of variation were calculated.

3.2.3.5. Effects of oxygen pressure on oxygen consumption by NuSun:corn oil Blends

The manufacturer recommends that 5 bars pure oxygen be used for all oxygen bomb analyses to provide maximum detection by the pressure transducer and maximum reaction to provide clear kinetics, and 5 bars or higher oxygen is standard for oil and grease analyses (ASTM 2007; Migdal et al 2008). Again, since testing at frying temperatures is a new application, and reactions under such conditions are much more rapid than at standard 90 to 120 °C, effects of oxygen pressure were evaluated to determine optimum conditions for high temperature studies. Twelve 10g samples of

fresh Blend oil were prepared as described above and heated at 180°C for 3 hours with cells pressurized to 0.5, 1, 2, 3, 4 or 5 bars pure oxygen. This allowed duplicates for each pressure.

The experiment was repeated pressurizing with air (oxygen concentrations 21% that of the oxygen runs), and under inert gas (nitrogen or argon).

3.2.3.6. Effects of temperature on oxygen consumption by NuSun:corn oil Blends

To test the response of the Oxipres system and determine changes in oxidation kinetics as a function of temperature, 10 g samples of fresh Blend oil were pressurized with 2 bars oxygen and then heated at 100, 120, 150, 160, 170 and 180°C for 3 hours, with duplicates for each temperature. The same experiment is run under 2 bars air. The data is recorded by Oxipres software.

3.2.3.7. Effects of pre-sparging oil with inert gas before heating

To test effects of pre-dissolved gases as well as oxygen diffusion into the oil during heating, 10 g samples of oil were loaded into the Oxipres cells and gently pre-sparged with argon for 15 minutes before heating. As controls, identical samples were prepared without argon sparging. Samples were heated under standard conditions (2 bars air, 180 °C, 3 hours).

3.2.3.8. Effects of periodic cell swirling on oxygen consumption

Questions arose regarding possible limitations in diffusion of oxygen into oils in the Oxipres cells. To test the role of oxygen diffusion in measured decreases in cell

pressures, duplicate 10 g samples of fresh Blend oil were heated at 180°C, pressurized with 2 bars air. The control group was heated constantly for 3 hours without disturbance. For the swirling test, one group was removed and swirled gently or vigorously for varying periods then returned to the heating block. In one test, samples were swirled for varying lengths of time from seconds to minutes. This experiment showed that sampling cooling during swirling was a complication, so in subsequent experiments, samples were typically withdrawn every 15 minutes and swirled for 15 seconds before returning to the heating block. To control for temperature effects, a parallel temperature control group was withdrawn at the same time and left on the bench top for identical periods without swirling.

3.2.3.9. Oxipres Oxygen Bomb Calculations

Total Volume of Oxipres Cells

Oxipres cells were filled with water with meniscus even with top. This volume was transferred carefully to a tared beaker, water drops clinging to cell were shaken into the beaker or taken up in a pipette and transferred to the beaker. The beaker was weighed, and water weight was converted to volume (density of water = 1 g/ml). Duplicate samples for each of six flasks were measured.

Average empty cell volume: 214.32 ± 0.24 g

Sample flask volume

Oxipres flasks and tops were submerged in 400 ml water in a graduated cylinder. Flask + lid volumes were determined from the volume increase. Duplicate samples for

each of six flasks were measured.

Average glass volume (flask + lid): 41.4 ± 2.1 ml

Oil volume

Density of oil (60% NuSun:40% corn oil)

NuSun ρ(20 C) = 0.914 g/ml (Warner 2003)

Corn oil ρ(20 C) = 0.922 g/ml (Elert 2000)

Experimental oil blend ρ(20 C) =0.60(0.914) + 0.40(0.922) = 0.9172 g/ml

Combined gas law (PV=nRT) calculations for Oxipres cells

Combined gas law calculations are required to determine the number of oxygen molecules available under various reaction conditions (i.e. oxygen limitation), the pressures that should be attained at different pressures, and the conversion of bars pressure to moles oxygen. Calculations used R=83.1447 (cm^3*bars/K*mol), cell loading T=298 K, 0.0113 mol TAG / 10 g sample based on average TAG mol wt of 885 (assuming ~50:50 oleic and linoleic acids).

Calculation of V (Gas headspace volume actually available under experimental conditions

Gas headspace volume = cell volume – flask/lid volume – oil sample volume

Oil volume = oil wt / oil density = oil weight / 0.9172

n mmol O_2 calculated from n = PV/RT

Results for various oil sample sizes are presented in Table 5.

Table 5. Calculations for headspace volumes and oxygen available with different oil sample sizes.

Sample wt (g)	mmol TAG	oil (ml)	Flask (ml)	Headspace (ml)	Available O_2 2 bars air mmol	mmol/ mol TAG	5 bars O_2 mmol	mmol/ mol TAG
3	3.39	3.3	41.4	169.6	2.88	0.85	34.24	10.1
5	5.65	5.5	41.4	167.5	2.84	0.5	33.8	5.98
10	11.3	10.9	41.4	162	2.75	0.24	32.69	2.89
15	16.95	16.4	41.4	156.6	2.65	0.16	31.59	1.86
20	22.6	21.8	41.4	151.1	2.56	0.11	30.49	1.35
30	33.9	32.7	41.4	140.2	2.38	0.07	28.29	0.83
40	45.2	43.6	41.4	129.3	2.19	0.05	26.09	0.58
50	56.5	54.5	41.4	118.4	2.01	0.04	23.89	0.42

Table 6. Calculation of n moles O_2 in headspace from PV=nRT as f(bomb pressure) under standard run conditions (Headspace V=162 for standard 10g samples)

gas	P (bars)	mols O_2	mol O_2/bar	mol O2 mol TAG
O2	5	0.03269	0.00654	2.89
	4	0.02615	0.00654	2.31
	3	0.01961	0.00654	1.74
	2	0.01308	0.00654	1.16
	1	0.00654	0.00654	0.58
air	5	0.00687	0.00137	0.61
	4	0.00549	0.00137	0.49
	3	0.00412	0.00137	0.36
	2	0.00275	0.00137	0.24
	1	0.00137	0.00137	0.12

Dividing n mols O_2 by bars P gives conversion factors for bars to mols O_2 of 0.00654/bar for pure oxygen and 0.00137/bar for air at room temperature.

Calculation of cell pressures as f(T) and conversion

When the cell is pressurized at room temperature then heated, the peak P should increase according to PV=nRT if the gas laws are followed. When the actual peak P reached during heating is different from these values, other factors are contributing to or detracting from the bomb pressure.

Table 7. Theoretical prediction of cell pressure according to ideal gas law

Temperature						
K	ºC	Cell Pressure (bars) expected				
273	25	5	4	3	2	1
373	100	6.2584	5.0067	3.755	2.5034	1.2517
393	120	6.594	5.2752	3.9564	2.6376	1.3188
423	150	7.0973	5.6779	4.2584	2.8389	1.4195
433	160	7.2651	5.8121	4.3591	2.906	1.453
443	170	7.4329	5.9463	4.4597	2.9732	1.4866
453	180	7.6007	6.0805	4.5604	3.0403	1.5201

P here is the total bomb pressure. $pO_2 = P$ when the pressurizing gas is oxygen.

$pO_2 = P * 0.21$ when air is the pressurizing gas.

Factors increasing peak P: volatiles released from oil

dissolved gases released from oil

Contribution of these factors increases at lower pO_2.

Factors decreasing peak P: rapid oxidation that begins even before oil reaches full temperature – contribution increases as pO_2 increases.

Dividing n mols O_2 at room temperature by expected bars P at each temperature gives

the conversion factors for bars to mols O_2 (Table 8).

Table 8. Converting factors for bars pressure to mols oxygen at different temperatures.

T°C	100	120	150	160	170	180
Oxygen	0.0052	0.005	0.0046	0.0045	0.0044	0.0043
Air	0.0011	0.001	0.001	0.0009	0.0009	0.0009

Sensitivity of oxygen detection

The digital pressure transducer sensor for the Oxipres system registers data to an infinite number of decimal places so the oxygen pressure change that it can detect is infinitesimally small. To determine the practical detection limit as signal to noise, empty cells were heated under the same conditions as oils (180 °C for 3 hours under 5 bars oxygen and 2 bars air). Curves were examined in the approximately constant region shown in the box (Figure 11).

The sensitivity limit of the sensor is 0.002442 bars (minimum registered pressure difference, i.e. successive data points in the noise differ by this value or multiples thereof), which corresponds to 1.05×10^{-5} mol O_2 under oxygen and 2.2 umol O_2 under air. Signal to noise for oxygen is ± 0.002442 bars, for air is ± 0.001221 bars.

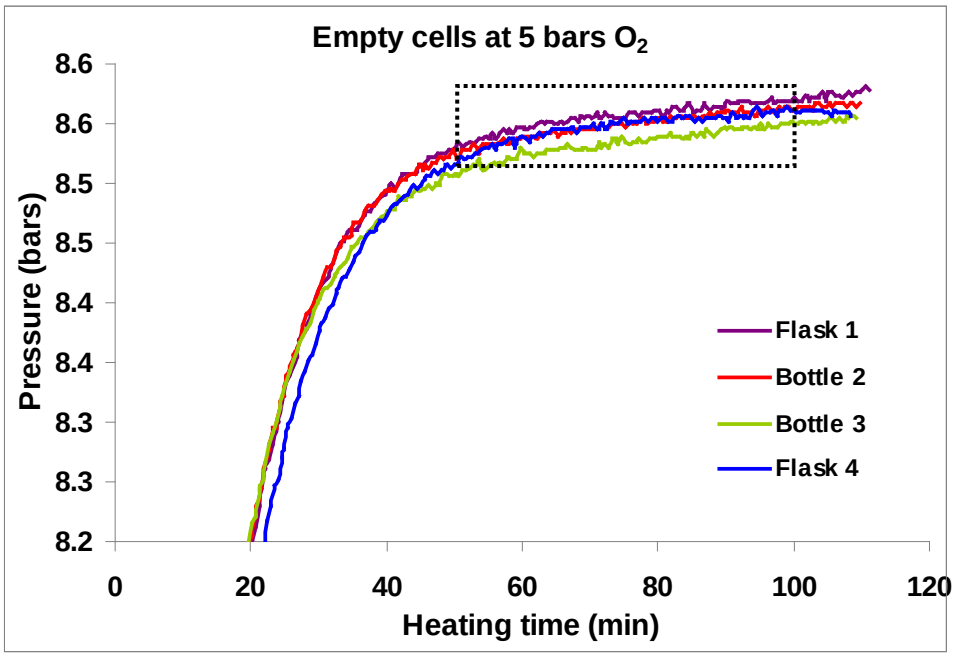

Figure 11. Oxipres curves for empty cells. Signal to noise and detection limits were determined from data in boxed region.

3.2.4. Analyses of Lipid Oxidation Products

Oxygen consumption reports the rate of oxidation independent of product pathways. However, in both research and industrial quality control, lipid oxidation is understood and interpreted in terms of products. Thus, to provide information about reactions and products underlying oxygen consumption, several standard lipid oxidation and hydrolysis products were measured in oils at the end of each heating period.

3.2.4.1. Conjugated dienes

Oil samples were first diluted with HPLC grade iso-octane, then optical absorbance was read at 234 nm against a blank of pure iso-octane in a Cary 50 Bio UV-Visble spectrophotometer. The concentration of the conjugated diene was calculated by the equation below.

$C=OD\times DF/29.5/2.98$

C: the concentration of the conjugated diene in oil sample in mmol/mol TAG

OD: absorbance at 234 nm

DF: dilution factor.

3.2.4.2. Peroxide Values

Before analysis, PeroxySafe^{TM} reagents A,B and C and standard curve calibrators were removed from the refrigerator and equilibrated to room temperature for at least 30 minutes. For standard curve preparation, 25 ul calibrator 1,2, 3, blank (distilled water) and reagent blanks were pipetted into 10 mm test tubes, with 3 replicates for each

calibrator. 1ml PeroxySafe^{TM} reagent A, 0.1ml PeroxySafe^{TM} reagent B and 0.16 ml PeroxySafe^{TM} reagent C were added to each calibrator, blank and reagent blank in sequence. Blank, reagent blank, and all calibrator samples were incubated at room temperature for 15 minutes, then each tube was inserted in the compartment of MicroChem II analyzer and optical absorbance at 550nm was measured. The calibration curve data was recorded and stored by computer.

For sample tests, 25 ul oil sample and reagent blank were added to 10 mm test tubes, 3 replicates for each. 1 ml PeroxySafe^{TM} reagent A, 0.1 ml PeroxySafe^{TM} reagent B and 0.16 ml PeroxySafe^{TM} reagent C were added to each sample and reagent blank, and all tubes were vortexed for 30 seconds, react at room temperature for 15 minutes, and optical absorbance at 550 nm was read and recorded for each tube using the MicroChem II analyzer. The concentration of peroxides in each sample was determined by comparison of sample absorbances to the calibration curve. When readings of oil samples were out of range for the test (as determined by computer notations), oil samples were diluted in HPLC grade 2-propanol until the concentration of the peroxide fell in the range of the calibration curve. The final concentration in the PeroxySaf Test was expressed as meq peroxide / kg oil. This was converted from meq/kg oil to meq/mol TAG (Triacylglycerol) by using the equation $C = c \times DF/1.13$

where C is the final peroxide concentration in meq/mol TAG,

c is the initial peroxide concentration in diluted oil in meq/kg oil, and

DF is the dilution factor

1.13 is moles TAG per kg oil

3.2.4.3. Aldehydes

Before analysis, AlkalSafe™ reagents A and B, Calibrators 1,2, 3, 4, and reagent blanks were removed from the refrigerator and equilibrated to room temperature for at least 30 minutes. For standard curve preparation, 75 ul calibrator 1,2, 3, 4, and blank (distilled water) were pipetted into 10mm test tubes, with 3 replicates for each calibrator. 1 ml AlkalSafe™ reagent A, 0.25 ml AlkalSafe™ reagent B were added to each calibrator and blank in sequence, all tubes were incubated at room temperature for 20 minutes, then optical absorbance at 570 nm was read and recorded for each tube using the MicroChem II analyzer. Data for the calibration curve were recorded and stored by computer.

For sample tests, 75 ul oil sample and blank were added to 10 mm test tubes, with 3 replicates for each sample. 1 ml AlkalSafe™ reagent A and 0.25 ml AlkalSafe™ reagent B were added to each sample and reagent black, all tubes were vortexed for 30 seconds, then incubated at room temperature for 20 minutes before reading optical absorbance at 570 nm. The aldehyde concentration of each sample was determined by comparison of sample readings to the calibration curve. When samples readings were out of calibration range, samples were diluted in HPLC grade 2-propanol and re-analyzed until the concentration of the aldehyde fell into the range of the calibration curve. The final concentration of aldehydes were expressed as nmol/ml by the AlkalSaf

Test. This was converted to mmol aldehyde/mol TAG by using the equation

$C=c\times DF\times 1.32/3.5/885$,

where C is the aldehyde concentration of original oil sample in mmol/mol TAG,

c is the aldehyde concentration of the diluted oil sample in nmol/ml,

DF is the dilution factor,

3.2.4.4. Free Fatty Acids

Before analysis, FASafe^{TM} reagents A and B, Calibrators 1,2, 3,4, and the reagent blank were removed from the refrigerator and allowed to equilibrate to room temperature for at least 30 minutes. For standard curve preparation, 50 ul calibrator 1,2, 3, 4, and blank (distilled water) were pipetted into 10 mm test tubes, with 3 replicates for each calibrator. 1 ml FASafe^{TM} reagent A and 0.1 ml FASafe^{TM} reagent B were added to each calibrator, and blank in sequence, all tubes were incubated at room temperature for 10 minutes, and optical absorbance at 570 nm for each tube was measured using the MicroChem II analyzer. Data for the calibration curve was recorded and stored by computer.

For analyses of free fatty acids in oil samples, 75ul oil and blank were added to 10 mm test tubes, 3 replicates for each sample. 1 ml FASafe^{TM} reagent A and 0.1 ml FASafe^{TM} reagent B were added to each sample and reagent blank, all tubes were vortexed for 30 seconds and incubated at room temperature for 10 minutes before reading, the the optical absorbance for each tube was measured at 570 nm using the

MicroChem II analyzer. Free fatty acid concentrations in each sample were determined by comparison of sample absorbances with the calibration curve. When oil sample readings were out of the calibration range, samples were diluted in HPLC grade 2-propanol and re-analyzed until the free fatty acid concentration fell into the range of the calibration curve. The free fatty acid concentration in the oil samples was calculated using the equation $C=c\times DF$,

where C is the % free fatty acid concentration in the original oil sample,

c is the % free fatty acid concentration of the diluted oil sample, and

DF is the dilution factor.

3.2.4.5. Total Volatiles

At normal temperatures, lipid oxidation rates are slow and release of volatile products into the Oxipres^{TM} cell headspace is trivial relative to 5 bars oxygen pressure. However, this study used lower oxygen pressures to prevent skewing product levels and distributions. In addition, oil degradation at frying temperatures is rapid and complex, and release of volatile products may be orders of magnitude higher than at 60 °C. Under such conditions, volatile products released from the oil may contribute significantly to headspace pressure (measured by a pressure transducer that does not differentiate oxygen from other molecules in the headspace) and even counteract loss of oxygen in reaction, resulting in decrease in the rate of oxygen consumption reported in the Oxipres curves.

To test for this possibility, Oxipres cells were vented through thermal desorption traps to collect headspace volatiles generated during heating. Thermal desorption traps (Scientific Instrument Services, Ringoes, NJ) were packed with Tenax (50mg) and carboxen (50mg) mixed in the ratio1:1 get remaining details of GC and MS analyses.

4. RESULTS AND DISCUSSION

Determining optimum experimental conditions

4.1. Effects of sample size on oxygen consumption curves and oil degradation.

A sample size of 5 g oil for standard analyses is recommended by the equipment manufacturer Mikrolab to maximize the surface to volume ratio. This amount is probably optimal for analyses at the 60 °C temperature commonly used and may be acceptable even at more elevated temperatures, e.g. 100 °C. However, early tests showed that at frying temperatures, 5 gram oil burns readily, even with short heating times. On the other hand, large oil volumes oxidizing rapidly may consume too much of the headspace oxygen, making the system oxygen limited with heating periods shorter than desired for testing. Thus, sample size was investigated to determine the optimum amount for high temperature operations.

A range of sample sizes from 3 to 50 g were tested with 3 and 6 hours heating at 180 °C. Absolute values of both initial oxygen consumption rate and net oxygen consumption increased with sample size (Figure 12), as might be expected. However, the increases were not linear, and when normalized to oxygen consumption per mole TAG, oxidation actually decreased with sample size (Figure 13, Table 9). This lower proportional oxidation probably occurs because the amount of oxygen available per mole of TAG decreases with sample size (see Table 5), so although oxygen is not strictly limiting and not all available oxygen is consumed, oxygen consumption per

mole TAG slows as diffusion of oxygen to radical sites becomes slower than other

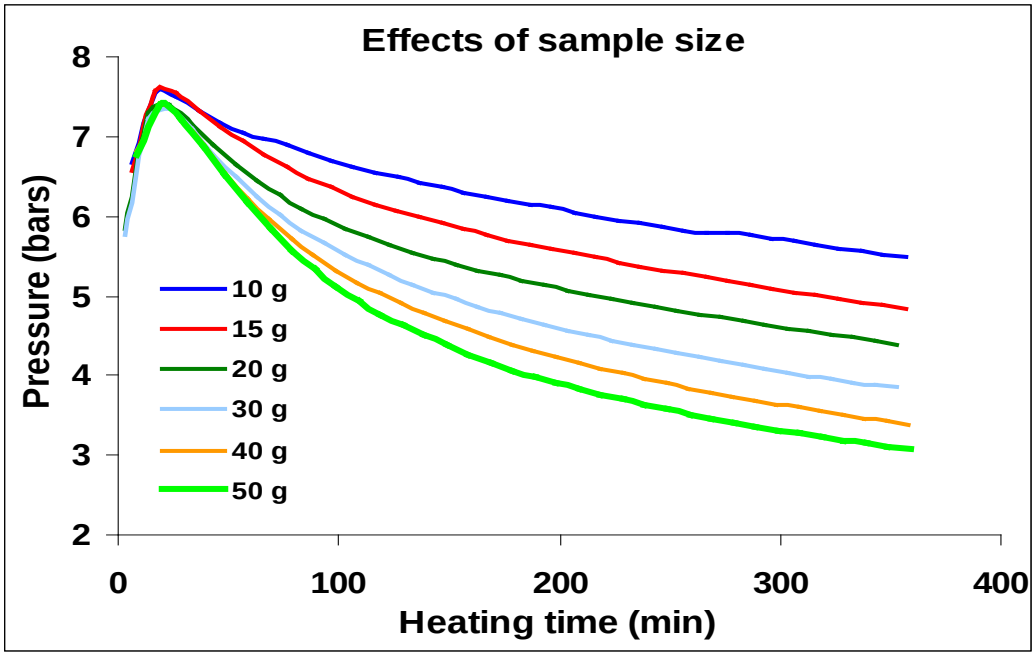

Figure 12. Oxygen consumption of different sample size under 5 bars oxygen pressure and 180°C for 6 hours.

Table 9. Effect of sample size on oxygen consumption parameters (180 °C, 5 bars O2).

Oil wt. (g)	Initial oxid. Rate/min			Net O2 consumption (6 hr)			% O2 consumed	
	mbar	mmol O_2	mmol O_2	bars O_2 /mol TAG	mol O_2	mol O_2 /mol TAG	avail.[a]	bars[b]
3	5.81	0.03	2.37	1.07	0.0049	0.43	13.4	14.2
5	9.66	0.04	3.93	1.58	0.0073	0.64	20.1	20.9
10	15.39	0.07	6.26	2.05	0.0094	0.84	27	27
15	20.27	0.09	8.25	2.74	0.0126	1.11	37.2	36
20	25.76	0.12	10.49	3.00	0.0138	1.22	42.3	39.5
30	29.55	0.14	12.03	3.50	0.0161	1.42	53.1	46
40	34.07	0.16	13.87	4.03	0.0185	1.64	66.4	53
50	35.53	0.16	14.46	4.31	0.0198	1.75	77.5	58.3

[a] mol O_2 per mol TAG consumed / mol O_2 available per mole TAG. basis
[b] bars O_2 consumed / peak bars O_2 basis.

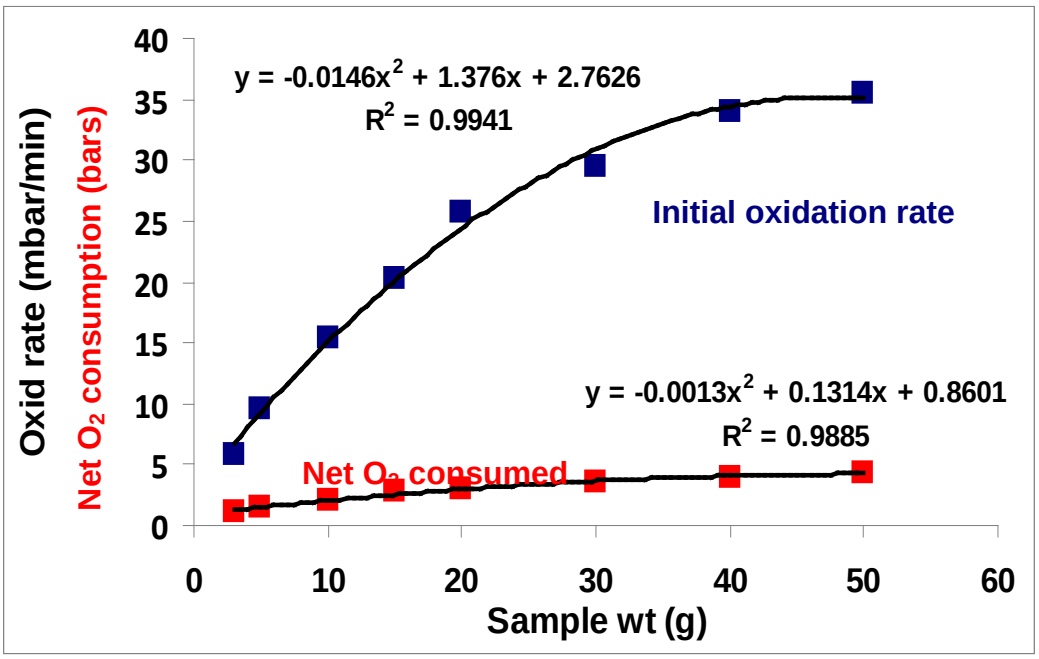

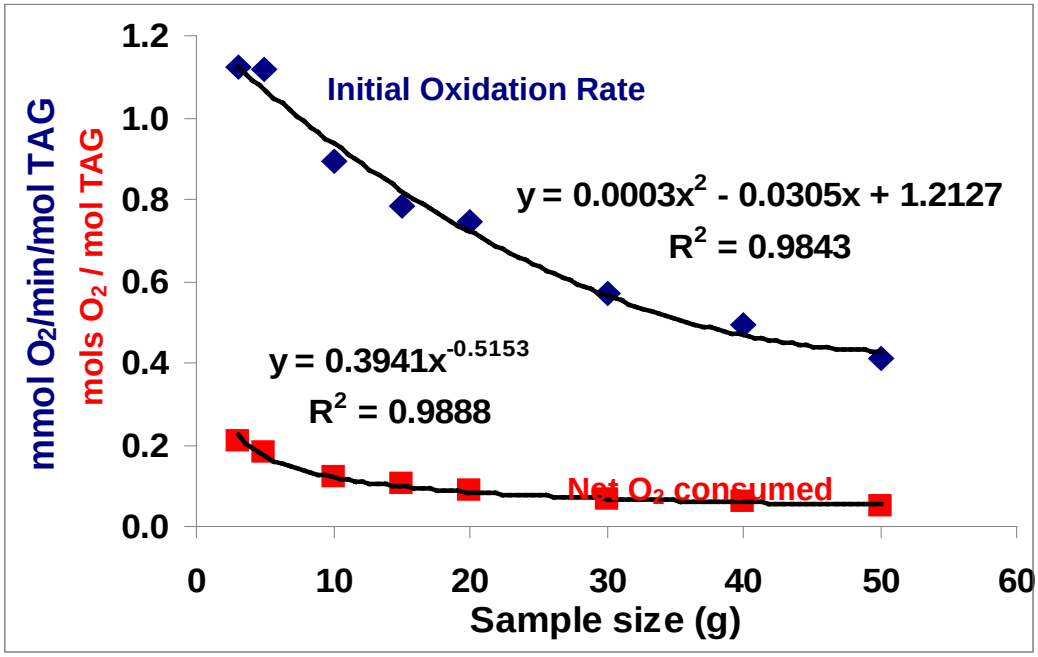

Figure 13. Change in initial oxygen consumption rates and net oxygen consumption as a function of sample size for Blend oil heated in the Oxipres for six hours at 180 °C under 5 bars oxygen.

radical reactions. Another possible explanation is that oxygen diffusion into the oil becomes more limiting for larger samples. The surface area and oxygen diffusivity are constant for all samples, so if there are not currents to circulate oxygen into lower layers of oil, only upper layers become oxygenated. Issues of diffusions, circulation, and surface versus bulk oil as oxidation sites will be discussed further later.

Browning decreased with sample size due to lower surface to volume ratio (Figure 14). Small volumes were especially prone to burning with long heating times (see Figure 15, next section).

From the curves in Figure 13 and considering limitation in oxygen availability at higher weights, 10 g was selected as the standard samples size to provide the maximum surface to ratio rate without over burning the oils.

3 hours

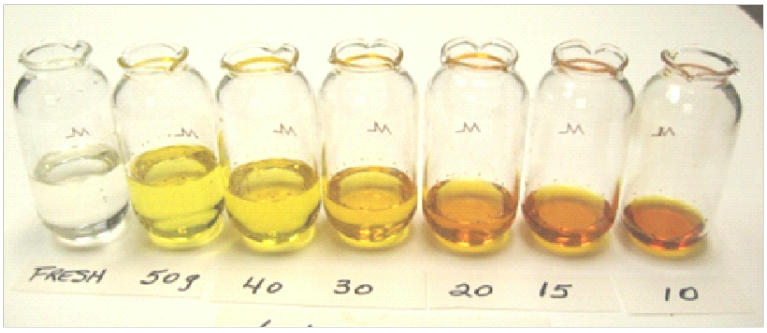

6 hours

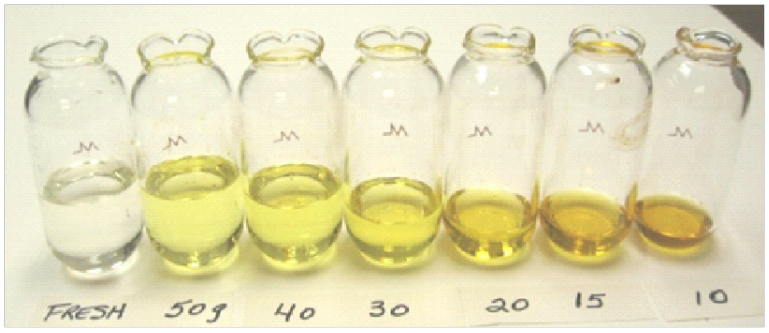

Figure 14. Browning due to the thermal degradation as a function of sample size after heating at 180 °C for 3 (top) and 5 (bottom) hours.

4.2. Effects of heating time

In commercial heating operations, oils are typically in continuous use for several days. Thus, in initial testing 5 g oil samples were heated for 48 hours. These were completely burned and oxidized into a sticky residue. Even with 24 hours heating and larger samples (10 and 20 g), oils burned (Figure 15). Sample sizes were then increased and oxygen consumption was followed over 24 hours to determine useful heating times. Results are shown in Figure 15.

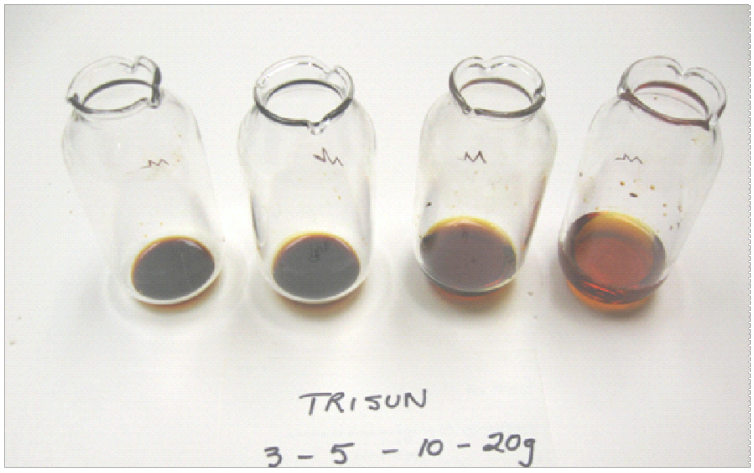

Figure 15. Excessive browning in Trisun oil heated at 180 °C for 24 hours.

The extensive browning makes it obvious that heating small oil volumes for long times in the Oxipres (or indeed anywhere) results in extensive degradation of the oil far beyond useful frying quality. Thus the heating time must be more limited. The curves in Figure 16 show that the oils oxidize in two phases: an initial rapid phase and a slow steady secondary phase. Though both phases are important to understand, the early reactions are most important to understand for determining reaction mechanisms and assessing oxidative stability of oils. This early phase is complete within three

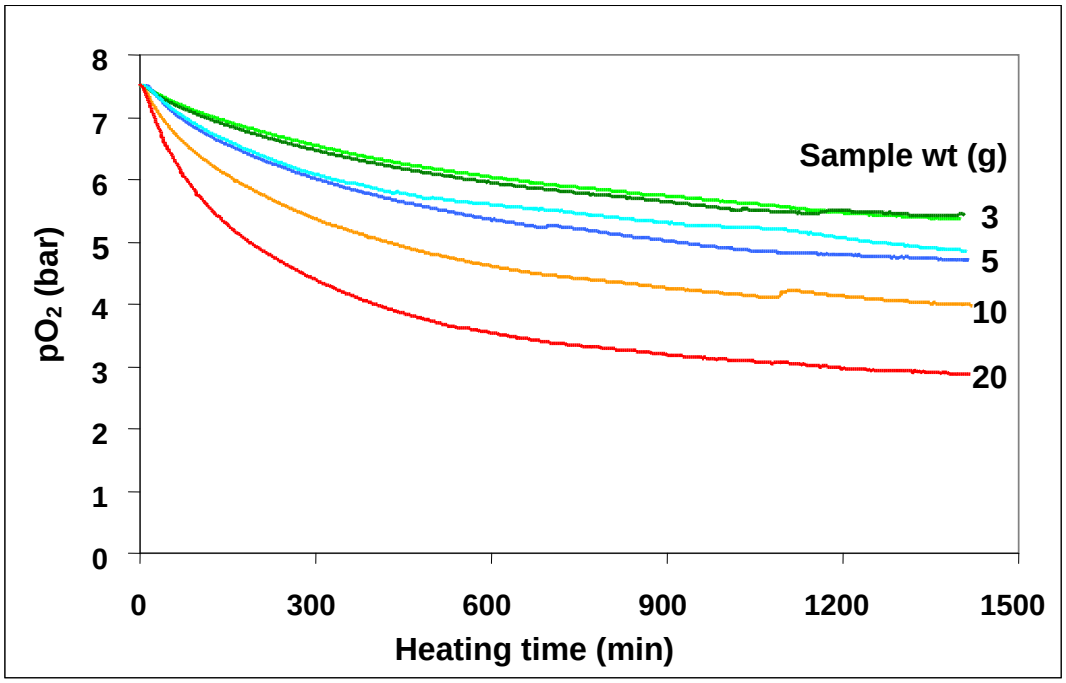

Figure 16. Effect of heating time on oxygen consumption by Trisun oil heated to 180 °C under 5 bars oxygen.

hours. Figure 14 shows that there is still notable browning with small oil volumes with 6 hours,but discoloration after three hours heating is still at an acceptable level. Three hours is also in the range of turnover times for industrial frying, so was selected as the standard heating time for this study.

4.3. Reproducibility of the oxygen bomb.

To verify the reproducibility of the oxygen bomb, commercial soybean oil, Trisun oil and olive oil were used for the test. 10 g of six samples of each kind of oil were heating under 180°C, 5 bars oxygen for 3 hours. Peak pressure, maximum oxygen consumption rate, and total oxygen consumption were measured. Oxygen consumption by the three different oils showed very high reproducibility (Figures 17-19). For soybean oil the variation was 0.85, 2.79 and 1.89 % for the peak pressure, max rate and total oxygen consumption, respectively (Table 10). The variation was 1.15, 2.79 and 1.89% respectively for Trisun oil (Table 11) and 0.48, 2.40 and 1.01 % for olive oil (Table 12). That soybean oil exhibited higher oxygen consumption rate than both olive oil and Trisun oil matches its polyunsaturation; in comparison, olive and Trisun oils are monounsaturated. The max oxygen consumption rate of Trisun oil and olive oil were similar, reflecting their composition high in oleic acid.

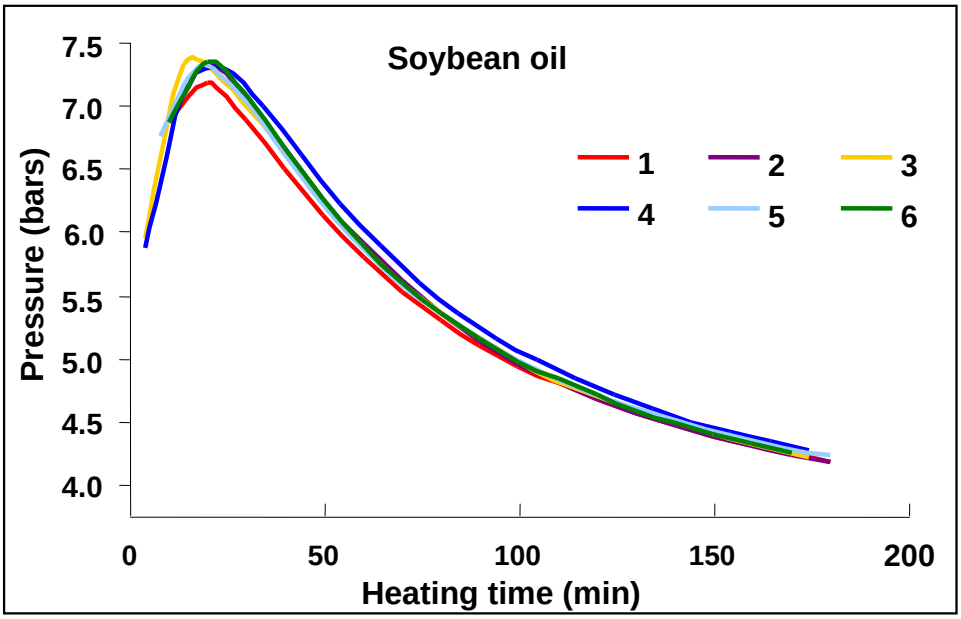

Figure 17. Reproducibility of oxygen consumption by soybean oil heated at 180 °C for three hours under 5 bars oxygen. Note the expanded scale.

Table 10. Peak pressure, maximum oxygen consumption rate, and total oxygen consumption of soybean oil heated at 180 °C for three hours under 5 bars oxygen.

Sample replicate	Peak pressure (bar)	Max rate (bars/min)	Total O_2 consumption (bar)
1	7.1844	0.0386	2.9915
2	7.3285	0.0400	3.1477
3	7.3284	0.0391	3.1111
4	7.2943	0.0389	3.0232
5	7.3236	0.0400	3.0891
6	7.3602	0.0418	3.0940
Average	7.3032	0.0397	3.0761
ST. Dev.	0.0619	0.0011	0.0580
% Var.	0.85	2.79	1.89

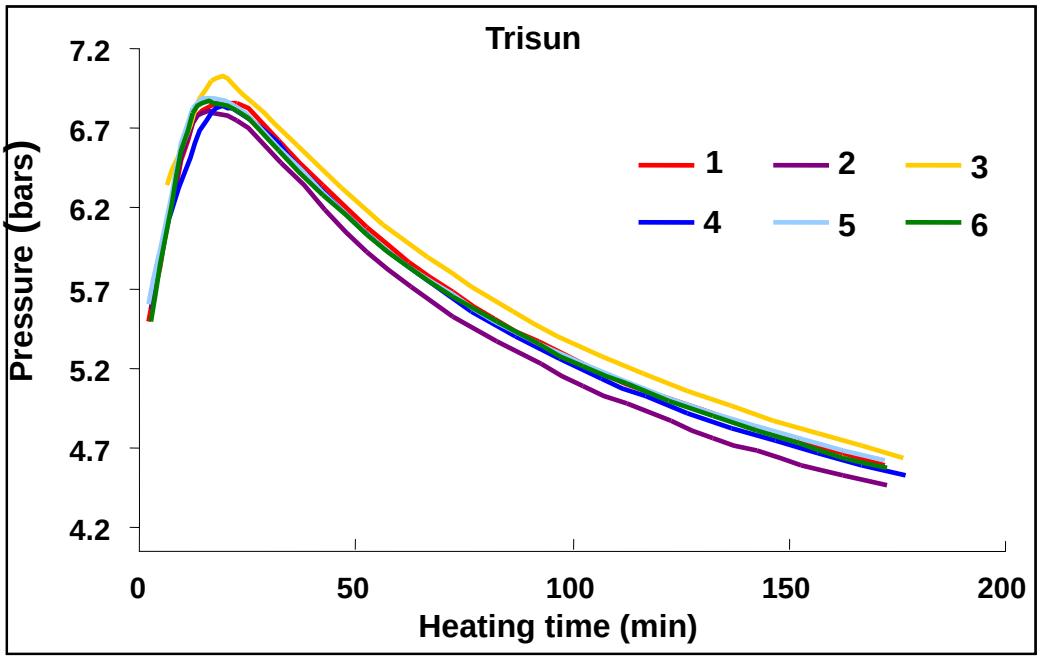

Figure 18. Reproducibility of oxygen consumption by Trisun oil heated at 180 °C for three hours under 5 bars oxygen. Note the expanded scale.

Table 11. Peak pressure, maximum oxygen consumption rate, and total oxygen consumption of Trisun oil heated at 180 °C for three hours under 5 bars oxygen.

Sample replicate	Peak pressure (bar)	Max rate (bars/min)	Total O_2 consumption
1	6.8596	0.0286	2.2637
2	6.7521	0.0293	2.2955
3	7.0037	0.0266	2.3761
4	6.8034	0.0276	2.2808
5	6.8498	0.0281	2.2369
6	6.8107	0.0276	2.2442
Average	6.8466	0.028	2.2829
ST. Dev.	0.0784	0.0009	0.0506
% Var.	1.15	3.3	2.2

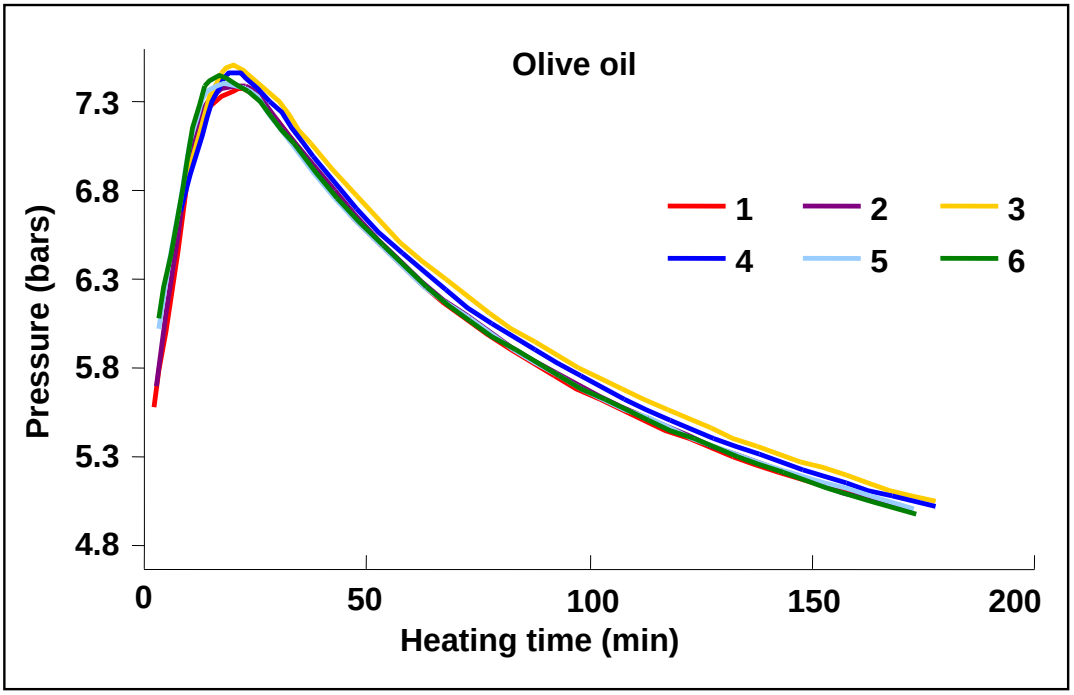

Figure 19. Reproducibility of oxygen consumption by olive oil heated at 180 °C for three hours under 5 bars oxygen. Note the expanded scale.

Table 12. Peak pressure, maximum oxygen consumption rate, and total oxygen consumption of olive oil heated at 180 °C for three hours under 5 bars oxygen.

Sample replicate	Peak pressure (bar)	Max rate (bars/min)	Total O_2 consumption (bar)
1	7.3797	0.0315	2.3810
2	7.3895	0.0313	2.3932
3	7.4701	0.0298	2.4225
4	7.4383	0.0298	2.4225
5	7.3748	0.0308	2.3614
6	7.3871	0.0310	2.4054
Average	7.4066	0.0307	2.3976
ST. Dev.	0.0352	0.0007	0.0241
% Var.	0.48	2.40	1.01

4.4. Oxipres sensitivity to differences in oil unsaturation and structure

To assess the ability of the Oxipres to distinguish oxidizability of oils with different levels of unsaturation, 10 g of soybean oil Trisun oil, olive oil, and Enova based on soybean oil were heated at 180 °C for three hours under five bars oxygen. Results show that the Oxpres is capable of correctly distinguishing differences in oxidizability of oils with varying fatty acid composition (Figures 20 and 21 and Tables 13 and 14).

It is interesting to note that although the oxygen consumption of Enova, a diacylglycerol based on soybean oil, was comparable to its parent oil, this oil browned to a much greater extent (Figure 22), so it must undergo different reactions during heating.

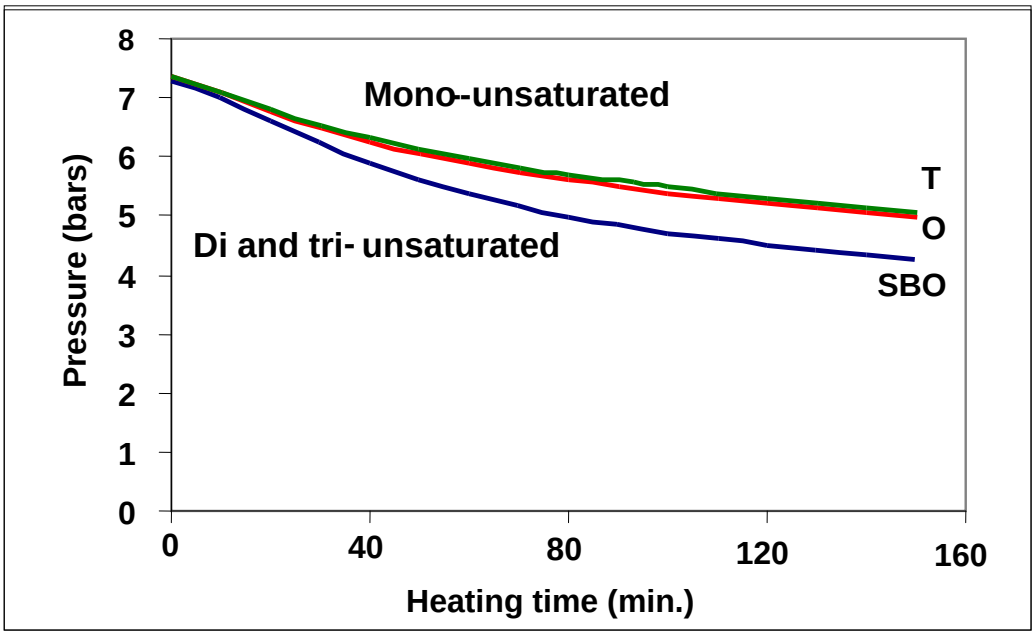

Figure 20. Comparison of oxygen consumption by mono-unsaturated Trisun (T) and olive (O) oils with polyunsaturated soybean oil (SBO). Oils were heated at 180 °C for three hours under 5 bars oxygen.

Table 13. Oxygen consumption and oxidation parameters Trisun, olive, and soybean oils oxygen in Oxipres oxygen bombs. 10 g samples, 180 °C, 3 hours, 5 bars oxygen

		Minutes To peak	Max P	Initial Rate mbars/min	Total O2 consumption bars	mol O2	mol/mol TAG
Trisun Oil	ave.	20.480	6.847	28.000	2.275	0.02	1.81
	Stdev.	2.970	0.086	0.900	0.022	---	---
Soybean Oil	ave.	18.910	7.283	39.600	3.056	0.03	2.43
	Stdev.	3.280	0.071	1.200	0.064	---	---
Olive Oil	ave.	24.470	7.362	30.900	2.353	0.02	1.87
	Stdev.	2.570	0.033	0.700	0.046	---	---

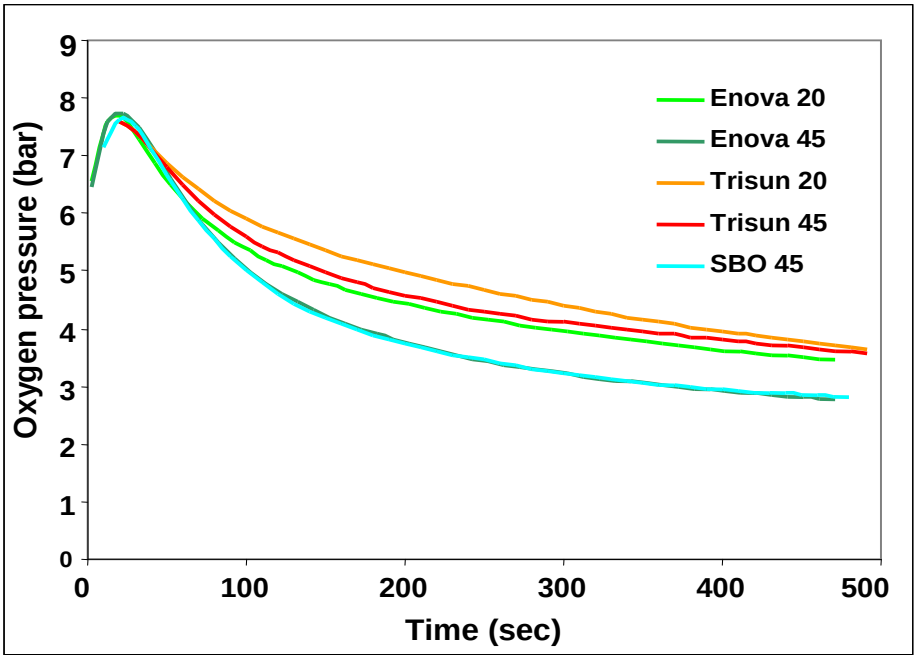

Figure 21. Comparison of oxygen consumption by mono-unsaturated Trisun (T) and olive (O) oils with polyunsaturated soybean oil (SBO). Oils were heated at 180 °C for eight hours under 5 bars oxygen. Sample weights were 20 and 45 g.

Table 14. Oxygen consumption and oxidation parameters for 5 g samples of food oils heated at 180 °C for 3 hour in Oxipres oxygen bombs

		Minutes To peak	Max P	Initial Rate mbars/min	Total O2 consumption bars	mol O2	mol/mol TAG
Trisun Oil	ave.	25.240	7.475	9.000	0.877	0.004	0.334
	Stdev.	0.270	0.204	0.686	0.010	---	---
Soybean Oil	ave.	21.390	7.656	19.300	1.317	0.006	0.501
	Stdev.	0.180	0.010	0.002	0.036	---	---
Olive Oil	ave.	22.440	7.540	17.100	1.171	0.005	0.446
	Stdev.	6.890	0.019	0.006	0.257	---	---

Figure 22. Browning differences in mono-unsaturated Trisun oil and polyunsaturated soybean and Enova oils heated at 180 °C for 24 hours under 5 bars oxygen.

4.5. Effects of Pressure (oxygen or air)

Oxygen pressure is probably the most critical factor controlling lipid oxidation at ambient temperature, and it should play an even greater role at elevated temperatures because oxygen is necessary to form reactive peroxyl radicals by addition to any radicals present and because oxygen solubility changes with temperature. For water, oxygen solubility decreases with temperatures, but oils are the opposite – oxygen solubility increases with temperature, possibly because the thermal energy disrupts some of the van der Waals associations between lipid acyl chains. This solubility increase is shown in table 15.

To test the response of the Oxipres^{TM} under different atmospheres and to determine effects of oxygen pressure on thermal oxidation/degradation of Blend oils,

Table 15. Effect of temperature on oxygen solubility in food oils (data based on hardened lard and olive oil) (Gunstone 1997).

Solubility at 1 bar (mg/kg oil)			Dissolved in oil sat'd w. air(mg/kg oil)	
Temp. °C	O_2	N_2	O_2	N_2
0	170	80		
25	180	85	38	66
50	185	90		
75	190	95		
100	200	105		
125	---	110		
150	---	115		

10 g samples were heated at 180°C under 0.5, 1, 2, 3, 4 and 5 bars pure oxygen and air. Oxygen consumption increased dramatically with oxygen concentration under oxygen (Figure 23, Table 16) and to a lesser extent under air (Figure 24, Table 17), which is to

be expected. However, there are three notable differences.

First, the increase in both rate of initial pressure drop and (Figure 25) and total oxygen consumption (Figure 26) was linear with pressure under oxygen, while in air both effects were non-linear and appeared to saturate with increased pressure. The most obvious explanation for this would be that the system is not limited under oxygen so reactions can be proportional to the oxygen pressure. Oxygen limitation under air which has only ~21% oxygen would explain non-linearity of reaction with oxygen pressure, but the shape of the curve should be opposite what was observed – i.e. oxygen limitation should be relieved as pressure increases.

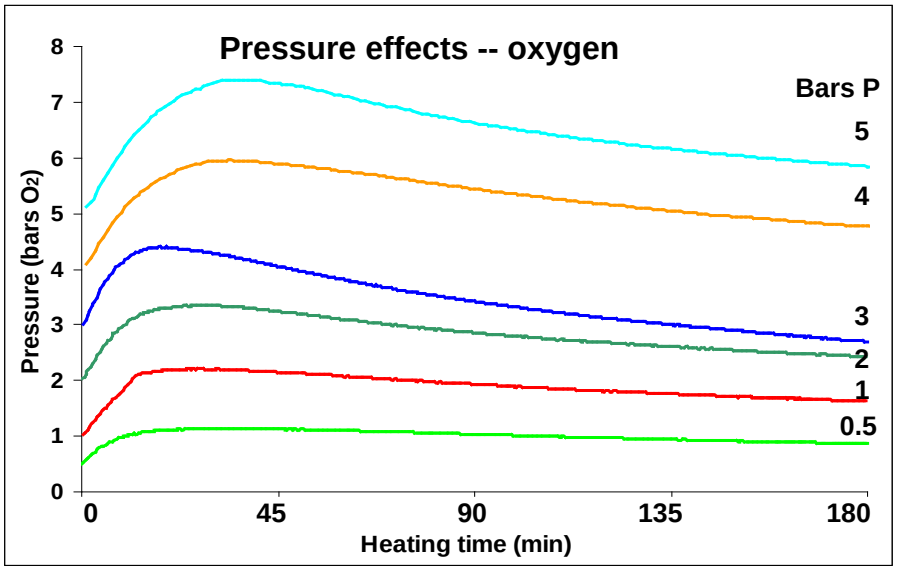

Figure 23. Effects of oxygen pressure on total oxygen consumption and rates of Blend oils heated at 180 °C for three hours. Top: full curves. Bottom: normalized to peak pressure.

Table 16. Effects of oxygen pressure on oxidation parameters of Blend oils heated at 180 °C for three hours under oxygen.

Pressure	Time to peak (min)	Peak Pressure	Initial rate/min mbars	mmol O_2	Total oxygen consumed bars	mol O_2	mol O_2/ mol TAG
0.5 bar	32.8	1.0146	2.6	0.0112	0.278	0.0013	0.1131
1 bar	24.38	2.3199	5.9	0.0271	0.65	0.0030	0.2646
2 bar	27.58	3.293	9.6	0.0442	0.883	0.0041	0.3594
3 bar	18.8	4.4676	16.8	0.0773	1.46	0.0067	0.5943
4 bar	18.25	5.9524	20.5	0.0943	1.706	0.0079	0.6945
5 bar	18	7.4383	30.2	0.138	2.248	0.0103	0.9151

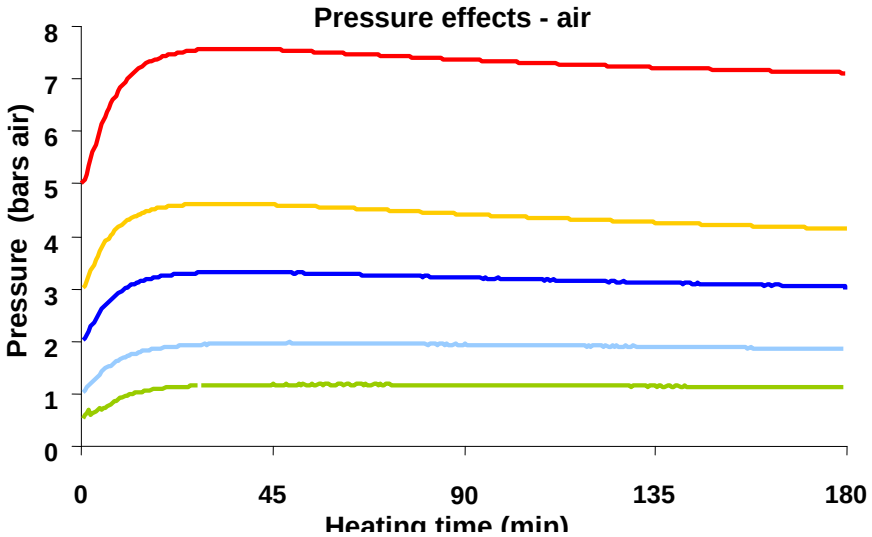

Figure 24. Effects of pressure (air) on total oxygen consumption and rates Blend oils heated at 180 °C for three hours.

Table 17. Effects of air pressure on oxidation parameters of Blend oils heated at 180 °C for three hours under air.

Pressure	Time to peak (min)	Peak Pressure	Initial rate/min mbars	umol O_2	Total oxygen consumed bars	mmol O_2	mmol O_2/ mol TAG
0.11	55.75	1.1819	0.72	3.31	0.123	0.57	50.07
0.21	51.34	1.9731	1.28	5.89	0.149	0.69	60.65
0.42	37.87	3.3223	2.5	11.5	0.337	1.50	137.2
0.63	31.89	4.6239	4.01	18.5	0.46	2.12	187.3
1.05	36.33	7.5788	4.71	21.7	0.485	2.23	197.4

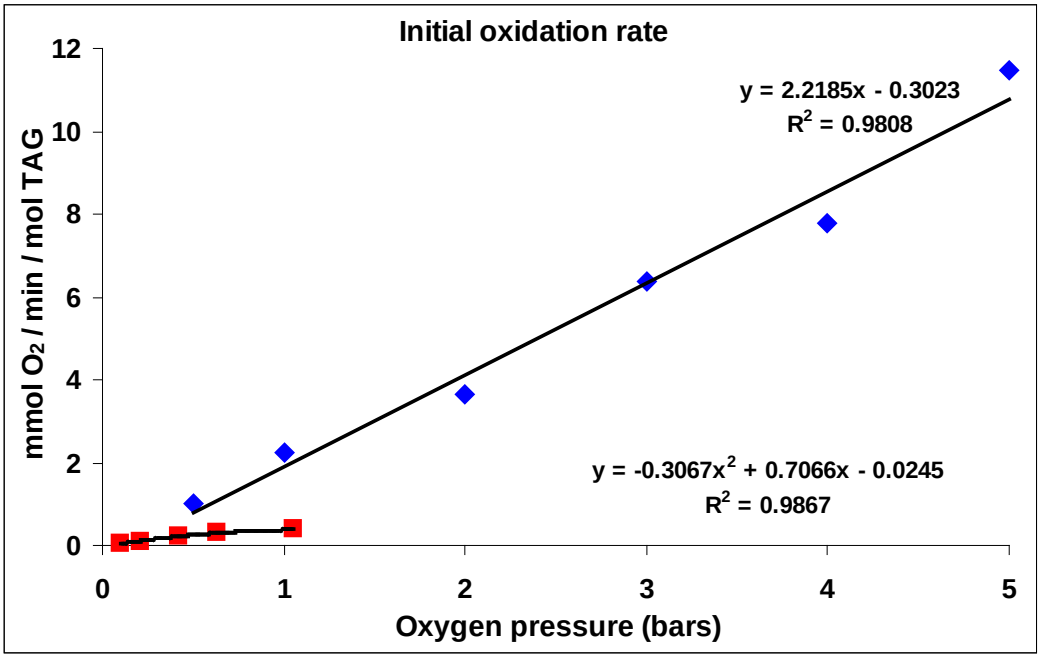

Figure 25. Effects of oxygen pressure on initial pressure drop for Blend oil samples heated under oxygen (blue) or air (red) at 180 °C for three hours. Best fit regression equations are shown

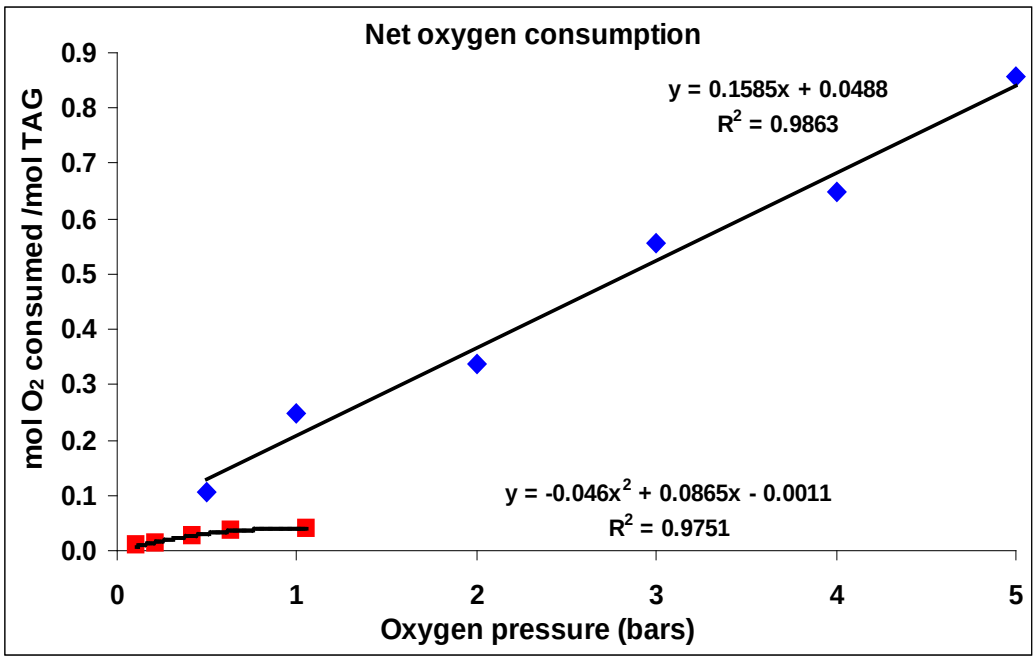

Figure 26. Effects of oxygen pressure on net oxygen consumption for Blend oil samples heated under oxygen (blue) or air (red) at 180 °C for three hours. Best fir regression equations are shown.

Second, against expectations, oxidation was not continuous with absolute oxygen concentration moving from air to oxygen. Total oxygen consumption in air averaged about 20% of the corresponding oxygen concentrations in pure oxygen (i.e. pO_2 in 5 bars air with 20% oxygen ≈ 1 bar pure oxygen) even after accounting for the partial pressure of oxygen in air (Table 18); initial oxygen consumption rates in air versus oxygen are slightly lower, about 15% (Table 19). The reasons for this difference need to be explored further.

To explore reasons for these behaviors more closely, actual oxygen consumption was compared to the theoretical amount of oxygen that should be present. As shown in Table 16, with oxygen pressurization the system is clearly not oxygen limited. Enough

oxygen is present that even at 0.5 bars pressure more than 1/3 of the total oxygen present was consumed. This % decreased with pressure, indicating that the reactions were saturated. That both first (k) and second order (k') rate constants are relatively constant with pressure under oxygen further supports this saturation, i.e. the reaction increases but the rate of increase does not change with pressure (Table 17). This means that the overall reaction is independent of oxygen (zero order) and the rate controlling factor is something else (e.g. thermal scissions to generate radicals).

In contrast, under air pressurization less than 10% of available oxygen was consumed. Thus, even though enough oxygen is present to fuel at least initial stages of oxidation and make the oil noticeably rancid (10% oxidized is considered quite rancid), reactions under these conditions must be very inefficient. The % available oxygen consumed increased with pressure, suggesting increased efficiency of contact and this could result either from increased diffusion into the oil or surface contact with increased O_2 concentrations in the headspace. The greatest effects are at the lowest concentrations, as shown in Table 17 and Figure 27. Adding a small amount of oxygen at 1-2 bars air has a very large effect on both oxygen consumption rates and total amount consumed because when too few oxygen molecules are available, diffusion of oxygen to radical sites becomes the rate-limiting process. Oxygen consumption increases with pressure because more oxygen molecules are present, but the impact of higher pressure diminishes as pressure increases, saturating levels of oxygen are reached, and initiation reactions (formation of $R^{\bullet}$) become rate controlling.

Table 18 . Effects of bomb and oxygen pressure on efficiency and proportionality of net oxygen consumption by Blend oil heated at 180 °C for three hours in oxygen or in air.

Bars (Total Pressure)	Bars (as P_{O2})	Theoratical O2 actually available mol/mol TAG	% consumed	% air vs O_2
O2				
5	5	2.89	29.6	
4	4	2.31	28.1	
3	3	1.74	31.94	
2	2	1.16	28.96	
1	1	0.58	42.62	
0.5	0.5	0.29	36.53	
air				
5	1.05	0.61	6.33	21.39
4	0.84	0.49	7.48	26.62
3	0.63	0.36	7.46	23.36
2	0.42	0.24	4.98	17.2
1	0.21	0.12	3.98	9.34

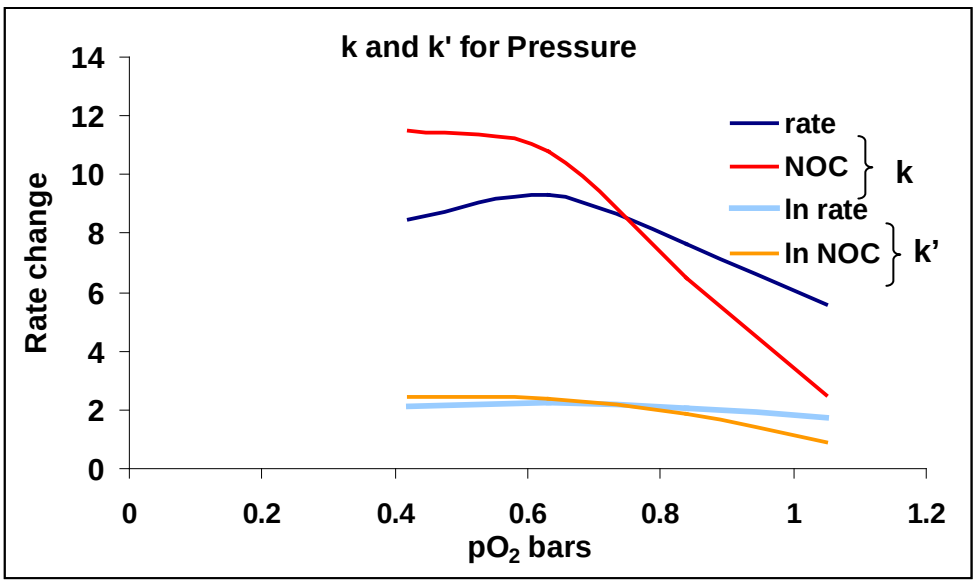

Figure 27. Oxygen pressure effects on rate of oxygen consumption increase in Blend oils heated for three hours at 180 °C under air at various pressures.

Table 19. Kinetic calculations for pressure effects on oxygen consumption rates and net oxygen consumption in Blend oils heated at 180 °C for three hours under varying pressures of oxygen or air. NOC = net oxygen consumption.

Bars (Total Pressure)	Bars (as P_{O2})	Rate mbar/min	% air/O_2	absolute Increase (n2-n1)/dP_{O2}	rate of Incr(k) (n2/n1)dP_{O2}
O2					
5	5	30.2		9.7	1.47
4	4	20.5		3.7	1.22
3	3	16.8		7.2	1.75
2	2	9.6		3.7	1.63
1	1	5.9		8.76	7.76
0.5	0.5	1.52			
air					
5	1.05	4.71	15.6	1.67	2.8
4	0.84	4.01	19.56	7.19	7.64
3	0.63	2.5	14.88	5.81	9.3
2	0.42	1.28	13.33	5.33	16.93
1	0.21	0.72	12.2		
		ave.	15.11		
			NOC		
O2					
5	5	2.25		0.542	1.32
4	4	1.71		0.246	1.17
3	3	1.46		0.577	1.65
2	2	0.88		0.233	1.36
1	1	0.65			
0.5		1.52			
air					
5	1.05	0.48	21.56	0.06	2.51
4	0.63	0.46	26.98	0.59	6.5
3	0.42	0.34	23.08	0.9	10.77
2	0.21	0.15	17.2	0.24	11.51
1	0.105	0.12	9.34		
		ave.	19.58		

Other studies also have reported larger rate increases at low oxygen, but the critical oxygen level varies from paper to paper depending on experimental condition. Andersson and Lingnert (Lingnert 1999) claim that when atmospheric oxygen is below 0.5% the influence of oxygen is greatly enhanced. Karel (Karel 1992) considers 4-5% oxygen the cut-off line, and Fredriksson (Fredriksson 1968) reports that oxidation rate increase much great from 1%-2% than the increase from 2%-21%.

These studies were all at ambient or moderately elevated temperatures where initiation reactions are isolated in space and time and oxidation rates are considerably lower than the frying temperatures used in this thesis. The 20%-30% oxygen showing higher acceleration in this study may be required for reaction with the extra radical load generated at high temperatures.

Overall, this pressure data suggests that in terms of linearity of response, it appears to be desirable to operate in oxygen atmospheres. However, as will be shown later, excess oxygenation under pure oxygen causes a shift in chemistry pathways and product distributions. In addition, pure oxygen is a poor model for real commercial frying operations that run under air or industrial frying operations that run under reduced oxygen atmospheres. Thus, for practical applications of results it will be desirable to run Oxipres experiments under air at the lowest pressure feasible. For such operation of the Oxipres system, several questions need to be answered:

1) Is the pressure transducer response as sensitive and accurate under air and low pressures as under pure oxygen at high pressures?

2) How does bomb pressure and concentration of oxygen in the headspace affect diffusion into the oil?

3) What are the actual oxygen concentrations attained in the oil under different oxygen pressures?

4) Where does oxygen consumption occur – at the oil surface, in the bulk oil, or both – and what are the differences in rates?

4.6. Effects of temperature

That lipid oxidation usually has an induction period in which little or no oxidation is detectable is well-documented in the literature, and induction periods are commonly used to assess the stability of oil or fat-containing foods. The longer the induction period, the more stable the food is. The Oxipres™ system was actually designed to determine induction periods, and calculations are included in its software. Standard Oxipres™ conditions are 60 °C, and most studies are conducted at this "accelerated shelf life" temperature (Trojakava 2001, Pokorny 2003, Reblova, 2006); few studies have used the Oxipres™ at higher temperatures, and no others have used this system at frying temperatures**.** If oil oxidation follows Arrhenius kinetics, the rate should double for each ten degrees increase in temperature, and this may eliminate induction periods under frying conditions.

To determine effects of high temperatures on induction periods and oxidation rates, Blend oils were heated for three hours under two and five bars air and oxygen at 100, 120, 150, 160, 170 and 180 °C. Oxipres curves in Figures 28-34 and rate data in Table 20 show very clearly that temperature has a tremendous effect on lipid degradation. An induction period of 650 minutes was present at 100 °C, it decreased to 150 minutes at 120 °C, and disappeared at higher temperatures. At the same time, the time to reach peak pressure decreased with temperature because oxidation began earlier, even during heating, and proceeded faster so that oxygen consumption by reactions counterbalanced pressure increase with temperature. This was particularly evident in

samples heated under 5 bars oxygen where the peak pressures were lower than expected from the temperature. In contrast, at 100 and 120 °C the peak pressures were higher than expected from PV=nRT with mere temperature rise. We hypothesize that volatile oxidation products released from the oils as the bombs are heated contribute to this increased pressure, and at low pressures these contribute a larger proportion of the headspace; at high pressures, especially under oxygen, rapid reaction of oxygen with radicals more than counterbalances this release.

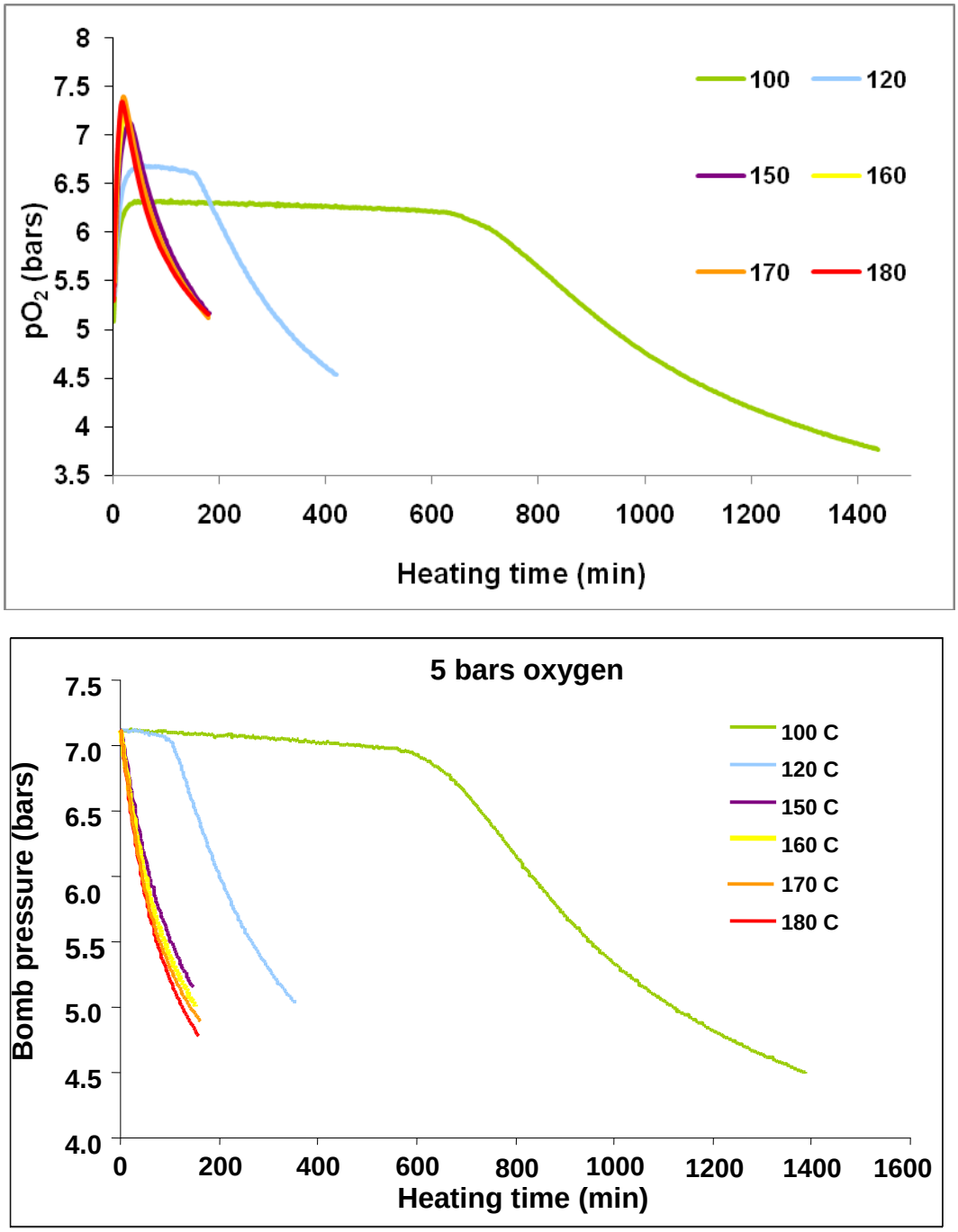

Figure 28. Oxygen consumption curves for Blend oil heated at temperatures ranging from100 to 180 °C under 5 bars oxygen. Top: full curves showing initial increase with heating (PV=nRT). Bottom: curves normalized to peak pressure to facilitate comparison of rates.

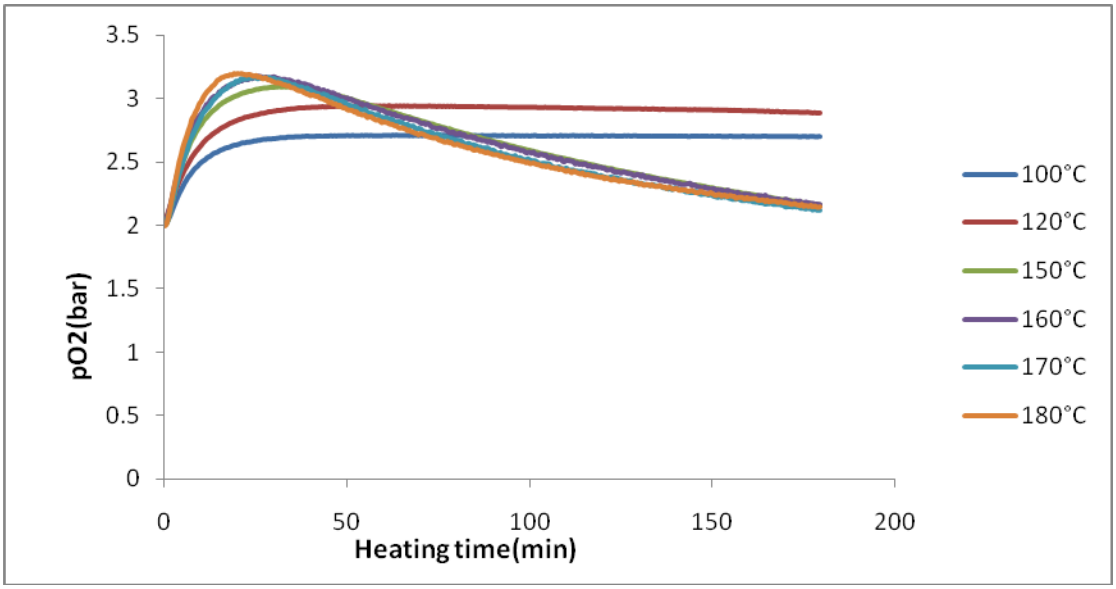

Figure 29. Oxygen consumption curves for Blend oil heated at temperatures ranging from100 to 180 °C under 2 bars oxygen. Top: full curves showing initial increase with heating (PV=nRT). Bottom: curves normalized to peak pressure to facilitate comparison of rates.

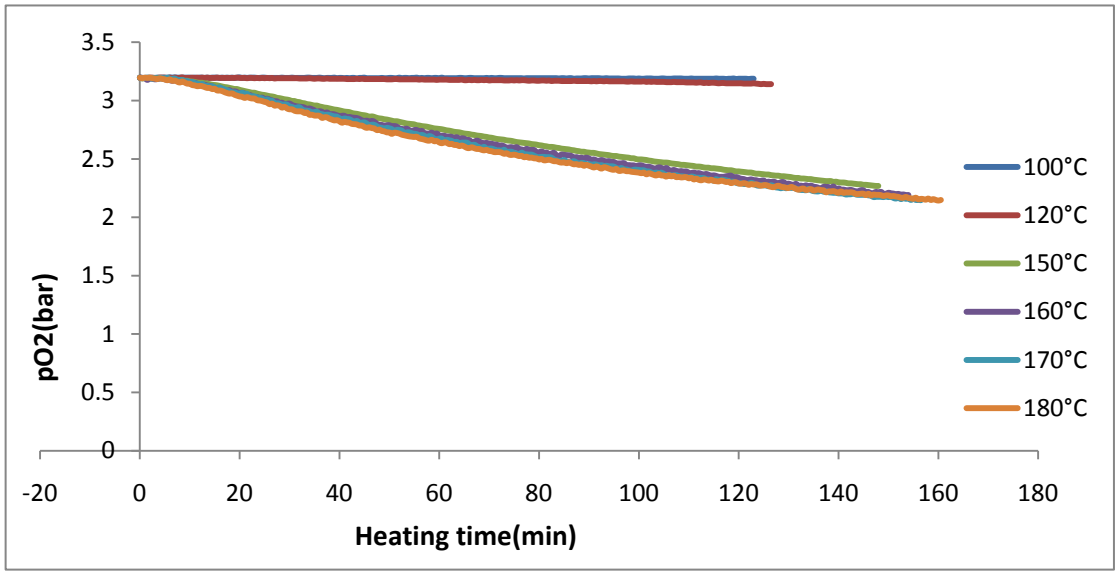

Figure 30. Peak-normalized Oxygen consumption curves for Blend oil heated at temperatures ranging from100 to 180 °C under 2 bars oxygen. Top: full curves showing initial increase with heating (PV=nRT). Bottom: curves normalized to peak pressure to facilitate comparison of rates.

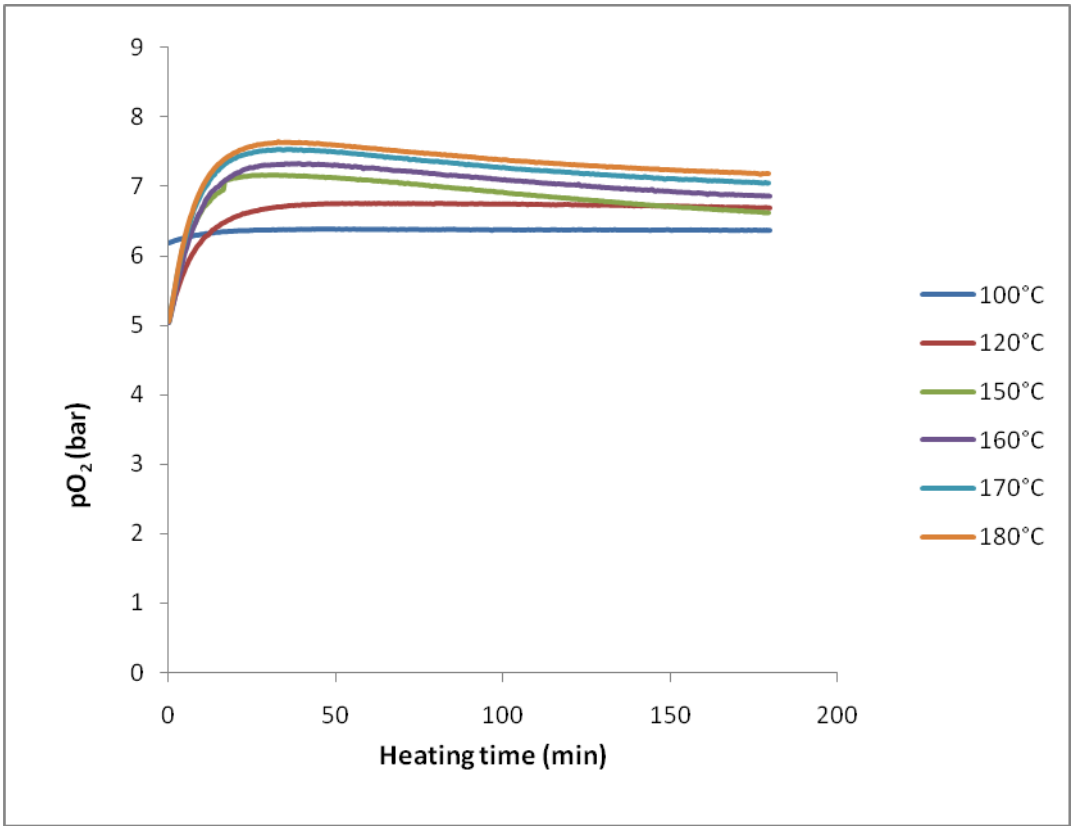

Figure 31. Oxygen consumption curves for Blend oil heated at temperatures ranging from100 to 180 °C under 5 bars air. Top: full curves showing initial increase with heating (PV=nRT). Bottom: curves normalized to peak pressure to facilitate comparison of rates.

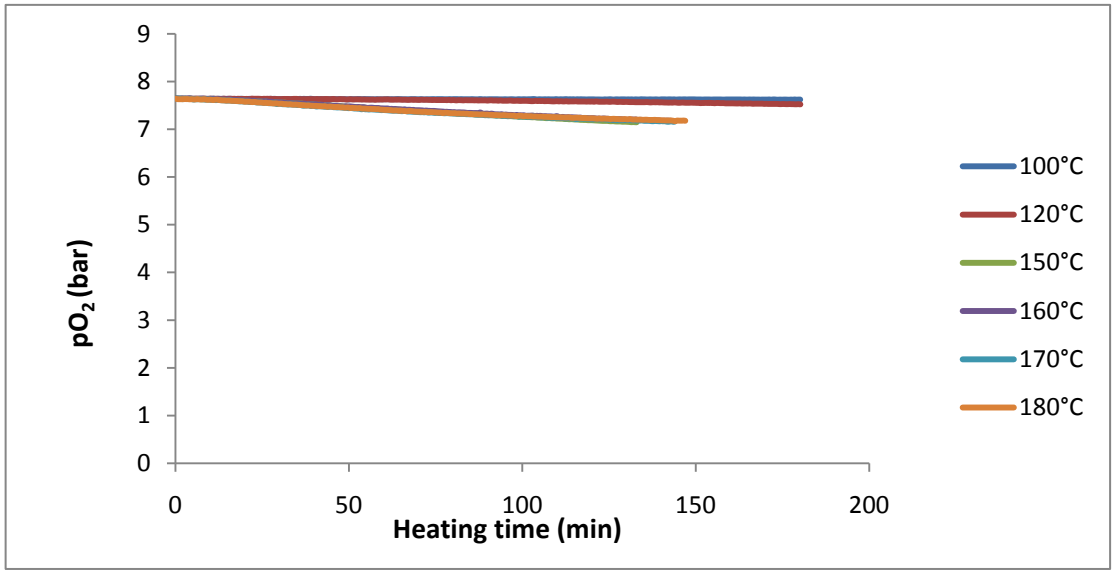

Figure 32. Peak-normalized Oxygen consumption curves for Blend oil heated at temperatures ranging from100 to 180 °C under 5 bars air. Top: full curves showing initial increase with heating (PV=nRT). Bottom: curves normalized to peak pressure to facilitate comparison of rates.

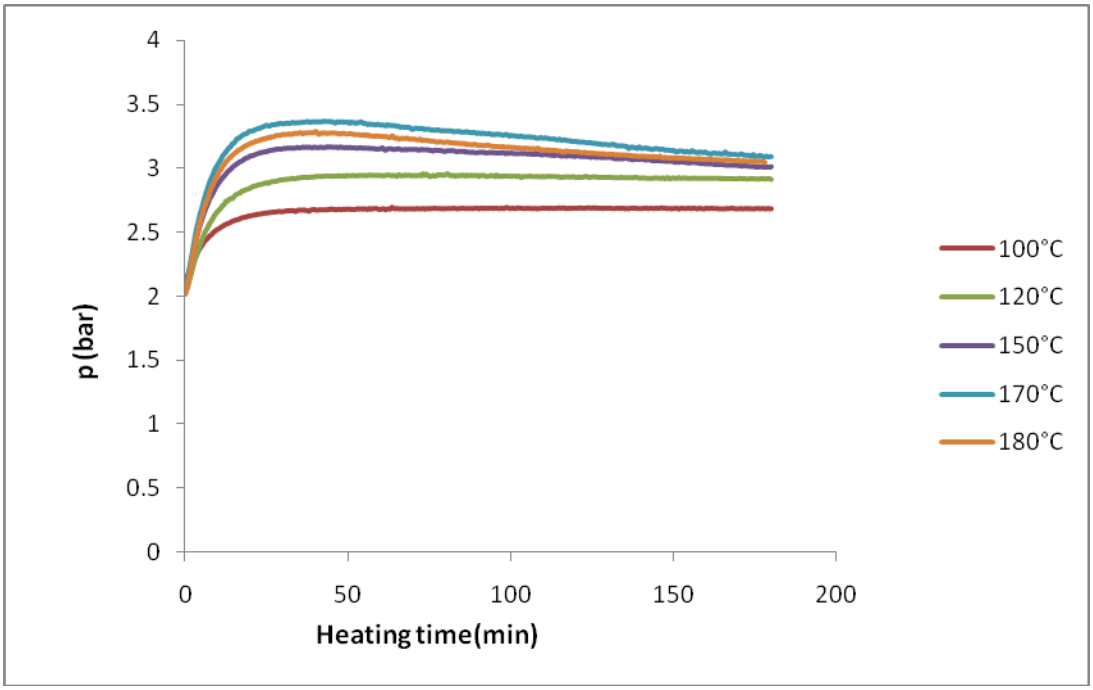

Figure 33. Oxygen consumption curves for Blend oil heated at temperatures ranging from100 to 180 °C under 2 bars air. Top: full curves showing initial increase with heating (PV=nRT). Bottom: curves normalized to peak pressure to facilitate comparison of rates.

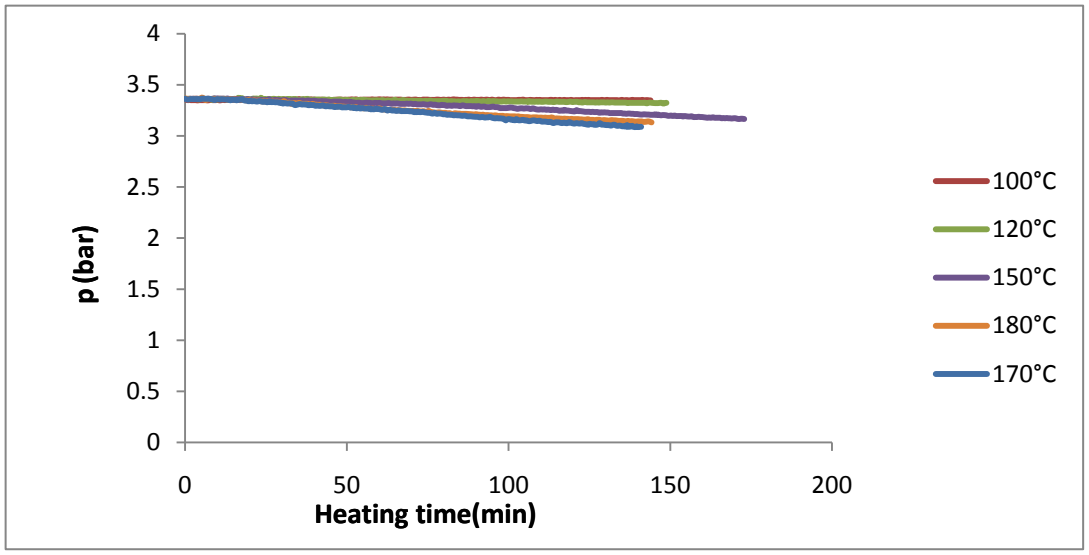

Figure 34. Peak-normalized Oxygen consumption curves for Blend oil heated at temperatures ranging from100 to 180 °C under 2 bars air. Top: full curves showing initial increase with heating (PV=nRT). Bottom: curves normalized to peak pressure to facilitate comparison of rates.

Table 20. Oxidation parameters from Oxipres curves of Blend oil heated at various temperatures for three hours under 5 bars O_2.

		Peak P.			Consumpt. rate		Total O2 consumption		
T °C	**Time to** peak P.	Pmax	expected	Δ	mbar	mmol O2/min	bars	moles O2	mol O2 mol/TAG
100	59.070	6.386	6.258	0.127	---	---	---	---	---
	60.917	6.359	6.258	0.101	---	---	---	---	---
ave	59.993	6.372	---	0.114	---	---	---	---	---
sd	0.923	0.013	---	0.019	---	---	---	---	---
120	54.870	6.670	6.594	0.076	---	---	---	---	---
	65.380	6.755	6.594	0.161	---	---	---	---	---
ave	60.125	6.713	---	0.119	---	---	---	---	---
sd	5.255	0.043	---	0.060	---	---	---	---	---
150	28.100	7.153	7.097	0.056	21.530	0.099	2.044	0.009	0.832
	29.600	7.138	7.097	0.041	26.460	0.122	2.276	0.010	0.927
ave	28.850	7.146	---	0.048	23.995	0.110	2.160	0.010	0.879
sd	0.750	0.007	---	0.011	2.465	0.016	0.164	0.001	0.067
160	24.033	7.167	7.265	-0.098	26.460	0.122	2.100	0.010	0.855
	25.817	7.257	7.265	-0.008	24.500	0.113	2.156	0.010	0.878
ave	24.925	7.212	---	-0.053	25.480	0.117	2.128	0.010	0.866
sd	0.892	0.045	---	0.064	0.980	0.006	0.040	0.000	0.016
180	17.450	7.355	7.601	-0.246	26.700	0.123	2.286	0.011	0.930
	17.333	7.309	7.601	-0.292	27.190	0.125	2.286	0.011	0.930
ave	17.392	7.332	---	-0.269	26.945	0.124	2.286	0.011	0.930
sd	0.058	0.023	---	0.033	0.245	0.002	0.000	0..000	0.00

Table 21. Oxidation parameters from Oxipres curves of Blend oil heated at various temperatures for three hours under 2 bars air

	Time	Peak P.			Consumpt. rate		Total O_2 consumption		
T °C	to peak	Pmax	expected	Δ	mbar	umol O_2/min	mbars	mmoles O_2	mmol O2 mol/TAG
100	100.18	2.70	6.26	0.13	---	---	---	---	---
120	56.60	2.94	6.59	0.08	---	---	---	---	---
150	47.70	3.17	7.10	0.06	1.47	1.31	156.3	0.14	0.0018
160	44.28	3.36	7.27	-0.10	2.20	1.98	275.9	0.25	0.0032
180	41.08	3.28	7.60	-0.25	2.32	2.08	236.9	0.21	0.0028

Table 22. Oxidation parameters from Oxipres curves of Blend oil heated at various temperatures for three hours under 5 bars air

								Total O_2 consumption	
T	Time to	Peak P	Pressure		Rate/min			mmoles	mmol O2
(°C)	peak (min)	bars	expected	Δ	mbar	umol O_2	bar	O_2	mol/TAG
100	42.08	6.38	6.26	0.12	---	---	---	---	---
120	55.32	6.75	6.59	0.16	---	---	---	---	---
150	32.37	7.17	7.10	0.07	4.52	4.10	1.97	0.49	0.0055
160	40.45	7.33	7.27	0.07	4.20	3.80	2.12	0.43	0.0049
170	33.48	7.54	7.43	0.11	4.76	4.30	2.31	0.44	0.0049
180	32.97	7.64	7.60	0.04	4.27	3.80	2.22	0.42	0.0047

Table 23. Oxidation parameters from Oxipres curves of Blend oil heated at various temperatures for three hours under 2 bars O_2

T (°C)	Time to peak (min)	Peak P bars	Pressure expected	Δ	Rate/min mbar	Rate/min mmol O_2	mbars	Total O_2 consumption mmoles O_2	Total O_2 consumption mmol O2 mol/TAG
100	54.05	2.71	2.50	0.21	---	---	---	---	---
120	53.50	2.94	2.64	0.31	---	---	---	---	---
150	31.60	3.09	2.84	0.25	8.79	0.040	929.60	4.28	378.4
160	25.58	3.17	2.91	0.27	7.77	0.036	1006.10	4.63	409.6
170	23.23	3.17	2.97	0.19	10.62	0.049	1050.00	4.83	427.4
180	19.15	3.20	3.04	0.16	10.62	0.049	1047.60	4.82	426.5

Surprisingly, after the large increase in rate between 120 and 150 °C, the variation in oxidation rate and net oxygen consumption were very small for temperatures above 150 °C. A Q_{10} of essentially 1.0 calculated from the data (Table 24) suggests that above 150 °C, the reaction rate is nearly independent of temperature. This can be an indication that when the working temperature is above some critical point, e.g. 150°C, some thermal reaction(s) becomes the dominant oxidation initiator(s) and occurs at a relatively constant rate that is the rate limiting step. Overall rates varied with oxygen pressure (5 or 2 bars oxygen vs 5 or 2 bars air), but the pattern of temperature effects was the same, further supporting thermal reactions as the controlling factors.

Table 24. Q10 values for oxygen consumption by Blend oil heated for 3 hours at temperatures ranging from 100 to 180 °C. Calculated for zero (k) and first (k') order reactions of oxygen.

	Calculated by (Kt-Ko)				Calculated by $[E_a/R/2.303]/[T_{0(T0-10)}]^b$			
	2 bars air		5 bars air		2 bars air		5 bars air	
T °C	k	k'	k	k'	K	k'	k	k'
100	---	---	---	---	---	---	---	---
120	1.10	(a)	0.50	0.80	0.86	(a)	0.86	0.87
150	0.70	0.70	1.30	2.00	0.87	0.87	0.87	0.87
160	1.10	1.30	1.60	1.40	0.88	0.88	0.88	0.88
170	2.40	2.00	0.80	1.00	0.89	0.88	0.89	0.88
180	1.00	1.10	1.10	1.00	0.89	0.88	0.89	0.89

a k = (Ao – At)/ t; k' = ln(Ao/At)/t. Running 20 minute slopes were determined and the maximum value was used for rate calculations.

b Determined by plotting ln k or k' vs 1/T (K); slope is Ea/R.

Table 25. Analysis of kinetic data – effects of temperature under 5 bar and 2 bar air pressurization

Temperature		5 bars air		2 bars air	
C	K	k	k'	k	k'
100	373	0.80	0.000038	0.23	0
120	393	0.84	0.000057	0.49	0.000134
150	423	3.37	0.000346	0.98	0.000273
160	433	4.30	0.000495	1.10	0.000365
170	443	4.73	0.000494	2.66	0.000725
180	453	5.38	0.000519	2.78	0.000777

4.7. What processes are being reflected in the Oxipres curves?

Pressure decrease results from oxidation-specific reactions in the oils

We have a reference of unidentified source that criticizes the Oxipres approach and claims that the decrease in headspace pressure during incubation is due exclusively to oxygen diffusion into the oil and is totally unrelated to reactions in the oil. To counter this claim, verify that the changes in pressure were directly and specifically related to oxidation reactions in the oil, and learn more about the physical and chemical processes that control sample behavior in the Oxipres, several control analyses were run.

a) **Empty Oxipres cells** heated under identical conditions as the oils showed pressure increasing with temperature but no subsequent oxygen consumption (Figure 35). The peak pressure reached was higher than with oil samples because the gas volume in the cell was higher without oil. The same behavior was observed with and without the glass containers present in the cells during heating.

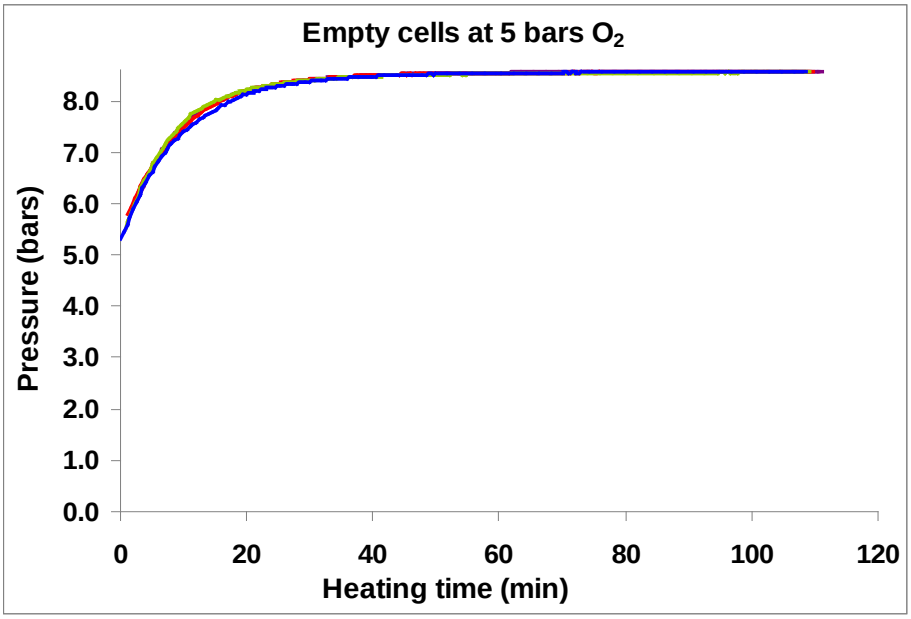

Figure 35. Lack of oxygen consumption in empty cells heated at 180 °C under standard conditions, 5 bars oxygen.

b) Oils heated under nitrogen. Since the Oxipres sensor is a pressure transducer, diffusion of any headspace gas into the oil should be reflected in loss of pressure. When oils were heated under nitrogen instead of oxygen pressurization, headspace pressure loss was negligible (Figure 36, Table 26). Although nitrogen solubility in oils is about half that of oxygen (Table 26), it is high enough to observe a pressure drop if diffusion is responsible for the Oxipres curve. Since there was no pressure drop at all under nitrogen, the gas consumption normally seen when oils are heated in air and oxygen cannot derive merely from diffusion of headspace gas into the oil.

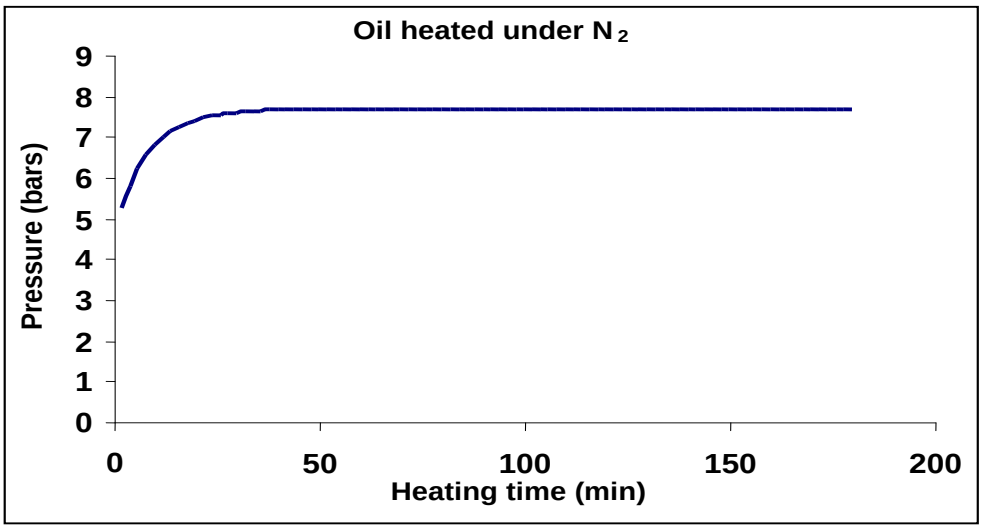

Figure 36. Oils heated in the Oxipres under nitrogen show no oxygen consumption.

Table 26. Comparison of pressure changes in Oxipres cells to oxygen and nitrogen solubilities in oils. Solubilities taken from Table 13.

	Solubility moles gas[a]			Actual Pressure decrease		
	mg/kg oil	/kg	/sample	bars P to satn	bars	mols	Satn[b]
O_2	230	0.00719	0.000072	0.01672	2.18315	0.009388	130.61
N_2	120	0.00429	0.000043	0.00997	0.00855	0.000037	0.86

[a] The factor 0.0043 mols gas/bar from Section 1.2.b. was used for conversion.

[b] Mols actually consumed / saturation solubility limit

c) Oxygen diffusion vs oxidation reactions

Questions have been raised about whether Oxipres curves reflect true reactions or only high oxygen pressure forcing oxygen diffusion into the oils. Oxygen solubility in oils is low (Table 15) and even high pressure cannot force solubilization that exceeds this limit. Extrapolating the oxygen solubility given in Table 15 to 175 °C, the solubility limit is 0.007 mole oxygen/kg oil or 6.2 mmol O_2/mol TAG in 10 g samples.

There are nearly 3 moles oxygen in the headspace of the Oxipres cells at 5 bar oxygen, so diffusion to oil saturation solubility would barely be detectable as a reduction of bomb pressure. In contrast, total oxygen uptake in 3 hr heating (850 mmol O_2/mol TAG, Table 15), far exceeds mere oxygen solubility. In addition, as will be shown later, lipid oxidation products (conjugated dienes, peroxides, and alkenals) are present at much higher levels than the oxygen solubility limit of 0.62 mmol O_2/mol TAG.. Thus, oxygen must continually be replenished to the oil over the heating time, and the oxygen consumption curves must reflect processes (e.g. reactions) other than oxygen diffusion into the oil. However, whether the reactions occur in the bulk oil, at the oil-headspace interface, or both remains an issue.

We have been unable to find an oxygen probe able to measure actual oxygen levels in hot oil. To obtain an indirect indication of how fast oxygen can diffuse into the oil from the headspace, samples of oils were pre-saturated with either argon or oxygen before heating in the oxygen bomb under standard conditions (180 °C, 3 hours, O_2). If oxygen diffusion is a dominant factor, the oxygen-saturated oil should show faster response because the oxygen solubility limit of the oil has already been reached. Argon-saturated oil should show slower initial response since it will outgas during heating, which will also yield a higher peak pressure; any argon remaining in the oil should provide some antioxidant effect. This is indeed what was observed (Table 22, Figure 35).

The oxygen-saturated oil reached equilibrium faster (16.6 minutes) because the

pre-gassing displaced other gases and left only oxygen which will not outgas against high pO_2; and it reached a lower peak pressure (7.15 bars) because it began oxidizing faster and earlier, consuming oxygen even during heating (Figure 35, top graph). Argon is heavier than oxygen and diffuses out of oil slowly, so it required more time to reach pressure equilibrium during heating (18.9 minutes), and the amount outgassed contributed to the higher peak equilibrium pressure (7.29 bars). Importantly, the rapid initiation of oxidation suggests that oxygen diffusion into the oil is very fast -- at least as fast as oil outgassing and heating to 180 °C, if not faster. This provides further evidence that the drop in oxygen pressure *after this equilibration point* in Oxipres curves is due to chemical reactions rather than oxygen diffusion into the oil.

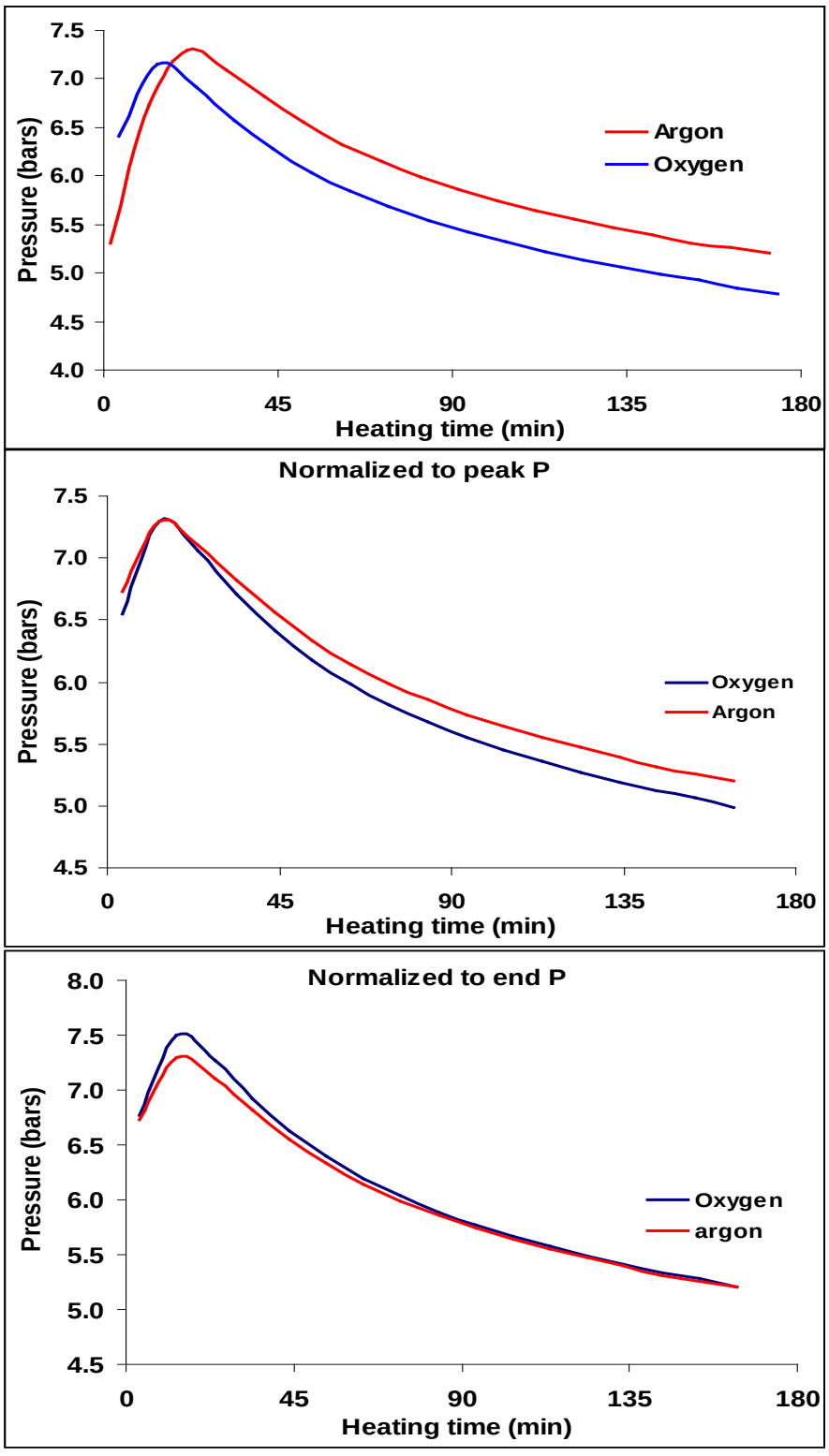

Figure 37. Effect of pre-sparging Blend oils with argon vs oxygen before heating for 3 hours at 180 °C under 5 bars oxygen. Top: direct curves as recorded. Middle: Curves normalized to peak pressure. Bottom: Curves normalized to final pressure to show points of divergence between oxygen and argon.

Table 27. Oxidation parameters for Blend oils pre-saturated with oxygen or argon before heating 3 hours at 180 °C under 5 bars oxygen.

	Oxygen	Argon
Minutes to peak O_2	16.64	18.94
Peak O_2 (bars)	7.15	7.29
Initiation rate (mbar O_2/min)	33.15	27.17
Total O_2 consumed (bars)	2.36	2.11

Normalization of the curves to peak pressure and to final pressure provides additional interesting information. The difference between the two sample curves is greatest at the peak pressure where the oxygen-sparged oil oxidizes faster but much less than might be expected (bottom graph, Figure 37), then it decreases from then until about 90 minutes, when the oxygen consumption rates for the two oils become the same. The difference in net oxygen consumption over the entire heating time is small – only 0.08 moles O_2/mole TAG (middle graph, Figure 37). These results support rapid oxygen diffusion into the oil, to almost complete saturation within 18 minutes, so that the argon-sparged oil begins oxidizing only slightly behind the oxygen-saturated oil. Another possible explanation is that most oxygen consumption by the oils occurs at the oil surface were there is greatest contact with high oxygen. Thus, the argon-sparged sample begins to oxidize at the surface even as the oil heats, while the bulk oil retains some protection until the argon is dissipated. At the present time, we cannot distinguish between these two processes, but it is likely that some combination of the two occurs.

4.8. Effect of agitation on lipid degradation.

The slow-down in oxygen consumption over time even while thermal stresses initiating reactions remained constant raises questions about oxygen limitation in the oils. It has already been shown that oxygen in the bomb chamber is sufficient to support much more oxidation than is observed. One possible explanation for this is that there is insufficient or no mixing in the oil by thermal currents, so oxygen diffuses into only a surface layer of the oil and does not get mixed into lower layers.

Laminar swirling. To test the role of mixing in oxygen consumption, a simple experiment was designed in which one group of samples were removed from the bomb periodically and swirled to produce agitation, then replaced in the bomb. A second set of samples were removed and held for the same time periods without swirling as temperature controls. These two sets were compared with a third that was not removed from the bombs.

Figure 38 (top) shows effects of gentle laminar swirling for different times from 2 minutes to 15 minutes. Pressures of the swirled group dropped notably with each swirling, proportional to swirling time (Figure 38, bottom), then returned to control levels. Pressures of the unswirled temperature controls, however, were nearly the same, indicating that most of the pressure drop was due to decreased temperature, following PV=nRT, rather than increased oxygen diffusion or access resulting from the swirling. The small differences in the swirled samples (Table 28), corresponding to 0.02 to 0.14 μmol oxygen, were most likely due to slightly greater cooling induced by swirling. The

combined gas law predicts a drop of 0.0069 bars per degree drop in temperature under the Oxipres conditions. Although the oil temperature could not be measured, the amount of cooling predicted by PV=nRT for the observed pressure drops were consistent with the rate of cooling when cells are removed from the bombs after heating, i.e. the temperature predicted for 15 min swirling matches what is seen after 15 min of system cool down. After each time out of the block, the pressures of swirled and unswirled samples both returned nearly to that of the control, and the overall curves tracked control curves almost identically. This further supports cooling as a major source of pressure drop.

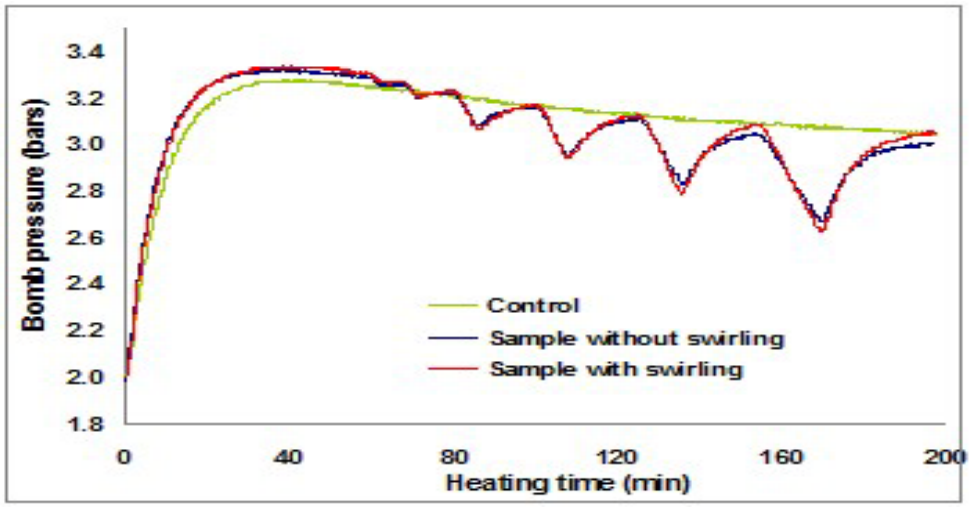

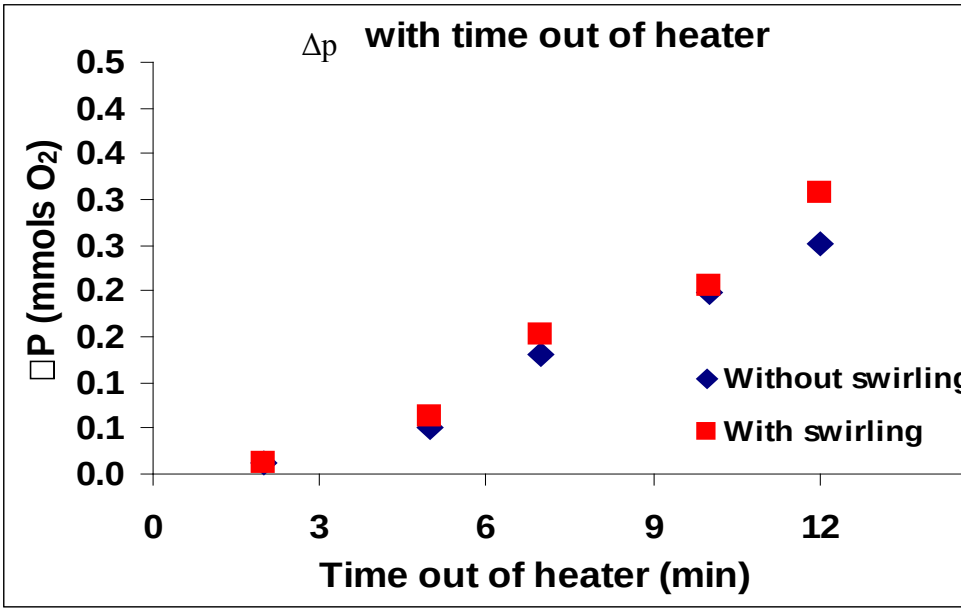

Figure 38. Top: Oxygen consumption curves for 10 g samples of Blend heated at 180 °C under 2 bars air pressure with and without gentle laminar swirling when the Oxipres cell was removed periodically from heater. Bottom: Change in pressure drop with time out of heater. Best fit curves with swirling: $y = 0.0035x^2 + 0.0596x - 0.092$, $R^2 = 0.9906$; without swirling: $y = 0.0016x^2 + 0.0719x - 0.1335$, $R^2 = 0.9927$.

Table 28. Calculation of swirling contributions to oxygen consumption.

Sw t (min)	−ΔP wo swirl	−ΔT °	−ΔP w swirling	−ΔT°	ΔT(w-wo)	Theoret Δmbars	Actual Δmbars	(act−theoret) mbars
2	0.021	14.93[a]	0.025	17.91	2.96	4.15[b]	4.18[c]	0.03[d]
5	0.038	27.47	0.048	34.63	7.11	9.95	10.03	0.08
7	0.070	50.33	0.079	58.85	8.45	11.83	11.93	0.10
10	0.075	53.74	0.082	56.12	2.36	3.31	3.34	0.03
12	0.080	57.22	0.098	69.66	12.34	17.27	17.41	0.14
15	0.086	61.70	0.106	75.63	13.82	19.35	19.50	0.15

Sw t = swirling time

[a] −ΔT° is the theoretical temperature change (calculated from the combined gas law) that would occur if all pressure change was due to cooling when Oxipres cells were removed from the heater.

[b] Theoretical pressure change calculated from ΔT(w-wo) assuming all ΔP due to cooling

[c] Pressure change actually measured

[d] Pressure change due to swirling, not cooling.

These results can be interpreted in two ways:

a) Oxygen diffusion was not limiting in the oil samples as normally run in the Oxipres and swirling the sample did not increase oxygen diffusion into the sample.

b) Oxygen solubility in the oil is extremely low, so measurable oxygen consumption must occur at the oil surface. Swirling the sample under these lateral laminar conditions does not change the surface area (surface not broken) so does not increase access to oxygen, hence there is no increase in net oxygen consumption.

Turbulent swirling. To distinguish between these two possibilities, another test was conducted in which cells were swirled with more force to create turbulence that can break the oil surface; the time for swirling was adjusted to 30 seconds to limit cooling effects (Figure 39, Table 29). In this experiment vigorous agitation initially increased the oxidation rate; the effect continued for a short time after swirling was stopped, and

then gradually returned toward control values. However, each successive swirling had less effect on the oxidation rate, suggesting that some processes were becoming saturated, and eventually, agitation had no effect on oxidation rate. Only with extremely vigorous agitation did one sample exhibit sustained enhanced oxidation (swirl 2, Figure 39). In later stages of heating, agitation barely affected oxygen consumption and in the last 60 minutes of heating, oxygen consumption slowed to a very slow rate. At the same time, the static controls removed from the heating block without swirling showed a constant small drop and recovery in the pressure curve with each swirling. The pressure drops were comparable to most swirled sessions, showing that again a major component of the pressure drop from swirling was from cooling. Finally, despite different treatments -- vigorous swirling in one set, parallel cooling in the second set, and neither in the third -- all three treatments ended with very close to the same total oxygen consumption. Turbulent swirling under 2 bars oxygen. To investigate whether the increased oxygen consumption induced by early swirling caused a rapid depletion of the headspace oxygen, swirling experiments were repeated under 2 bars oxygen instead of air. Three separate experiments were run; swirling times in each were 15 sec. Similar patterns as in air were observed: the pressure drop increased with initial swirls, decreased with subsequent swirls, and showed negligible effects in later curves (Figure 39). Under oxygen, the curves did not return to the control level during the normal three hours of heating but after extended heating (five hours) the swirled sample curve did return to the control level (bottom graph, Figure 40), indicating that the pattern was

the same, but just takes longer to consume the higher levels of oxygen.

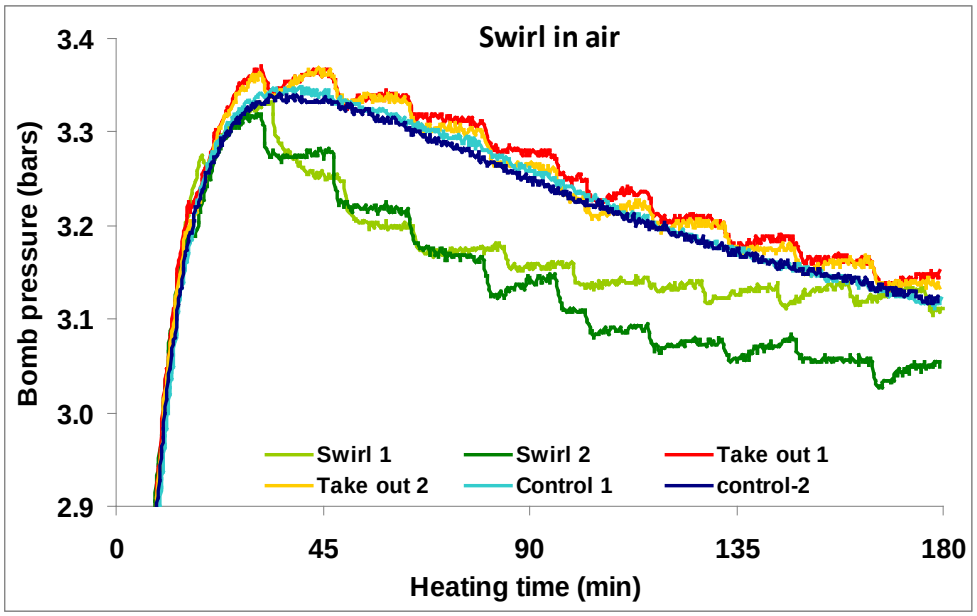

Figure 39. Effect of vigorous swirling on oxygen consumption curves of Blend oil heated at 180 °C for three hours under 2 bars air pressure.

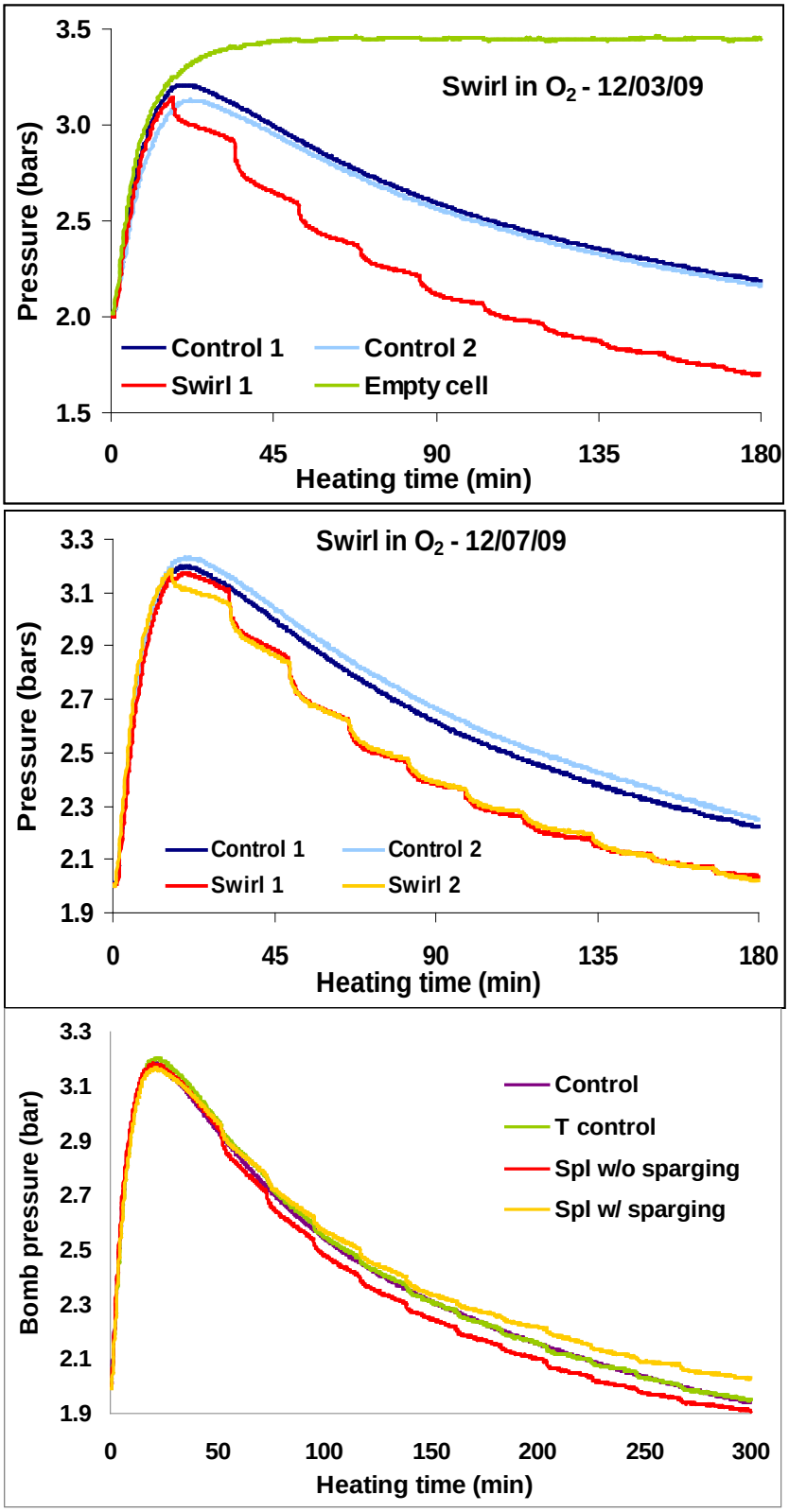

Figure 40 Oxygen consumption curves for 10 g oil samples heated at 180 °C under 2 bars oxygen pressure static or with swirling during periodic removal of the Oxipres cell from the heating block for three minutes. Swirl times: 30 seconds every 15 minutes.

How can these results be explained? What do they indicate about reactions in the Oxipres cells? The major issues needing clarification are:

a) whether oxygen is lost from the headspace by diffusion into the oil or by reaction with radicals in the oil,

b) whether reactions leading to oxygen consumption occur in the oil, at the surface, or both, and in what proportion.

Oils used in these experiments are stored under argon headspace but are not routinely sparged with nitrogen before heating in the oxygen bombs, so some oxygen is already present. Samples pick up some additional oxygen during weighing and transfer to the Oxipres cells, and there is some further diffusion of oxygen into the oil during pressurization. Since solubility of oxygen in oil is very low, it is likely that under most normal conditions, the oil has already reached its oxygen saturation limit by the time the oil reaches frying temperature, so shaking or swirling cannot increase diffusion into the oil except to restore saturation, i.e. to replace any dissolved oxygen already consumed in reaction. This amount is very small, limited by the low solubility of oxygen.

Does oxygen consumption occur in the oil or at the surface? The formation of $LOO^{\bullet}$ from $L^{\bullet}$ is controlled by the rate at which oxygen can diffuse to $L^{\bullet}$. $L^{\bullet}$ radicals in oil have very short lifetimes so oxygen molecules must be located close to the radicals to compete with radical annealing and recombination. Dissolved oxygen does react

with radicals in the bulk oil but not efficiently because the oil viscosity is high. Oxygen reacts with lipid radicals much faster at the oil surface where oxygen concentrations are orders of magnitude greater and oxygen molecules have free movement.

Oils heated under the normal Oxipres conditions (10 g, 180 minutes) are not in thermal equilibrium – there is enough temperature difference from top to bottom of the cell to maintain slow circulation of the oil. The existence of thermal convection microcurrents in the Oxipres system has been verified by computer simulation (calculations by Dr. M. Karwe and students, Dept. of Food Science, Rutgers University). This microcirculation brings new oil constantly to the surface for reaction in a slow equilibrium process. When the oils are swirled gently in laminar flow, little new surface is created and the real increase in oxidation rate (ΔP not due to cooling) is negligible. However, when the oil is agitated so as to create turbulence, new surface area for reaction is increased and increased oxygen consumption is observed while the agitation is maintained. When the agitation is stopped, the oil returns to equilibrium conditions. Oxygen enhances the initial rate increase but not long term reactivity, again indicating that the surface is the site of action.

How can agitation affect reaction rates if increased oxygen diffusion is not involved? What is happening at the surface? We propose the following explanation. Research of Nawar (Nawar 1969) has shown that heating oils at 180 °C induces thermal scission reactions in the acyl chains of lipids. When thermal energy breaks bonds in fatty acid chains, two $C^{\bullet}$ scission radicals are generated:

$$-CH_2-CH_2-CH_2-CH_2- \rightarrow -CH_2-CH_2^{\bullet} + {}^{\bullet}CH_2-CH_2-$$

The radicals have several possible fates depending on the degree of agitation of the oil and the concentration of oxygen molecules close to the radicals (angstroms).

a) reaction with O_2 to form peroxyl radicals, $ROO^{\bullet}$, or with $-O^{\bullet}$ formed at high temperatures to generate alkoxyl radicals, $RO^{\bullet}$.

$$-CH_2-CH_2^{\bullet} + {}^{\bullet}CH_2-CH_2- \xrightarrow{O_2} -CH_2-CH_2OO^{\bullet} + {}^{\bullet}OOCH_2-CH_2-$$

$$-CH_2-CH_2^{\bullet} + {}^{\bullet}CH_2-CH_2- \xrightarrow{O^{\bullet}} -CH_2-CH_2O^{\bullet} + {}^{\bullet}OCH_2-CH_2-$$

These are the reactions accounting for oxygen consumption. They are favored by agitation which creates more surface area and constantly brings new oil to the surface, and by high oxygen pressures which decrease diffusion distance and increase the probability that an oxygen atom or molecule will be close enough to a scission radical to compete with radical recombination reactions.

b) recombination to reform the original fatty acid

$$-CH_2-CH_2^{\bullet} + {}^{\bullet}CH_2-CH_2- \rightarrow -CH_2-CH_2-CH_2-CH_2-$$

This is probably the dominant reaction in oils being heated with little swirling or agitation because there is no force to move the radicals apart.

c) recombination with other fragments to form new dimer and polymer products, particularly alkanes and ketones of various lengths

$$-CH_2-CH_2^{\bullet} + {}^{\bullet}CH_2-CH_2-CH_2-CH_2- \rightarrow CH_2-CH_2-CH_2-CH_2-CH_2-CH_2-$$

Formation of mixed dimer products is favored as motion in the oil increases and scission radicals are pushed out of their initial reaction cage; dimers are also enhanced

under low oxygen pressures where competition from O_2 reactions is limited.

d) H abstraction to form short alkanes

$$-CH_2-CH_2^{\bullet} + RH \rightarrow -CH_2-CH_3 + R^{\bullet}$$

This reaction is favored by low oxygen and should not be affected much by agitation.

e) internal rearrangement of radicals to generate alkenes

$$-CH_2-CH_2-CH_2^{\bullet} \rightarrow -CH-CH=CH_2 \leftrightarrow -CH=CH-CH_3$$

This reaction is favored by low oxygen which limits peroxyl radical formation and by agitation which disrupts radical recombinations.

Why does agitation increase oxygen consumption only during active swirling? Agitation increases all the reactions shown above except radical recombination b), resulting in formation of volatile products that are released to the headspace. In addition, when peroxyl radicals form in close proximity or in high local concentrations, they recombine to form alkoxyl radicals and release a molecule of oxygen via the Russell reaction:

$$R_1OO^{\bullet} + {}^{\bullet}OOR_2 \rightarrow R_1O^{\bullet} + O_2 + {}^{\bullet}OR_2$$

Both the released oxygen and the product volatiles add to the headspace. The result is that while swirling increases contact with oxygen and hence the rate of reaction with radicals from thermal scission or any autoxidation chains initiated, it also paradoxically increases the rate at which volatile secondary products (including oxygen) are formed and it brings volatile products more rapidly to the surface for release.

Increased release of volatiles then counterbalances enhanced oxygen consumption.

In the oxygen bomb, thermal scissions are active initiators of radical reactions that consume oxygen, and the balance between oxygen consumption, radical recombinations, scission to short alkanes, and scission with oxidation to hydroperoxides and aldehydes is controlled by rate of agitation and availability of oxygen. Supporting this explanation are initial analyses of volatiles released when the Oxipres cells were opened and trapped on thermal desorption traps, as will be discussed in the next section.

4.9. Correlation of oxygen consumption with chemical assays of lipid oxidation products and volatile oxidation products

While the oxygen bomb provides kinetic information about the oxidation process and the oxidation curves tell researchers how far and how fast the reactions proceed, when used alone it is a blind assay – it provides no information about underlying reactions, products, or mechanisms. To demonstrate that the oxygen consumption curves do indeed reflect frying chemistry accurately, and to better understand what reactions are happening during elevated temperature frying, oils after heating were analyzed for conjugated dienes, hydroperoxides, aldehydes, and free fatty acids, and exploratory volatiles analyses were conducted

Products formed under various conditions are shown in Table 28. Several interesting patterns were observed. At all high temperatures, very low levels of hydroperoxides and conjugated dienes were detected Low concentrations of hydroperoxides are expected since heat decomposes hydroperoxides. Low concentrations of conjugated dienes indicates very low levels of autoxidation initiation, supporting thermal scissions as major initiators in short-time heating at frying temperatures. From table 30 it’s found, once the heating temperature is set, the concentration of hydroperoxides has little connection with oxygen. Surprisingly, extremely high concentrations of aldehydes were detected, all these points that thermal scission reaction is the dominant reaction in high heat system. To test this, the headspace gas was collected by short path thermal desorption trap by venting through it.

The volatiles were analyzed by GC-MS. From table 31, it's shown that the GC-MS analysis indicate that in the headspace, there are all kinds of small fraction of degradation products, specifically, alkanes, alkenes, aldehydes, carboxylic acid, alcohols, epoxides, free fatty acid and so forth, in all chain length from 2 carbons to 12 carbons.

Table 29. Major oxidation product of Swirl test, Temperature test and Pressure test.

	P.V. (meq/mol TAG)	ALK Mmol/mol TAG	C.D.	FFA %
Swirl test[a]				
Swirl	1.212	265.320	18.700	1.250
Stdev	0.200	17.890	0.283	0.011
Control	2.208	361.020	23.521	0.910
Stdev	0.019	11.860	1.253	0.113
Take-out	3.044	408.080	23.036	1.115
Stdev	0.038	9.210	0.607	0.014
Pressure Test[b](Bar)				
1	1.420	41.174	4.428	0.240
Stdev	0.344	2.056	0.045	0.001
2	1.783	74.464	6.431	0.805
Stdev	0.081	1.916	0.424	0.060
3	1.782	71.152	7.368	1.220
Stdev	0.275	11.621	0.602	0.057
4	1.509	116.868	8.800	2.085
Stdev	0.081	4.711	0.008	0.021
5	1.668	128.210	8.118	1.685
Stdev	0.357	22.946	0.275	0.149
Temperature[c] °C				
100	63.363	ND	5.471	17.570
Stdev	17.021	N/A	0.599	0.806
120	40.531	17.175	34.091	13.230
Stdev	3.755	3.229	0.806	5.487
150	7.973	21.845	40.063	9.565
Stdev	0.638	0.307	2.574	2.256
160	4.088	19.790	34.819	11.018
Stdev	0.626	0.322	4.325	2.388
180	1.257	17.438	35.681	8.155
Stdev	0.125	0.404	5.982	0.912

a: Experiment conducted under 2 bars oxygen, heated under 180°C for 3 hours.
b: Experiment conducted under 1-5 bars air, heated under 180°C for 3 hours.
c: Experiment conducted under oxygen, heated under 100-80°C for 3 hours
note: All the concentrations of products are reported in the average of 2 duplicate.

In further research on agitation, it's found that not only can agitation consume more oxygen by surface renewal; it also has positive effect on helping stabilize oil during frying. The figure 41 shows GC-MS diagram of swirled and control samples. Some peaks came out at the later stage of the GC-MS run in sample with swirling, which means there're some molecules with large molecular weight. However in the control sample these peaks did not show up. From table 3, it's also found that the total volatiles released in swirled samples are significantly more than that of controls. For test ran under 2 bars air, volatiles released from swirled sample are 4.7 time more than that of control and over 20 times more for swirled test ran under 2 bar pure oxygen. Oxygen concentration also played a role in competing with the thermal scission reaction. When running under air, the total volatiles released are 1.6 times and 7.3 times more than that run under pure oxygen, respectively. Combine the agitation research, some suggestions can be made to industrial frying are that first, if the agitation can be control during the early stage of frying, oil oxidation can be significantly reduced by cutting the access of oil with oxygen. On another hand, in the later stage of the frying, when the oil quites down, if artificial agitation can be made, for example, by flushing nitrogen through the oil, formation of dimmers and other large molecular weight compounds will greatly reduce, furthermore, by agitating the oil, release of volatiles will be facilitated which otherwise will stick on the fried food products and affect the safety and shelf life of the food products.These showing homologous series of alkanes, alkenes, aldehydes, carboxylic acids, and alcohols.

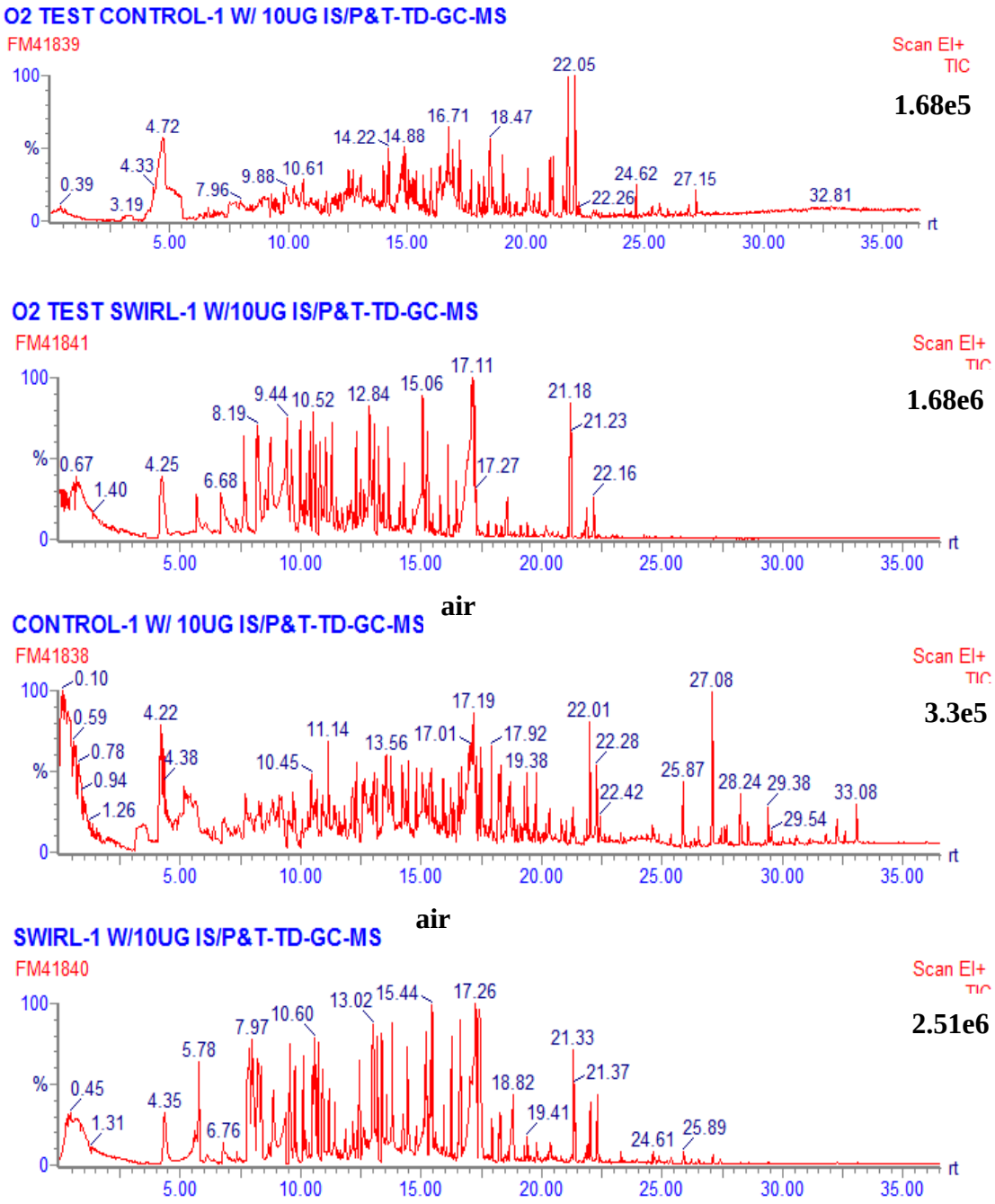

Figure 41 Effects of swirling under 2 bars oxygen or air on distribution and quantities of volatile products released from oil heated at 180 °C in the Oxipres system. Top two curves, heating under oxygen without (control) and with swirling. Bottom two curves, same but heating under air. Numbers shown at the right end of each chromatogram are the total area under the curve.

Table 30 Effect of swirling on volatile products released from oils heated at 180 °C for three hours under 2 bars oxygen or air.

	2 bars O_2		2 bars air	
	Control[a]	Swirl	control[a]	swirl
Acids	4.6	141.70	17.36	180.02
Alcohols	2.15	66.69	74.47	157.13
Aldehydes	0.77	4.81	2.05	12.59
CON	1.26	21.88	6.11	63.00
Esters	1.38	18.76	3.50	26.39
Furans	1.92	23.87	2.75	32.43
Hydrocarbons	2.10	31.09	9.81	48.22
IS	1.05	41.42	3.58	42.15
Ketones	1.37	29.82	3.26	67.44
Unknnow	0.66	2.42	2.13	9.57
TOTAL	17.12	367.21	124.92	588.93

a Control not removed from heater, not swirled

note: All units are as % of the largest peak of the internal standards

4.10. Thermal scission versus autoxidation.

From this project, it's found that, oxygen bomb is an excellent alternative method for study of frying chemistry in several ways. First, it provides a perfect closed system that allows researchers to monitor the oxygen consumption without worrying about leakage, also since it's closed system, all the oxidative volatile products will stay in the cylinder and can be easily collected and prepared for other analyses. Secondly, it provides accurate and stable temperature and pressure control throughout the entire project.. Thirdly, data acquisition frequency can be set from 10-second, which is for short-term experiment, to 600-second interval, which can be used for long term storage study. Fourthly, it provides easy means to control and interpret how far and how fast the reaction proceeds. However, during the project, several drawbacks were also found. First, the pressure transducer sensor causes problems, since oxygen consumption is the major concern and needs to be accurately monitored, but the pressure transducer picks up the total pressure. In this case, when oil degrades volatiles released would obscure the real total oxygen consumption, therefore, in order to detect only oxygen change during the experiments, the pressure transducer sensor needs to be replaced with a sensor that is only sensitive to oxygen. Secondly, the temperature detected by the machine is from the heating block, since the oil or the fat containing sample is the main concern for investigating oil frying chemistry, the temperature of the heating block may not reflect the real situation of the oil, especially during the heating up stage, it's recommended that a thermometer should be embedded in the reaction cylinder,

therefore the real time temperature can be monitored completely and accurately. Thirdly, it's known that when frying, because of the water contained in most of the foods, agitation happens at the early stage of the frying. During the agitation test, the agitation is created by swirling manually, this cause a lot of labor to do this, furthermore, manual handling of agitation may vary from people to people and batch to batch, even agitation between two sample in the same batch by the same operator can vary. Thus, it's suggested that stirrer should be installed in the cylinder for better and easier control of the agitation. Last but not least, data provided by oxygen bomb gives information of how fast and how far the oil degradation proceeds, this is measured by the total oxygen consumption and oxygen consumption rate when conducting at elevated temperature, and induction period for experiment at ambient temperature. However, for mechanism study, it's hard to extract helpful information from it since products should be known to map out all the possible reaction mechanisms.

5. Summary and Conclusion

The main purpose of this project was to evaluation the feasibility of using oxygen bomb to study frying chemistry. Since this technology had been used for food oils and fats only at ambient temperature where induction period can be used as the primary parameters for the determination of the stability of oils and fats, for elevated temperature, the shifted reaction mechanism requires new thinking and method to interpret the data obtained.

This is further proved by the temperature study of this project. It's found that when working temperature is below 150°C, induction period still showed up, which matches the result from other people's work. Nevertheless, when temperature is above that point, oxygen consumption started immediately after it reached the peak pressure or even before that. In this case, oxidation rate, net oxygen consumption, the comparison between observed peak pressure and theoretical peak pressure were measured and used as the parameters for studying the chemistry. Oxidation rate of the temperature test for sample run at temperature above 150°C did not show significant variance, which indicates that once temperature is above the critical point (may vary dependent on oil type, antioxidant proxidant and so fourth), enough thermal energy will trigger the scission reaction proceed at a constant rate. Excess energy will not have significant effect on the oxidation rate once the critical point is passed.

In the pressure test, the effect of oxygen was tested at the typical frying temperature-180°C. First, it's found that oxygen pressure affect the oxidation rate as it

would be expected, however, when under careful examination, result turns out that low oxygen, specifically, from 0.5 to 1 bar oxygen the oxidation rate increase more dramatically than that at relative high oxygen, namely from 1 bar to 5 bars. From the literature, same phenomenon had also been reported, only the cut-off pressure varies from work to work.

Furthermore, from the GC-MS data, it's found that oxygen concentration also played a role in competing with thermal scission reaction. 7.3 times more volatiles from the air-control group were detected compare to oxygen control group, and 1.6 time more volatile from the air-swirl groups compare to oxygen swirl group.

From the swirl test, it's found that agitation, which is always happen during practical frying, can either do good or bad to oils and therefore the food fried. First, when oil is agitated, oxygen consumption, in another word, oxidation rate is significant increased. Because, agitation will bring new oxygen into oils more effectively, and meantime, it breaks the oil surface, which allows the new fresh oil gain access to oxygen. This can cause the oil quality and safety go south much fast. Nevertheless, from the result of GC-MS, it's found that with agitation, it help to release much more volatile out of the oil phase and generate less high molecular weight products, which are possibly dimmers and polymers that can stick onto the fried foods. The benefit of this is that, less oxidized oil products will stick to the fried products, therefore enhance the quality, safety and shelf life. Furthermore, it's also found from the swirl test that, agitation initially had tremendous effect on the increase of oxidation rate, however less

and less effect was observe during the last few operations, more surprisingly, the experimental group ended up with the same amount the total oxygen consumption with the control group, which indicates that in the control group, slow convection still exists that keep circulating the oil from bottom to top bringing new fresh oil to react.

In order to understand what is really happening in the cylinder during experiment, products analyses was conducted by Saftest^{TM} kits for the oil phase, and by GC-MS for the volatile test. Four major oxidative products from oil phase was conducted, namely hydroperoxide, aldehyde, conjugated diene and free fatty acid. From the result, very little hydroperoxide and conjugated diene were detected, however, huge amount of aldehyde was detected. This suggests thermal scission reaction is the dominant reaction at elevated temperature. This suggestion was also further proved by the GC-MS data, in which homologous series of short chain products, namely from 2 carbons to 12 carbons, were detected.

In summary, oxygen bomb is a reliable and stable equipment that provides easy means to control and interpret the data obtain. However, for more accurate measurements, several modifications to the hardware design of the machine should be made. Last but not least, since the oxygen bomb only provides information about kinetics, for mechanism study, the data gain from it should be combined with products analyses

6. Future work

First, because of the drawbacks of the equipment mentioned above are very critical for accurate and precise quantitative analysis, suggestions will be made to the manufacturer for modifications, including changing the pressure transducer to oxygen sensor for real oxygen consumption analysis, and adding inert stirrer into the reaction cylinder to provide circulation. Inserting a thermometer in the reaction cylinder to monitor the temperature of the oil sample will be necessary to verify the heating time for research and to determine appropriate monitoring times, but is probably not critical for commercial design once reproducible patterns have been established.

Secondly, to data, single factors that affect oil oxidation has been done by using this methodology, including, temperature, pressure, agitation, water, metal ions, phospholipids and oxidized products. (The data of latter 5 factors are not shown here). Considering the practical situation in which multiple proxidants exist in foods, the synergistic effect of either two or three factor will be investigated in future.

Finally, since the current products analyses method, the Saftest^{TM} kits are only good for qualitative or semi quantitative determination, sophisticated analytical methods are under developing. For oxidized products in oil phase, HPLC-ECD method for detailed products determination will be developed. Since the current GC analysis for volatiles was done by cooperating with other labs, GC method for determination of volatiles by our own lab should be developed.

.

REFERENCES

Kaufmann, A, Suter, B (2001). "Comparison of different methods to determine polar compounds in frying oils." Eur. Food Res. Technol. **213**: 377-380.

American Oil Chemistry Society. Free Fatty Acid. **Ca 5a-40**.

American Oil Chemistry Society Official method (1986). Peroxide Value. **Cd 8-53**.

American Oil Chemistry Society Official method (1989). 2-Thiobarbituric Acid Value. Direct Method. **Cd 19-90**.

American Oil Chemistry Society Official method (1989). p-Anisidine value. **Cd 18-90**.

American Oil Chemistry Society Official method (2003). Spectrophometric Determination of Conjugated Dienoic Acid. **Ti 1a-64**.

ASTM (2007). Standard test method for oxidation stability of lubricating grease by oxygen vessel method. **D942-02**.

Muik, B., Molina-Diaz, A., Ayora-Canada, M.. (2005). "Direct monitoring of lipid oxidation in edible oil by Fourier transform Raman spectroscopy." Chemistry and Physics of Lipids **134**: 173-182.

Blankenship, R., Holaday, E., Barnes, J,. Pearson, L.. (1973). "Comparison of oxygen bomb method to other methods for measuring oxidative stability of peanuts and peanut products." J. Amer. Oil Chem. Soc. **50**(9): 377-380.

Byrdwell, C., Neff, E. (1998). "Analysis of Hydroxy-containing seed oils using atmospheric pressure chemical ionization mass spectrometry." J. Liquid Chromatogr. **21**: 1485-1501.

Byrdwell, C., Neff, E.. (1999). "Non-volatile products of triolein produced at frying temperatures characterized using liquid chromatography with online mass spectrometric detection." J. Chromatography A **852**: 417-432.

Summo, C., Caponio, F.. (2008). "Assessment of the oxidative and hydrolytic degradation of the lipid fraction of mortadella by means of HPSEC analyses of polar compounds." Meat Science **79**: 722-726.

Choe, E., Min, D.. (2006). "Mechanisms and Factors for Edible Oil Oxidation " Comprehensive reviews in Food Science and Food Safety **5**: 169-186.

Claxson, A., Hawkes, G., Richardson, D., Naughton, D., Haywood, R., Chander, C., Atherton, M., Lynch, E.. (1994). "Generation of lipid peroxidation products in culinary oils and fats during episodes of thermal stressing: a high field ^{1}H NMR study." Federation of European Biochemical Societies **355**: 81-90.

Coni, E., Podesta, E., Catone, T.. (2004). "Oxidizability of different vegetables oils evaluated by thermogravimetric analysis." Thermochimica acta **418**: 11-15.

Cooper, R., Matzinger, D. P., Furia. T. E.. (1979). "An improved apparatus for oxygen bomb testing." J. Amer. Oil Chem. Soc. **56**(1): 1-5.

Dobarganes, M. C., Velasco, J.. (2002). "Analysis of lipid hydroperoxides." Eur. J. Lipid Sci. Technol **104**: 420-428.

Dobson, G., Christie, W. W., Sebedio, J. L.. (1997). "Saturated bicyclic fatty acids formed in heated sunflower oils " Chemistry and Physics of Lipids **87**: 137-147.

Drozdowsk, B., Szukalska, E. (1987). "A rapid instrumental method for the evaluation of the stability of fats." J. A. Oil Chem. Soc. **64**(7): 1008-1011.

Eldin, A. K. (1997). "Characterisation of aldehydic acid in used and unused frying oils " J. Chromatography A **776**: 245-254.

Ellis, R., Gaddis, A. M., Currie, G. T.. (1966). "Carbonyls in oxidizing fat. IX. Aldehydes isolated from autoxidized methyl arachidonate." J. Food Sci. **31**(2): 191-195.

Ellis, R., Gaddis, A.M., Currie, G.T. & Powell. S.L.. (1968). "Carbonyls in oxidizing fat: XII. The isolation of free aldehydes from autoxidized triolein, trilinolein and trilinoleinin." J. Amer. Oil Chem. Soc. **45**(8): 553-559.

Esterbauer, H., Zollner., H.. (1989). "Methods for determination of aldehydic lipid peroxidation products." Free Radical Biology & Medicine **7**: 197-203.

Farhoosh, R., Moosavi, R.. (2008). "Carbonyl value in monitoring of the quality of used frying oils." Analytical chimica ACTA **617**: 18-21.

Caponio, F., Gomes, T., Pasqualone, A., Summo, C.. (2006). "Use of the high performance size exclusion chromatography analysis for the measurement of the degree of hydrolytic and oxidative degradation of the lipid fraction of biscuits." Food Chemistry **102**: 232-236.

Frankel, E. (1982). "Volatile lipid oxidation products." Prog. Lipids Res. **22**: 1-33.

Frankel, E. (1987). "Secondary products of lipid oxidation " Chem. Phys. Lipids **44**: 73-85.

Frankel, E., Neff, W., Selke, E., Brooks, D. (1987). "Thermal and metal-catalyzed decomposition of methyl linolenate hydroperoxides " Lipids **22**: 322-327.

Frankhauser-Noti, A., Fiselier, K., Biedermann-Brem, S., Grob, K.. (2006). "Assessment of epoxidized soy bean oil (ESBO) migrating inito foods: Comparison with ESBO-like epoxy fatty acids in our normal diet." Food Chemical Toxicology **44**: 1279-1286.

Fredriksson, P., Marcuse, R. (1968). "Fat oxidation at low oxygen pressure.i. kinetic studies on the rate of fat oxidation in emulsion." Journal of American Oil Chemistry Society. **45**: 400-407.

Gertz, S. K. C., Kochhar, S. P.. (2000). "Testing and comparing oxidative stability of vegetable oils and fats at frying temperature." European Journal of Lipid Science and Technology **102**: 543-551.

Gillat, P. (2001). Flavour and Aroma Development in Frying and Fried Foods. Boca Raton, CRC Press.

Gonzaga, F. B., Pasquini, C.. (2006). "A new method for determination of the oxidative stability of edible oils at frying temperatures using near infrared emission spectroscopy." Analytical Chimica Acta **570**: 129-135.

Gordon, V. (2001). Food Testing System: Rapid and routine analysis of food quality and stability. AOAC. Gordon, V. (2005). "Rapid testing for fats and oils and food products." Food Technology **19**(9): 594-595.

Guillen, M. D. (2009). "Oxidation of corn oil at room temperature: Primary and

secondary oxidation products and determination of their concentration in the oil liquid matrix from H nuclear magnetic resonance data." Food Chemistry **116**: 183-192.

Gunstone, F. D. a. P., F. B.. (1997). Lipid Technologies and Application. New York, NY, Marcel Dekker**:** 181-182.

J. Pokorny, Parkanyiova, L., Reblova, Z., Trojakova, L., Sakurai, H., Miyahara, M., Yano, T.. (2003). "Changes on storage of peanut oils containing high levels of tocopherols and beta-carotene." Czech J. Food Sci. **21**: 19-27.

Jin-Hyang, S., Cho-Ook, C., Terao, J., Ki, P. D.. (1993). "Electrochemical detection of triacylglycerol hydroperoxides by reversed phase high-performance liquid chromatography." Biosci. Biotechnol. Biochem. **57**: 479-480.

Jonsdottir, R., Bragadottir, M. Arnarson, G.. (2005). "Oxidatively derived volatile compounds in microencapsulated fish oil monitored by solid-phase microextraction (SPME)." J. Food Sci. **70**: 433-440.

Kamal-Eldin, A., Marquez-Ruiz, J., Dobarganes, C., Appelqvist, A.. (1997). "Characterisation of aldehydic acids in used and unused frying oils." J. Chromatography A **776**: 245-254.

Karel, M. (1992). In Physical Chemistry of Foods. New York, Marcel Dekker.

Kerwin, J. L., Torvik, J. J.. (1996). "Identification of monohydroxy fatty acids by electrospray mass spectrometry and tandem mass spectrometry." Anal. Biochem. **237**: 56-64.

Kinter, M. (1995). "Analytical technologies for lipid oxidation products analysis." Journal of Chromatography **671**: 223-236.

Kochi, J. K. (1973). Free Radicals. New York, John Wiley.

Labuza, T. P. (1971). "Kinetics of lipid oxidation in foods." CRC Crit. Rev. Food Sci. Nutr. **2**(3): 355-405.

Liang, C. (1998). "Comparison of four accelerated stability methods for lard and tallow with and without antioxidants." Journal of American Oil Chemistry Society **75**(10): 1441-1443.

Lingnert, K. A. a. H. (1999). "Kinetic studies of oxygen dependence during initial lipid oxidation in rapeseed oil." Journal of Food Science **64**(2): 262-266.

Trojakova, L. Reblova, Z., Pokorny, J.. (2001). "Determination of oxidative stability in mixtures of edible oil with nonlipidic substances." Czech Journal of Food Science. **19**(1): 19-23.

Trojakova, L.,Reblova, Z., Thu, T., Pokorny, J.. (2001). "Antioxidant activity of rosemary and sage extracts in rapeseed oil." J. Food Sci. **8**: 1-13.

Lundberg, W. O. and J. R. Chipault (1947). "The oxidation of methyl linoleate at various temperatures." Journal of American Chemistry Society **69**: 833-836.

Moreno, M., Olivares, D., Lopez, F., Martinez, V., Reig, F..(1999). "Study of the formation of carbonyl compounds in edible oils and fats by H-NMR and FTIR." Journal of Molecular Structure **482-483**: 557-561.

Makinen, M., Piironen, V., Hopia, A.. (1996). "Postcolumn chemiluminescence,

Ultraviolet and evaporative light-scattering detectors in high-performance liquid chromatography determination of triacylglycerol oxidation products." Journal of. Chromatography. **734**: 221-229.

De Maria, C., Santos, M., Dias, U., Marana, M.. (2000). "Stabilization of soybean oil with heated quercetin and 5-caffeoylquinic acid in the presence of ferric ion." J. Agric. Food Chem. **48**: 3935-3938.

Marmeasat, S., Velasco, J., Dobarganes, M. C.. (2008). "Quantitative determination of epoxy acids, keto acids and hydroxy acids formed in fats and oils at frying temperatures." J. Chromatography A. doi: 10.1016/j.chroma.2008.09.077

Moreno, M.. (1998). "Study of the formation of carbonyl compounds in edible oils and fats by H-NMR and FTIR." J. of Molecular Structure.

Moros, J., Roth, M., Garrigues, S., Guardia, M.. (2009). "Preliminary studies about thermal degradation of edible oils through attenuated total refectance mid-infrared spectrometry." Food Chemsitry **114**: 1529-1536.

Mullertz, A., Schmedes, A., Holmer, G.. (1990). "Separation and detection of phospholipid hydroperoxides in the low nano-molar range by a high performance liquid chromatography/ironthiocianate assay." Lipids **25**: 415-418.

Nawar, W. W. (1985). Food chemistry. New York, Marcel Dekker, Inc.

Oliw, E. H., Su, C., Skogstrom, T., Benthin, G.. (1998). "Analysis of novel hydroperoxides and other metabolites of oleic, linoleic and linolenic acids by liquid chromatography-mass spectrometry with Ion trap MS." Lipids **33**: 843-852.

Osawa, C., Goncalves, L. A. G., Ragazzi, S.. (2007). "Correlation between free fatty acids of vegetable oils evaluated by rapid test and by the official method." J. Food Composition Analysis **20**: 523-528.

Osawa, C., Goncalves, L. A. G., Ragazzi, S.. (2007). "The use of fast methodologies (Kits) in evaluating deep-frying oils." Journal of American Oil Chemistry. Society. DOI 10.1007/s11746-007-1124-7

Palmer, D., Anderson, M., Jolly, R.. (1984). "Separation of some neutual lipids by normal-phase high-performance liquid chromatography on a cyanopropyl column: Ubiquinone, dolichol, and cholesterol levels in sheep liver." Anal. Biochemitry **140**(2): 315-319.

Pellegrini, N., Visioli, F., Buratti, S., and Brighenti, F.. (2001). "Direct analysis of total antioxidant activity of olive oil and studies on the influence of heaing " J. Agric. Food Chem. **40**: 2532-2538.

Pohle, W. D., Gregory, R. L., Taylor, J. R.. (1962). "A comparison of several analytical techniques for prediction of relative stability of fats and oils to oxidation." J. Amer. Oil Chem. Soc. **39**(4): 226-229.

Pohle, W. D., Gregory, R. L., Van Giessen, B.. (1963). "A rapid oxygen bomb method for evaluating the stability of fats and shortenings." J. Amer Oil Chem. Soc. **40**(11): 603-605.

Pokorny, J., Parkanyiova, L., Reblova, Z., Trojakova, L., Sakurai, H., Miyahara, T.,

Yano, T.. (2003). "Changes on storage of peanut oils containing high levels of tocopherols and beta-carotene." Czech J. Food Sci. **21**: 19-27.

El-Abssy, R., Donfack, P., Materny, A.. (2009). "Assessment of conventional and microwave heating induced degradation of carotenoids in olive oil by VIS Raman spectroscopy and classical methods." Food Research International, doi: 10.1016/foodres.2009.10.021

Reblova, Z. (2006). "The effect of temperature on the antioxidant activity of tocopherols " Eur. J. Lipid Sci. Technol. **108**: 858-853.

Reiners, W. A. (1972). "Comparison of oxygen-bomb combustion with standard ignition techniques for determining total ash." Ecology **53**(1): 132-136.

Rossell, J. (1994). Measurement of Rancidity, in Rancidity in Foods. London, Blackie Academic.

Saguy, I. S., Dana, D.. (2003). "Integrated approach to deep fat frying: engineering, nutrition, health and consumer aspects." J. Food Engineering **56**: 143-152.

Schaich, K. M. (1992). "Metals and lipid oxidation. Contemporary Issues." Lipids **27**(3): 209-218.

Schaich, K. M. (2005). Lipid oxidation: Theoretical Aspects, Bailey's Industrial Oil and Fat Products. F. Shahidi, ed., John Wiley & Sons, NY**:** 269-310.

Schaich, K. M. (2008). Culinology 101: Frying, Rutgers University Continuing Education Course. New Brunswick, NJ, U.S., Rutgers University.

Schneider, C., Schreier, P., Herderich, M.. (1997). "Analysis of lipoxygenase-derived fatty acid hydroperoxides by electro-spray ionization tandem mass spectrometry." Lipids **32**: 331-336.

Schulte, E. (2002). "Determination of higher carbonyl compounds in used frying fats by HPLC of DNPH derivatives." Anal. Bioanal.Chem. **372**: 644-648.

Shahina Naz, R. S., Hina Sheikh, Syed Asad Sayeed (2005). "Deterioration of olive, corn and soybean oil due to air, light, heat and deep-frying." Food Research International **38**(127-134).

Shen, N., Fehr, W., White, P.. (1997). "Oxidative stabilities of soybean oils with elevated palmitate and reduced linolenate contents." J. Am. Oil Chem. Soc. **74**(3): 299-302.

Sheppard, H.. (1962). "Determination of H3 and C14 in biological materials using oxygen bomb combustion." Analytical Biochemistry **4**(3): 246.

Sjovall, O., Kuksis, A., Marai, L., Muher, J. J.. (1997). "Elution factors of synthetic oxotriacylglycerols as an aid in identification of peroxidized natural triacylglycerols by reverse-phase high performance liquid chromatography with electro-spray mass spectrometry." Lipids **32**(1211-1218).

Spickett, C. M., Pitt, A. R., Brown, A. J.. (1998). "Direct observation of lipid hydroperoxides in phopholipid vesicles by electro-spray mass spectrometry." Free Radical Biology & Medicine **25**: 613-620.

Stephanie A. Smith, R. E. K., David B. Min (2007). "Oxidative and thermal stabilities of genetically modified high oleic sunflower oil " Food Chemistry **102**:

1208-1213.

Stuckey, B. N., Sherwin, E. R., (1958). "Improved techniques for testing fats and oils by the oxygen bomb method." Journal of American Oil Chemistry Society **35**(11): 581-584.

Foo, S. Y., Cuppett, S., Schlegel, V.. (2006). "Evaluation of Saftest method for monitoring frying oil quality " Journal of American Oil Chemistry Society **83**: 15-20

Tomaino, A., Cimino, F., Zimbalatti, V., Venuti, V., Sulfaro, V., De Pasquale, A., Saija, A.. (2005). "Influence of heating on antioxidant activity and the chemical compostion of some spice essential oils." Food Chemistry **89**: 549-554.

Toth, K., Stulik, K., Kutner, W., Feher, Z., and Lindner, E.. (2004). "Electrochemical detection in liquid flow analytical techniques: Characterization and Classification." Pure Appl. Chem. **76**(6): 1119-1138.

Uran, S., Larsen, A., Jacobsen, P., and Skotland, T.. (2001). "Analysis of phospholipid species in human blood using normal-phase liquid chromatography coupled with electrospray ionization ion-trap tandem mass spectrometry." J. Chromatography B: Biomedical Sciences and Applications **758**(2): 265-275.

Walker, M. D., Hughes, P.S., Simpson, W. J.. (1996). "Use of chemiluminescence HPLC for measurement of positional isomers of hydroperoxy fatty acids in malting and rest stage of mashing. J. Sci. Food Agric. **70**: 341-346.

Warner, K. (2008). Food Lipids: Chemistry, Nutrition and Biotechnology. Boca Raton, CRC Press.

Warner, K., Vick, B. A., Kleingartner, L., Isaac, I., and Doroff, K.. (2003). "Composition of sunflower, Nusun (mid-oleic sunflower), and high oleic sunflower oils. In Proc. Sunflower ResearchWorkshop, Fargo, ND." http://www.sunflowernsa.com/research/research-workshop/documents/107.pdf

Yamada, K., Brodsky, M. E., Baker, J. C., Ames, B. N.. (1987). "Detection and characterization of lipid hydroperoxides at picomole levels by high-performance liquid chromatography. ." Anal. Biochem. **160**: 7-13.

Yang, G. C. (1992). "Detection of lipid hydroperoxides by high performance liquid chromatography coupled with post-column reaction." Trends Food Sci. Technol. **3**: 15-18.

Yu, J.(1997). "Thermal Decomposition of C10-C14 Normal Alkanes in Near-Critical and Supercritical Regions: Products Distribution and Reaction Mechanism." Ind. Eng. Chem. Res. **36**: 574-584.